Dipl.-Ing. Bojana Stojčić

Affinity tagging of (phospho)lipolytic enzymes in cultured cells

Dissertation

zur Erlangung des akademischen Grades einer

Doktorin der technischen Wissenschaften

eingereicht an der

Technischen Universität Graz

Betreuer:

Ao. Univ.-Prof. Dr. phil. Albin Hermetter

Institut für Biochemie

Graz, Juni 2013

Thesis Committee Members:

Professor Saša Frank

Institute of molecular Biology and Biochemistry

Medical University of Graz

Professor Hans-Jörg Leis

Department of Pediatrics and Adolescence Medicine

Medical University of Graz

Захваљујем се,

професору Албину Херметру на могућности да урадим овај рад, те на савјетима и смјерницама током последње три године.

радним колегама са истутута и из групе на подршци, као и колегама и професорима са других института који су додатно доприносили радној атмосфери.

свим познаницима, рођацима и пријатељима на великој подршци, и који су ми свјесно или несвјесно отварали видике према новим тајнама живота и остварењу циљева. Овом приликом се захваљујем и Бранки Рачић која ме је у дјетињству охрабривала и својим савјетима подржавала. Посебне захвале дугујем партнеру Мартину Фолмајер на великој толеранцији и моралној подршци у последњих годину дана.

својој породици, родитељима Михајлу и Гордани и сестри Јовани, који су ми са љубављу пружали сталну подршку. Вама, дугујем пуно више од ријечи захвалности. Хвала вам пуно на савјетима и бескрајној љубави којом ме окружујете.

на крају, али не и по важности, покојној баки Веселки, која је несебичном љубављу испунила дане мога дјетињства и зато овај рад и посвећујем Њој.

Стојчић Бојана

Срећа је једина ствар на свијету која кад се дијели, расте.

Непознати аутор

Покојној баки Веселки,

с љубављу

Eidesstattliche Erklärung

Ich erkläre an Eides statt, dass ich die vorliegende Arbeit selbstständig verfasst, andere als die angegebenen Quellen/Hilfsmittel nicht benutzt und die den benutzten Quellen wörtlich und inhaltlich entnommenen Stellen als solche kenntlich gemacht habe.

Graz, am …… ……..

Unterschrift

Abstract

Fluorescently labeled and lipophilic p-nitrophenyl phosphonate esters were developed as suicide inhibitors for the selective detection of (phospho)lipolytic enzymes. These activity-based probes (ABPs) are substrate analogous compounds that covalently react with serine (lipid) hydrolases. They preferentially label active (phospho)lipolytic proteins in complex protein mixtures. After fluorescence detection, the tagged enzyme candidates can be isolated and identified by MS/MS analysis. In this study, we used phospholipid and fatty acid ester analogues as ABPs. We characterized the reaction of these lipids with reference phospholipases and used them for functional proteomic analysis of lipolytic enzymes in cultured macrophages. The identified proteins were lipases, phospholipases, lipid transferases and lipid-unrelated proteins. For the identification of protein targets of drugable enzyme inhibitors, a differential activity-based gel electrophoresis (DABGE) method was established. This technique is based on two types of fluorescent probes that are suicide inhibitors of lipases. The respective compounds are hydrophobic phosphonic esters that contain the same reactive group but differ by the fluorophores. In a typical experiment, a control sample A and a sample B preincubated with the drug are separately labeled with a green (dye swap: red) and a red (dye swap: green) fluorophore, respectively. After mixing the protein samples A and B, labeled proteins are separated by gel electrophoresis. Emission of fluorophore A shows all protein targets, whereas fluorophore B emission only shows proteins that do not bind the drug. Thus, the difference in the fluorescence patterns is representative for the drug targets in a given sample. This method was applied to identify protein targets of two commercial serine hydrolase inhibitors, namely Orlistat and CAY10499 in lysates of HepG2 cells and mouse adipocytes. The same technique was used for the identification of protein targets of Orlistat in cultured human squamous carcinoma cells. Various cancer cells were studied including the cell lines SCC12 and SCC13 as well as immortalized keratinocytes (HaCaT). The identified protein targets included fatty acid synthase, (phospho)lipases and lipid-unrelated proteins. Targeting of some of these polypeptides by Orlistat explains at least in part the profound apoptotic activity of this anti-obesity drug in cancer cells.

Kurzfassung

Fluoreszenzmarkierte lipophile p-Nitrophenyl-Phosphonatester wurden als Suizid-Inhibitoren für die selektive Detektion (phospho)lipolytischer Enzyme entwickelt. Diese aktivitätsbasierten Proben (ABPs) sind substratanaloge Verbindungen, die kovalent mit Serin(lipid)hydrolasen reagieren. Sie markieren bevorzugt (phospho)lipolytische Proteine in komplexen Proteingemischen. Nach der Fluoreszenzdetektion können die markierten Enzymkanditaten isoliert und massenspektroskopisch identifiziert werden. In dieser Studie haben wir Phospholipid- und Fettsäureester - Analoge als ABPs verwendet. Wir haben die Reaktion dieser Lipide mit Referenz-Phospholipasen charakterisiert und in der Folge für die funktionelle Proteomanalyse lipolytischer Enzyme in kultivierten Makrophagen eingesetzt. Die identifizierten Proteine waren Lipasen, Phospholipasen, Lipidtransferasen und „lipidunabhängige“ Proteine. Für die Identifizierung der Proteintargets von pharmakologisch relevanten Enzyminhibitoren wurde eine differenzielle, aktivitätsbasierte Elektrophorese (DABGE) Methode etabliert. Die betreffenden Verbindungen sind hydrophobe Phosphonatester, die dieselbe reaktive Gruppe, aber verschiedene Fluorophore enthalten. In einem typischen Experiment werden eine Kontrollprobe A und eine Probe B, die mit dem Pharmakon vorinkubiert wurde, separat mit einem grünen und einem roten Fluorophor markiert. In einem „Dye swap“ Experiment wurden die Fluorophor umgekehrt verwendet. Die Proteinproben A und B werden gemischt und die markierten Proteine werden durch Elektrophorese getrennt. Die Emission des Fluorophors A zeigt alle Proteintargets an, während die Emission des Fluorophors B nur die Proteine anzeigt, die das Pharmakon nicht binden. Daher ist die Differenz der Fluoreszenzmuster repräsentativ für die Targets des Pharmakons in einer gegebenen Probe. Diese Methode wurde eingesetzt um die Proteintargets von zwei kommerziellen Serinhydrolase-Inhibitoren (Orlistat und CAY10499) in Lysaten von HepG2 Zellen und Maus-Adipozyten zu bestimmen. Dieselbe Technik wurde für die Identifikation der Proteintargets von Orlistat in kultivierten menschlichen Hautkrebszellen verwendet. Wir studierten verschiedene Hautkrebszellen einschließlich der Zelllinien SCC12 und SCC13 (squamous carcinoma cells) sowie immortalisierte Keratinozyten (HaCaT). Die identifizierten Proteintargets waren Fettsäuresynthase, (Phospho)lipasen und „lipidunabhängige“ Proteine. Das Targeting einiger dieser Polypeptide durch Orlistat erklärt zumindest teilweise die ausgeprägte apoptotische Aktivität dieser Verbindung in Krebszellen, die primär als Medikament gegen Fettleibigkeit entwickelt wurde.

Table of Contents

1. Chapter 1 1

General Introduction

1.1 Abbreviations 2

1.2 General introduction 3

1.3 References 10

2. Chapter 2 17

Phosphonate probes for activity-based screening of (phosoho)lipolytic enzymes

2.1 Abbreviations 18

2.2 Abstract 19

2.3 Introduction 20

2.4 Experimental procedures 22

2.4.1 Cell Culture 22

2.4.2 Preparation of cell lysates 22

2.4.3 Preparation and handling of fluorescent inhibitors 23

2.4.4 Transient expression of phospholipase A_2 group IVB and platelet-activating factor acetylhydrolase in COS 7 cells 24

2.4.5 Microscopy of PLA_2 - GFP fusion proteins 25

2.4.6 One dimensional gel electrophoresis 25

2.4.7 Two dimension gel electrophoresis 26

2.4.8 Fluorescence detection of labeled proteins in electrophoresis gels 26

2.4.9 LC-MS/MS analysis of target proteins....27
2.5 Results....28
2.6 Discussion....36
2.7 Acknowledgment....39
2.8 References....40

3. Chapter 3....43

Functional proteome analysis of (phospho)lipases as targets of Orlistat in HepG2 and 3T3-L1 cells

3.1 Abbreviations....44
3.2 Abstract....46
3.3 Introduction....47
3.4 Experimental procedures....50
3.4.1 Cell culture....50
3.4.2 Preparation of cell lysates....51
3.4.3 Drug targeting and activity tagging of (phospho)lipolytic enzymes in cell lysates (DABGE)....51
3.4.4 One dimensional gel electrophoresis....52
3.4.5 Fluorescence detection of proteins in electrophoresis gels....52
3.4.6 LC-MS/MS analysis of target proteins....53
3.4.7 Lipid extraction and analysis....54
3.5 Results....56
3.6 Discussion....66
3.7 Acknowledgment....71
3.8 References....72

3.9 Supplemented Data 76

4. Chapter 4 78

Toxicity and protein targets of Orlistat in cultured human squamous carcinoma cells

4.1 Abbreviations 79

4.2 Abstract 81

4.3 Introduction 82

4.4 Experimental procedures 84

4.4.1 Cell culture 84

4.4.2 Preparation of cell lysates 85

4.4.3 Drug targeting and activity tagging of (phospho)lipolytic enzymes in cell lysates (DABGE) 86

4.4.4 One dimensional gel electrophoresis 87

4.4.5 Fluorescence detection of proteins in electrophoresis gels 87

4.4.6 LC-MS/MS analysis of target proteins 87

4.4.7 Lipid extraction and analysis 88

4.4.8 Microscopy 89

4.4.9 Caspase 3 activity Assay 90

4.5 Results 91

4.6 Discussion 99

4.7 Acknowledgment 103

4.8 References 104

List of Figures

Figure 2. 1 Chemical structures of fluorescent p-nitrophenyl phosphonate probes 24

Figure 2. 2 The mechanism of enzyme labeling by activity-based probes 28

Figure 2. 3 Detection of recombinant phospholipases A2 (PLA_2) with Ethyl-Cy-tagged inhibitors: group IVB (GIVB) and platelet-activating factor acetylhydrolase (PAF-AH) 30

Figure 2. 4 Fluorescence detection of transiently expressed PLA_2 - GIVB in COS 7 cells after tagging with NBD-labeled inhibitors (NBD-PC and NBD-HE-HP) 31

Figure 2. 5 Fluorescence microscopic images of GFP- tagged phospholipases (PLA2 - GIVB and - PAFAH) in COS 7 cells 32

Figure 2. 6 Lipolytic proteomes of murine RAW 264.7 cells 33

Table 2. 1 (Phospho)lipolytic and esterolytic proteomes of murine RAW 264.7 cells 35

Figure 3. 1 Chemical structure of (fluorescent) lipase inhibitors 56

Figure 3. 2 DABGE imaging of drug/inhibitor-targeted (phospho)lipases 57

Figure 3. 4 DABGE analysis of CAY10499 – tagged (phospho)lipolytic enzymes in HepG2 cell lysates 61

Figure 3. 6 Effects of Orlistat on glycerol(phospho)-lipid profiles in HepG2 cells 64

Table 3. 1 Orlistat targets in (phospho)lipolytic proteome of HepG2 (human) and differentiated 3T3-L1 (mouse) cell lysates in one dimensional gel electrophoresis 65

Figure S 1 Effects of Orlistat on triacylglycerol species analysis 76

Figure S 2 Effects of Orlistat on diacylglycerol species 76

Figure S 3 Effects of Orlistat on glycerophospholipid – phosphatidylcholines species 77

Figure S 4 Effects of Orlistat on glycerophospholipid – phosphatidylethanolamine species 77

Figure 4. 1 DABGE analysis of Orlistat – tagged “(phospho)lipolytic” enzymes in SCC13 cell lysates 92

Figure 4. 2 DABGE analysis of Orlistat – tagged “(phospho)lipolytic” enzymes in lysates of different non-melanoma squamous cancer cells (SCC) and keratinocytes (HaCaT) 94

Figure 4. 3 Effects of Orlistat on glycero(phospho)-lipid profiles in SCC13 cells 95

Figure 4. 4 Time dependent effects of Orlistat on morphology of human non-melanoma skin cancer cells 96

Figure 4. 5 Caspase 3/7 activity assay in skin cancer cells (SCC13) 97

Table 4. 1 Orlistat targets in a “(phospho)lipolytic” proteome of human non-melanoma SCC13 cell lysates 98

Chapter 1

General Introduction

1.1 Abbreviations

Apo	Apolipoprotein
ATGL	Adipose triacylglycerols lipase
CCK	Cholecystokinin
CE	Cholesterol ester
EL	Endothelial lipase
FAS	Fatty acid synthase
FFA	Free fatty acid
GAPDH	Glycerin aldehyde pyruvate dehydrogenase
GL	Gastric lipase
HDL	High density lipoprotein
HL	Hepatic lipase
HSL	Hormone sensitive lipase
IDL	Intermediate density lipoprotein
LDL	Low density lipoprotein
LPL	Lipoprotein lipase
MGL	Monoacylglycerol lipase
NBD	Nitrobenzo-2-oxa-1,3-diazole
PL	Pancreatic lipase
RPL	Ribosomal protein L
THL	Triacylglycerol hydrolase
VLDL	Very low density lipoprotein

1.2 General introduction

Development of obesity, type 2 diabetes mellitus and cardiovascular disease are constantly increasing and almost reaching an epidemic outbreak in the modern society (1, 2). These lipid-associated disorders are mainly due to impaired metabolism and cellular retention of lipids (3). In this context, lipolysis plays an important role. (Phospho)lipolytic enzymes are responsible for the degradation of acylglycerols, cholesterol esters and phospholipids releasing free fatty acids into the circulation and inside the cells. The localization, structure and selectivity of (phospho)lipolytic enzymes influence the metabolic fate of free fatty acids and their lipid metabolites. If not used for energy expenditure, free fatty acids will be stored in chemically bound form. Upon energy demand, they are released by lipolytic enzymes (1). Inappropriate life style and nutritional behavior contribute to lipid accumulation over longer periods of time and can lead to overweight/obesity. Genetic predispositions as well as dietary habits can lead to an elevated risk of obesity and other lipid-associated disorders (1).

In healthy mammals, lipids are stored in adipose tissue and are the primary source of energy during phases of high energy demand. In order to avoid harmful effects, excess of free fatty acids are intracellularly stored in triacylglycerols and cholesterol esters (4). The balance of lipid storage and mobilization is directly associated to body energy homeostasis. Many different physiological processes are involved in the regulation of lipid metabolism (1) such as: food resorption in the gut, the partitioning of energy substrates among tissues and the *de novo* synthesis and catabolism of lipids (1, 4). Any of these components may be involved in lipid-associated disorders. Fluctuations of circulating fatty acid are among the main risk factors for development of lipid-mediated disorders (5-8).

Lipid-mediated disorders such as obesity or insulin resistance (type 2 diabetes) are frequently associated. Therefore, it is believed that obesity and insulin resistance may be causally related. They both share impairment of carbohydrate and fat metabolism in muscle and fat tissue (8). Some studies suggest that elevated free fatty acid (FFA) competes with glucose for energy production in cardiac muscle (7). It is also believed that the elevation of FFAs in muscle cells leads to an increase of DAG. This effect influences the phosphorylation of the insulin receptor substrate 1. As a consequence, insulin cannot bind, hence preventing translocation of GLUT4 vesicles and uptake of glucose (9). According to another model chronically elevated FFAs are lipotoxic, due to nitric oxide formation, which causes dysfunction of β-cells of the pancreas leading to the development of type 2 diabetes (10-12). Even though the exact correlation between increased FFA, insulin resistance and β-cells dysfunction is unknown, many evidences support the assumption that elevated FFA are causally related to the development of type 2 diabetes (7). Next to many other lipid metabolizing enzymes lipolytic enzymes are responsible for the apparent level of FFAs and their (patho)physiological consequences. Therefore, further investigations of lipolytic enzymes are of big importance.

Many lipolytic enzymes such as triacylglycerol lipases and cholesteryl esterases are important enzymes in lipid mobilization. However, until now not all of them are identified and understood on the molecular level. Many extracellular and intracellular lipases have been characterized. Some secretory or extracellular proteins are vascular lipases (lipoprotein lipase - LPL (13), hepatic lipase – HL (14) and endothelial lipase - EL (15)). Enzymes of the digestive tract are pancreatic lipase – PL (16), gastric lipase – GL (17, 18) and others. The main intracellular lipases responsible for the degradation of mono-, di- and triacylglycerols are monoacylycerol lipase – MGL (19), hormone sensitive lipase –

HSL (20), adipose triacylglyceride lipase – ATGL (21) and triacylglycerols hydrolase – THL (22).

Human gastric lipase and pancreatic lipase are two well studied digestive enzymes. It is known that up to 95% of the daily lipid intake is absorbed due to the action of lipases in the stomach and small intestine and the enzymes secreted by the liver and pancreas (23, 24). Enzymatic lipid degradation requires several components including emulsification and lipolysis (24). Human gastric lipase is a lipolytic enzyme, which is secreted in the fundus mucosa. It is stimulated by pentagastrin and participates in the formation of large fat globules (25, 26). The fat globules mix with bile salts synthesized in the liver and secreted from the gallbladder and pancreatic juice (secreted from the pancreas) in duodenum. Degradation of globules by pancreatic lipase leads to the formation of small lipid droplets (27). The human pancreatic lipase is expressed in the acinar cells of the pancreas and localizes to the zymogen granulas together with other digestive enzymes. These zymogen granules stay inactive until stimulation by the intestinal hormones secretin and cholecystokinin (CCK) releasing the enzyme into the intestinal lumen (28, 29). Interestingly the gastric lipase is inhibited by these hormones (25). Another important protein secreted from the pancreatic acinar cells is carboxyl ester lipase. This enzyme is involved in hydrolysis of triacylglycerols, cholesterol ester (CE), monoacylglycerols, phospholipids, lysophospholipids, ceramides and sphingolipids. It is involved in the release of long chain fatty acyl groups but it requires bile salt for its activation (30). Fatty acid, cholesterol and glycerol released by the lipases are taken up from the enterocyte and are re-assembled to triacylglycerols and cholesterol esters as components of chylomicrons. The chylomicrons are triacylglycerols- and cholesterol ester- rich particles secreted from the intestine into the blood system through the lymph (1). They also carry fat-soluble vitamins. In the blood vessels triacylglycerols of chylomicrons are degraded

mainly by endothelial lipoprotein lipase (LPL) leading to the formation of chylomicron remnants which recruit apolipoprotein E (ApoE) and cholesterol from HDL. In contrast to other vascular lipases (HL and EL), lipoprotein lipase is activated by apolipoprotein-CII (15). Its expression level is a rate limiting process for the uptake of triacylglycerols derived fatty acids (10). The liver synthesizes and releases an endogenous lipoprotein namely very low-density lipoprotein (VLDL). In plasma, these cholesterolester-rich particles are also degraded by lipoprotein lipase thereby forming intermediate density lipoproteins (IDL or also known as VLDL-remnants) which are finally converted to LDL. The final lipoprotein particles are recognized by the ApoE receptor (for LDL-Clearance) in the liver after hydrolytic modification by hepatic lipase. LDL is recognized by the cells of other tissues by the ApoB-100 receptor (31, 32). Hepatic lipase, mainly expressed in liver, hydrolyzes triacylglycerols and phospholipids in the triacylglycerols rich low-density lipoprotein (VLDL and/or IDL) and high-density lipoprotein (HDL) particles (33). Hepatic lipase also has a role in HDL metabolism (14). In contrary to LPL and HL (mainly responsible for hydrolization of the triacylglycerol-rich lipoproteins, chylomicrons, VLDL, and IDL), EL is more efficient in hydrolysis of HDL. The intracellular lipases (e.g. ATGL, HSL) expressed in adipocytes play an important role in fatty acid mobilization and its delivery to oxidative tissues such as skeletal muscle and heart for energy production. It is known that fat tissue and fat depot in the cell is the most important energy source in vertebrates. For the energy supply it is necessary to release free fatty acids (FFAs) from stored fat, which requires the enzymatic activity of lipases (intracellular lipases). ATGL is considered a key enzyme in triacylglycerols hydrolysis in adipose tissue. If ATGL is inactivated, it can be causally related to cardiac dysfunction and insulin sensitivity (34). HSL is also an intracellular neutral lipase, which is capable of hydrolyzing cholesterol esters, diacylglycerols and to lesser extent triacylglycerols in adipose tissue (1, 20). MGL preferentially catalyzes

monoacylglycerol hydrolysis by completing the last step in the hydrolysis of stored triglycerides in the adipocyte (19). TGH is involved in mobilization of triacylglycerols and the VLDL secretion in liver (22). It is also highly expressed in adipose tissue (35).

Impairment of lipolysis in macrophages, liver and adipose tissue are not only causally linked to several lipid-associated disorders such as obesity, diabetes 2 and atherosclerosis. They are also essential for survival of cancer cells (36).

Nowadays, many attempts are being made to treat or avoid obesity by pharmacotherapy (37). One of the clinically approved anti-obesity drugs still in use is Orlistat (Xenical;Roche), which reduces absorption of dietary fat in the intestinal lumen by inhibition of digestive lipases (37). Orlistat is a derivative of the well known lipase inhibitor lipstatin. Lipstatin is a lipid produced by *Streptomyces toxytricini* (38) and can covalently bind to the serine residue in the active site of a serine hydrolase by ester formation with its β-lactone group (39-42). It has been shown that therapeutic doses of Orlistat (120 mg three times daily) reduce fat absorption up to 30%, while undigested fat is excreted (37, 43). The bioavailability of Orlistat is rather poor but there is a small amount still absorbed into systemic circulation (44). Thus, it is not surprising that unwanted adverse side effects have been observed. They are mainly related to the gastrointestinal tract including fatty/oily stool (45). However, abdominal pain, facial spotting, pancreatitis etc. have also been described. Due to impairment of lipid resorption by Orlistat the uptake of cholesterol and fat-soluble vitamins can also be reduced. Uptake of other lipophilic drugs is also affected (45). Several studies showed that Orlistat may display unfavorable effects: pancreatitis (99 reports) (46), serious hepatic side effects such as cholestatic hepatitis (47), subacute liver failure (two reports) (48, 49), severe hepatic injury (one report) (50). Some beneficial effects have been seen in non-alcoholic fatty liver disease (51, 52).

Therefore, it is important to understand the molecular mechanisms underlying these phenomena and to identify primary targets or off-targets of Orlistat in different cells that are essential for lipid metabolism.

Orlistat inhibits human pancreatic lipase, gastric lipase, carboxyl ester lipase and lipoprotein lipase and others (39). Recently, a new important target has been identified, namely fatty acid synthase (FAS) (53). Orlistat likely binds to the thiol domain of FAS and inhibits the activity of this enzyme. It is believed that inhibition of FAS in cancer cells such as breast, prostate and melanoma leads to anti-proliferative effects and apoptosis and thus could be important for the development of anti-cancer therapies. Expression levels of FAS are much higher in cancer cells than in most normal cells (53, 54). It is upregulated in several malignancies e.g. prostate, breast, melanoma, ovary and soft tissue sarcoma (55-68). Inhibition of FAS reduces proliferation of cancer cell by blocking DNA replication during S-phase, which in the end promotes apoptosis (69, 70). Studies in mouse melanoma B16-10 cells have demonstrated that inhibition of FAS leads to apoptosis (71) since energy supply is short. This effect induces a signaling cascade stimulating release of cytochrome c from mitochondria eventually leading to cell death. Nevertheless, the exact mechanism of Orlistat-induced apoptosis is still not perfectly understood and needs to be elucidated. Yang and colleges found additional Orlistat targets (e.g. β-tubulin, GAPDH, heat shock protein 90 ab1, annexin A2 and ribosomal proteins: RPL7a, RPL14 and RPS9) in HepG2 cells (72), which might be causally related to apoptosis. For all these reasons, discovering more targets and/or off targets of Orlistat is significant.

In our study, we mainly focused on the identification of “(phosho)lipolytic” proteomes in cultured cells using activity-based fluorescent probes and the use of these probes for the discovery of Orlistat targets in liver cells (HepG2), adipocytes (3T3-L1) and skin cancer cells (SCC13). The former two cells were chosen as they are useful for studying lipid-

associated disorders. SCC13 cells were included to test the potential of Orlistat as a potential anti-cancer drug. For lipase screening, we used lipophilic phosphonate acid p-nitrophenyl esters that can covalently bind to the nucleophile serine and cysteine in the active site of serine hydrolases, which is a component of the catalytic triad Ser-His-Asp/Glu (73). In contrast to esterases lipases contain a lid which controls the access of substrate at the water/lipid interface. Once the lipase binds to a water/lipid interface the lid opens and the active site is accessible for a hydrophobic substrate (74). We used different fluorescent phosphonate inhibitors, which represent substrate analogues as activity-based probes for (phospho)lipolytic enzymes. They all contain (i) a reactive group, which covalently binds to a target enzyme; (ii) a fluorescent tag as a reporter group, which allows visualization through fluorescence in-gel detection and (iii) a binding group as a recognition site, which is responsible for the selectivity towards certain enzymes. In our studies, NBD and Ethyl-Cy fluorophores have been used for the labeling of the phosphonate inhibitors carrying single hydrophobic chains or glycerophospholipid moieties. A combination of these probes was successfully used to identify lipases, phospholipases and other lipid-related enzymes, e.g. FAS, in HepG2 cells and skin cancer cells. A novel differential method using combination of inhibitors with different dyes was developed to identify targets of pharmacologically interesting drugs (Orlistat) in cultured cells. This new technology enabled us to find many more targets than previously shown and confirm others (FAS) that have already been identified as promising candidates.

1.3 References

1. Birner-Gruenberger, R., A. Hermetter. 2007. Activity-based proteomics of lipolytic enzymes. *Current Drug Discovery Technologies* **4:** 1-11.
2. Yach, D., D. Stuckler, and K. D. Brownell. 2006. Epidemiologic and economic consequences of the global epidemics of obesity and diabetes. *Nat. Med.* **12:** 62-66.
3. Kopelman, P. G., N. Finer. 2001. Reply: Is obesity a disease? *Int. J. Obes.* **25:** 1405-1406.
4. Flier, J. S. 2004. Obesity Wars: Molecular Progress Confronts an Expanding Epidemic. *Cell* **116:** 337-350.
5. Bergman, R. N., G. W. Van Citters, S. D. Mittelman, M. K. Dea, M. Hamilton-Wessler, S. P. Kim, and M. Ellmerer. 2001. Central role of the adipocyte in the metabolic syndrome. *J. Invest. Med.* **49:** 119-126.
6. Arner, P. 2002. Insulin resistance in type 2 diabetes: Role of fatty acids. *Diabetes. Metab. Res.* **18:** S5-S9.
7. Boden, G., G. I. Shulman. 2002. Free fatty acids in obesity and type 2 diabetes: Defining their role in the development of insulin resistance and β-cell dysfunction. *Eur. J. Clin. Invest.* **32:** 14-23.
8. Blaak, E. E. 2003. Fatty acid metabolism in obesity and type 2 diabetes mellitus. *Proc. Nutr. Soc.* **62:** 753-760.
9. Hesselink, M. K. C., M. Mensink, and P. Schrauwen. 2007. Lipotoxicity and mitochondrial dysfunction in type 2 diabetes. *Immunology, Endocrine and Metabolic Agents in Medicinal Chemistry* **7:** 3-17.
10. Unger RH. 1995. Lipotoxicity in the pathogenesis of obesity-dependent NIDDM. Genetic and clinical implications. *Diabetes.* **44:** 863-870.
11. McGarry JD, Dobbins RL. 1999. Fatty acids, lipotoxicity and insulin secretion. *Diabetologia.* **42**: 128-138.

12. Unger RH, Zhou YT. 2001. Lipotoxicity of beta-cells in obesity and in other causes of fatty acid spillover. *Diabetes.* **50** Suppl 1:S118-21.
13. Preiss-Landl, K., Zimmermann, R., Hammerle, G. and Zechner, R. 2002. Lipoprotein lipase: the regulation of tissue specific expression and its role in lipid and energy metabolism. *Curr. Opin. Lipidol.*, **13:** 471-481.
14. Thuren, T. 2000. Hepatic lipase and HDL metabolism. *Curr .Opin. Lipidol.*, **11:** 277-283.
15. McCoy, M.G., Sun, G.S., Marchadier, D., Maugeais, C., Glick, J.M. and Rader, D.J. 2002. Characterization of the lipolytic activity of endothelial lipase. *J. Lipid Res.*, **43:** 921-929.
16. Semeriva, M. and Desnuelle, P. 1979. Pancreatic lipase and colipase. An example of heterogeneous biocatalysis. *Adv. Enzymol. Relat. Areas Mol. Biol.*, **48:** 319-370.
17. Bodmer, M.W., Angal, S., Yarranton, G.T., Harris, T.J.R., Lyons, A., King, D.J., Pieroni, G., Riviere, C., Verger, R. and Lowe, P.A. 1987. Molecular cloning of a human gastric lipase and expression of the enzyme in yeast. *Biochim. Biophys. Acta*, **909:** 237-244.
18. Canaan, S., Roussel, L., Verger, R. and Cambillau, C. 1999. Gastric lipase: crystal structure and activity. *Biochim. Biophys. Acta-Mol. Cell. Biol. Lipids*, **1441:** 197-204.
19. Karlsson, M., Contreras, J.A., Hellman, U., Tornqvist, H. and Holm, C. 1997. cDNA cloning, tissue distribution, and identification of the catalytic triad of monoglyceride lipase. Evolutionary relationship to esterases, lysophospholipases, and haloperoxidases. *J. Biol. Chem.*, **272:** 27218-27223.
20. Kraemer, F.B. and Shen, W.J. 2002. Hormone-sensitive lipase: control of intracellular tri-(di-) acylglycerol and cholesteryl ester hydrolysis. *J. Lipid Res.*, **43:** 1585-1594.
21. Zimmermann, R., Strauss, J.G., Haemmerle, G., Schoiswohl, G., Birner-Gruenberger, R., Riederer, M., Lass, A., Neuberger, G., Eisenhaber, F., Hermetter, A. and Zechner, R. 2004. Fat mobilization in adipose tissue is promoted by adipose triglyceride lipase. *Science,* **306:** 1383-1386.
22. Dolinsky, V.W., Sipione, S., Lehner, R. and Vance, D.E. 2001. The cloning and expression of a murine triacylglycerol hydrolase cDNA and the structure of its corresponding gene. *Biochim. Biophys. Acta*, **1532:** 162-172.

23. Desnuelle, P. 1986. Pancreatic lipase and phospholipase. *Molecular and Cellular Basis of Digestion* 275-296.
24. Carey, M. C., D. M. Small, and C. M. Bliss. 1983. Lipid digestion and absorption. *Annu. Rev. Physiol.* **45:** 651-677.
25. Miled, N., S. Canaan, L. Dupuis, A. Roussel, M. Rivière, F. Carrière, A. De Caro, C. Cambillau, and R. Verger. 2000. Digestive lipases: From three-dimensional structure of physiology. *Biochimie* **82:** 973-986.
26. Miled, N., C. Bussetta, A. De Caro, M. Rivière, L. Berti, and S. Canaan. 2003. Importance of the lid and cap domains for the catalytic activity of gastric lipases. *Comparative Biochemistry and Physiology - B Biochemistry and Molecular Biology* **136:** 131-138.
27. Brockman, H. L. 2000. Kinetic behavior of the pancreatic lipase-colipase-lipid system. *Biochimie* **82:** 987-995.
28. Lairon, D. 1978. Possible roles of bile lipids and colipase in lipase adsorption. *Biochemistry (N. Y.)* **17:** 5263-5269.
29. Borovicka, J., W. Schwizer, C. Mettraux, C. Kreiss, B. Remy, K. Asal, J. B. M. J. Jansen, I. Douchet, R. Verger, and M. Fried. 1997. Regulation of gastric and pancreatic lipase secretion by CCK and cholinergic mechanisms in humans. *American Journal of Physiology - Gastrointestinal and Liver Physiology* **273:** G374-G380.
30. Wang, C. -., J. A. Hartsuck. 1993. Bile salt-activated lipase. A multiple function lipolytic enzyme. *Biochimica et Biophysica Acta - Lipids and Lipid Metabolism* **1166:** 1-19.
31. Ernst J. Schaefer, M.D. Overview of the diagnosis and treatment of lipid disorders.
32. G. Hellige, P.G. Spieckermann, A. Zieglier. Lipoproteins and Atherogenese.
33. Henry J. Pownall. Fatty acid, hyperlipidemia and atherogenesis: a hypothesis.
34. Haemmerle, G., Lass, A., Zimmermann, R., Gorkiewicz, G., Meyer, C., Rozman, J., Heldmaier, G., Maier, R., Theussl, C., Eder, S., Kratky, D., Wagner, E.F., Klingenspor, M., Hoefler, G. and Zechner, R. 2006. Defective lipolysis and altered energy metabolism in mice lacking adipose triglyceride lipase. *Science* **312:** 734-737.

35. Soni KG, Lehner R, Metalnikov P, O'Donnell P, Semache M, Gao W, Ashman K, Pshezhetsky AV, Mitchell GA. 2004.Carboxylesterase 3 (EC 3.1.1.1) is a major adipocyte lipase. *J Biol Chem.* **279:** 40683–40689.

36. Mashima, T., H. Seimiya, and T. Tsuruo. 2009. De novo fatty-acid synthesis and related pathways as molecular targets for cancer therapy. *Br. J. Cancer* **100:** 1369-1372.

37. Uusitupa, M. 1999. New aspects in the management of obesity: Operation and the impact of lipase inhibitors. *Curr. Opin. Lipidol.* **10:** 3-7.

38. Weibel, E. K., P. Hadvary, and E. Hochuli. 1987. Lipstatin, an inhibitor of pancreatic lipase, produced by Streptomyces toxytricini. I. Producing organism, fermentation, isolation and biological activity. *J. Antibiot.* **40:** 1081-1085.

39. Borgstrom, B. 1988. Mode of action of Orlistat: A derivative of the naturally occurring lipase inhibitor lipstatin. *Biochimica et Biophysica Acta - Lipids and Lipid Metabolism* **962:** 308-316.

40. Hadvary, P., H. Lengsfeld, and H. Wolfer. 1988. Inhibition of pancreatic lipase in vitro by the covalent inhibitor Orlistat. *Biochem. J.* **256:** 357-361.

41. Stalder, H., G. Oesterhelt, and B. Borgstrom. 1992. Orlistat: Degradation products produced by human carboxyl-ester lipase. *Helv. Chim. Acta* **75:** 1593-1603.

42. Drahl, C., B. F. Cravatt, and E. J. Sorensen. 2005. Protein-reactive natural products. *Angewandte Chemie - International Edition* **44:** 5788-5809.

43. Denke, M. A. 2001. Connections between obesity and dyslipidaemia. *Curr. Opin. Lipidol.* **12:** 625-628.

44. Zhi, J., A. T. Melia, H. Eggers, R. Joly, and I. H. Patel. 1995. Review of limited systemic absorption of orlistat, a lipase inhibitor, in healthy human volunteers. *J. Clin. Pharmacol.* **35:** 1103-1108.

45. Filippatos, T. D., C. S. Derdemezis, I. F. Gazi, E. S. Nakou, D. P. Mikhailidis, and M. S. Elisaf. 2008. Orlistat-associated adverse effects and drug interactions: A critical review. *Drug Safety* **31:** 53-65.

46. Napier, S., M. Thomas. 2006. 36 Year old man presenting with pancreatitis and a history of recent commencement of orlistat case report. *Nutrition Journal* **5:** .

47. Kim, D. H., E. H. Lee, J. C. Hwang, J. H. Jeung, H. Kim, J. Y. Cheong, S. W. Cho, and Y. B. Kim. 2002. A case of acute cholestatic hepatitis associated with Orlistat. *Taehan Kan Hakhoe chi = The Korean journal of hepatology* **8:** 317-320.

48. Montero, J. L., J. Muntané, E. Fraga, M. Delgado, G. Costán, M. Serrano, J. Padillo, M. De la Mata, and G. Mio. 2001. Orlistat associated subacute hepatic failure [1]. *J. Hepatol.* **34:** 173.

49. Thurairajah, P. H., W. K. Syn, D. A. Neil, D. Stell, and G. Haydon. 2005. Orlistat (Xenical)-induced subacute liver failure. *European journal of gastroenterology & hepatology.* **17:** 1437-1438.

50. Lau, G., C. L. Chan. 2002. Massive hepatocullular necrosis : Was it caused by orlistat? *Medicine, Science and the Law* **42:** 309-312.

51. Athyros, V. G., D. P. Mikhailidis, T. P. Didangelos, O. I. Giouleme, E. N. Liberopoulos, A. Karagiannis, A. I. Kakafika, K. Tziomalos, A. K. Burroughs, and M. S. Elisaf. 2006. Effect of multifactorial treatment on non-alcoholic fatty liver disease in metabolic syndrome: A randomised study. *Curr. Med. Res. Opin.* **22:** 873-883.

52. Diakou, M. C., E. N. Liberopoulos, D. P. Mikhailidis, E. V. Tsianos, A. K. Burroughs, and M. S. Elisaf. 2007. Pharmacological treatment of non-alcoholic steatohepatitis: The current evidence. *Scand. J. Gastroenterol.* **42:** 139-147.

53. Kuhajda, F. P. 2000. Fatty-acid synthase and human cancer: New perspectives on its role in tumor biology. *Nutrition* **16:** 202-208.

54. Weiss, L., G. E. Hoffmann, R. Schreiber, H. Andres, E. Fuchs, E. Körber, and H. J. Kolb. 1986. Fatty-acid biosynthesis in man, a pathway of minor importance. Purification, optimal assay conditions, and organ distribution of fatty-acid synthase. *Biol. Chem. Hoppe-Seyler* **367:** 905-912.

55. Alò, P. L., P. Visca, M. L. Framarino, C. Botti, S. Monaco, V. Sebastiani, D. E. Serpieri, and U. Di Tondo. 2000. Immunohistochemical study of fatty acid synthase in ovarian neoplasms. *Oncol. Rep.* **7:** 1383-1388.

56. Pizer, E. S., C. Jackisch, F. D. Wood, G. R. Pasternack, N. E. Davidson, and F. P. Kuhajda. 1996. Inhibition of fatty acid synthesis induces programmed cell death in human breast cancer cells. *Cancer Res.* **56:** 2745-2747.

57. Pizer, E. S., F. D. Wood, H. S. Heine, F. E. Romantsev, G. R. Pasternack, and F. P. Kuhajda. 1996. Inhibition of fatty acid synthesis delays disease progression in a xenograft model of ovarian cancer. *Cancer Res.* **56:** 1189-1193.

58. Gansler, T. S., W. Hardman III, D. A. Hunt, S. Schaffel, and R. A. Hennigar. 1997. Increased expression of fatty acid synthase (OA-519) in ovarian neoplasms predicts shorter survival. *Hum. Pathol.* **28:** 686-692.

59. Dhanasekaran, S. M., T. R. Barrette, D. Ghosh, R. Shah, S. Varambally, K. Kurachi, K. J. Pienta, M. A. Rubin, and A. M. Chinnaiyan. 2001. Delineation of prognostic biomarkers in prostate cancer. *Nature* **412:** 822-826.

60. Swinnen, J. V., T. Roskams, S. Joniau, H. Van Poppel, R. Oyen, L. Baert, W. Heyns, and G. Verhoeven. 2002. Overexpression of fatty acid synthase is an early and common event in the development of prostate cancer. *International Journal of Cancer* **98:** 19-22.

61. Innocenzi, D., P. L. Alò, A. Balzani, V. Sebastiani, V. Silipo, G. La Torre, G. Ricciardi, C. Bosman, and S. Calvieri. 2003. Fatty acid synthase expression in melanoma. *J. Cutan. Pathol.* **30:** 23-28.

62. Rossi, S., E. Graner, P. Febbo, L. Weinstein, N. Bhattacharya, T. Onody, G. Bubley, S. Balk, and M. Loda. 2003. Fatty acid synthase expression defines distinct molecular signatures in prostate cancer. *Molecular Cancer Research* **1:** 707-715.

63. Takahiro, T., K. Shinichi, and S. Toshimitsu. 2003. Expression of fatty acid synthase as a prognostic indicator in soft tissue sarcomas. *Clinical Cancer Research* **9:** 2204-2212.

64. Visca, P., V. Sebastiani, C. Botti, M. G. Diodoro, R. P. Lasagni, F. Romagnoli, A. Brenna, B. C. De Joannon, R. P. Donnorso, G. Lombardi, and P. L. Alo. 2004. Fatty Acid Synthase (FAS) is a marker of increased risk of recurrence in lung carcinoma. *Anticancer Res.* **24:** 4169-4173.

65. Kapur, P., D. Rakheja, L. C. Roy, and M. P. Hoang. 2005. Fatty acid synthase expression in cutaneous melanocytic neoplasms. *Modern Pathology* **18:** 1107-1112.

66. Van de Sande, T., T. Roskams, E. Lerut, S. Joniau, H. Van Poppel, G. Verhoeven, and J. V. Swinnen. 2005. High-level expression of fatty acid synthase in human prostate cancer tissues is linked to activation and nuclear localization of Akt/PKB. *J. Pathol.* **206:** 214-219.

67. Rossi, S., W. Ou, D. Tang, N. Bhattacharya, A. P. Dei Tos, J. A. Fletcher, and M. Loda. 2006. Gastrointestinal stromal tumours overexpress fatty acid synthase. *J. Pathol.* **209:** 369-375.

68. Dowling, S., J. Cox, and R. J. Cenedella. 2009. Inhibition of fatty acid synthase by orlistat accelerates gastric tumor cell apoptosis in culture and increases survival rates in gastric tumor bearing mice in vivo. *Lipids* **44:** 489-498.

69. Pizer, E. S., F. J. Chrest, J. A. DiGiuseppe, and W. F. Han. 1998. Pharmacological inhibitors of mammalian fatty acid synthase suppress DNA replication and induce apoptosis in tumor cell lines. *Cancer Res.* **58:** 4611-4615.

70. Furuya, Y., S. Akimoto, K. Yasuda, and H. Ito. 1997. Apoptosis of androgen-independent prostate cell line induced by inhibition of fatty acid synthesis. *Anticancer Res.* **17:** 4589-4593.

71. Carvalho, M. A., K. G. Zecchin, F. Seguin, D. C. Bastos, M. Agostini, A. L. C. A. Rangel, S. S. Veiga, H. F. Raposo, H. C. F. Oliveira, M. Loda, R. D. Coletta, and E. Graner. 2008. Fatty acid synthase inhibition with Orlistat promotes apoptosis and reduces cell growth and lymph node metastasis in a mouse melanoma model. *International Journal of Cancer.* **123:** 2557-2565.

72. Yang, P. -., K. Liu, M. H. Ngai, M. J. Lear, M. R. Wenk, and S. Q. Yao. 2010. Activity-based proteome profiling of potential cellular targets of orlistat - An FDA-approved drug with anti-tumor activities. *J. Am. Chem. Soc.* **132:** 656-666.

73. Cygler, M., P. Grochulski, R. J. Kazlauskas, J. D. Schrag, F. Bouthillier, B. Rubin, A. N. Serreqi, and A. K. Gupta. 1994. A structural basis for the chiral preference of lipases. *J. Am. Chem. Soc.* **116:** 3180-3186.

74. Jaeger, K. -., B. W. Dijkstra, and M. T. Reetz. 1999. Bacterial biocatalysts: Molecular biology, three-dimensional structures, and biotechnological applications of lipases. *Annual Review of Microbiology* **53:** 315-351.

Chapter 2

Phosphonate probes for activity-based screening of (phospho)lipolytic enzymes

Bojana Stojčić[1], Gerald Rechberger[2], Manfred Kollroser[3]and Albin Hermetter[1]

[1] Institute of Biochemistry, Graz University of Technology, Austria

[2] Institute of Molecular Bioscience, University of Graz, Austria

[3] Institute of Forensic Medicine, University of Graz, Austria

2.1 Abbreviations

ABP	Activity-based probe
DMEM	Dulbecco's Modified Eagle Medium
DMSO	Dimethyl Sulfoxide
FCS	Fetal Calf Serum
GIVB	Group IVB
HPLC	High pressure liquid chromatography
NBD	Nitrobenzo-2-oxa-1,3-diazole
PAFAH	Platelet-activating factor acetylhydrolase
PBS	Phosphate buffered saline
Pen/Strep	Penicillin/ Streptomycin
PLA_2	Phospholipase A_2
QTOF	Coupled to quadrupole time-of-flight
RuBPS	Ruthenium-tris-bathophenanthrolinedisulfonate tetrasodium salt
SDS-PAGE	Sodium dodecyl sulfate - polyacrylamide gel electrophoresis
UPLC	Ultra-performance liquid chromatography

2.2 Abstract

Fluorescently labeled and lipophilic p-nitrophenyl phosphonate esters were developed as suicide inhibitors for the selective detection of (phospho)lipolytic enzymes. These activity-based probes (ABPs) are substrate analogous compounds that covalently react with serine (lipid) hydrolases. They preferentially label active (phospho)lipolytic proteins in complex protein mixtures. After fluorescence detection, the tagged enzyme candidates can be isolated and identified by MS/MS analysis. In this study, we used phospholipid and fatty acid ester analogues as ABPs. We characterized the reaction of these lipids with reference phospholipases and used them for functional proteomic analysis of lipolytic enzymes in cultured macrophages. The identified proteins were lipases, phospholipases, lipid transferases and lipid-unrelated proteins.

2.3 Introduction

Maintenance of energy homeostasis, signal transduction and the development of lipid-associated disorders (obesity, atherosclerosis) are tightly associated with the activities of (phospho)lipolytic enzymes (1, 2). Determination of (phospho)lipolytic enzymes and in particular their activities is a difficult task, since these proteins act on water-lipid interfaces and therefore depend not only on the structure of the substrate but also substrate solubilization. For the selective detection of such enzymes fluorescently labeled lipophilic p-nitrophenyl phosphonate esters were developed as suicide inhibitors of lipases and esterases according (3-6). These activity-based probes (ABPs) are substrate analogous compounds that covalently react with serine (lipid) hydrolases (7-13). They preferentially labeled active (phospho)lipolytic proteins in complex protein mixtures and are therefore useful tools of functional proteomic (5). Identified proteins can be further studied with respect to substrate selectivity and biological function using appropriate *in vitro* and *in vivo* methodology. The catalytic mechanism of acyl esters hydrolysis is frequently due to the nucleophile attack of serine in the active site of an enzyme, which in most cases is part of catalytic triade together with histidine and aspartate. This is the first reaction step of catalytic mechanism leading to formation of a tetrahedral transition state (intermediate state). The intermediate state is cleaved leading in release of free fatty acid, the alcohol component and the nucleophilic serine (3). Even though many serine hydrolases show strong structural and sequential similarity (14-16), their substrate selectivity may largely differ (17, 18). Phosphonate inhibitors irreversibly and specifically react with serine hydrolases by formation of stable lipid-protein complexes freezing the reaction at the initial tetrahedral transition state (3, 19). If the inhibitor carries a fluorophore, this allows for detection of the labeled protein in an electrophoresis gel and further analysis by mass

spectrometry (5). This method is very sensitive and can be used for quantification of moles active enzymes since the labeling is stoichiometric (protein/label 1/1) (8-10, 13).

Here we report on the development and application of five activity-based probes. The focus of our study was on detection of phospholipases next to other lipolytic proteins. The respective probes were NBD- and Cy- tagged phosphonic acid esters with single hydrophobic chains or diacylglycerophospholipid residues as amphipathic moieties. Here we characterized the reaction of these lipids with reference phospholipases and used them for functional proteomic analysis of lipolytic enzymes in cultured macrophages.

2.4 Experimental procedures

2.4.1 Cell Culture

The macrophage-like cells RAW 264.7 (ATCC No. TIB-71, American Type Culture collection, Rockville, MD, USA) were grown in DMEM, high glucose (4,5 g/L), 25 mM HEPES from Invitrogen (Lofer, Austria) supplemented with 10% FCS and 1% Pen/Strep (100 U).

The COS 7 cell line (ATCC No. CRL-1651, American Type Culture collection, Rockville, MD, USA) was a gift from Prof. Dr. Rudolf Zechner (Institute of Molecular Bioscience, Karl Franz University of Graz, Austria). This cell line is derived from the kidney of the African Green Monkey, *Cercopithecus aethiops*. It was immortalized by transformation of an origin-defective mutant of SV40 in CV-1 simian cells. Cells were grown in DMEM low glucose (1 g/L), 25 mM HEPES and L-Glutamine from PAA (Pasching, Austria) supplemented with 10% FCS and 1% Pen/Strep (100 U).

Both cell lines were grown under an atmosphere containing 5% CO_2 at 37°C.

2.4.2 Preparation of cell lysates

Cells were scraped and sonicated in 50 mM Tris/HCl buffer containing protease inhibitors (20 µg/ml leupeptin, 2 µg/ml antipain and 1 µg/ml pepstatin) at 40 W for 20 seconds. Cell debris was removed by centrifugation at 1.000 x g at 4°C for 15 minutes. Protein concentration in the supernatant was determined using the Bio-Rad protein assay based on the Bradford method (20).

2.4.3 Preparation and handling of fluorescent inhibitors

The chemical structures of the five fluorescent p-nitrophenyl phosphonate inhibitors used in this study are depicted in Figure 2.1. Compounds A were synthesized as described by Morak et al. (4). Compound B was prepared as described for the preparation of fluorescent organo-phosphonate (3), but using lysophosphatidylcholines as an alcohol component (A. Hermetter and E. Zenzmeier, unpublished). Compound C was synthesized according to Oskolova et al. (6).

For labeling of proteins, 150 µl cell lysate containing 150 µg protein were incubated with fluorescent inhibitors as follows: 1,5 µl of 100 mM Triton X-100 in $CHCl_3$ (final sample concentration: 1 mM) and a solution of 1,5 nmol and 7,5 nmol of activity-based probes (Ethyl-Cy-tagged inhibitors; NBD-PC and NBD-HE-HP, respectively) in $CHCl_3$ (final concentration: 10 µM and 50 µM, respectively) were mixed. The organic solvent was removed under a stream of argon. Cell lysates (1 µg protein/µl) were incubated with the activity-based probes at 37°C and 550 rpm for 2h30. Protein was precipitated by addition of 500 µl acetone and the samples were stored overnight at -20°C. Precipitated protein was collected by centrifugation at 14.000 x g at 4°C for 20 min and resuspended in 1-D SDS-PAGE sample buffer (20 mM KH_2PO_4, 6 mM EDTA, 6 % SDS, 10 % glycine and 0,05 % bromophenol blue, pH 6,8 and 20 µl/ml mercaptoethanol). Samples were preheated for 5 minutes at 95°C prior to loading onto the gel.

For 2-D gel electrophoresis, samples were diluted in 2-D buffer (7 M urea, 2 M thiourea, 4% CHAPS, 2% Pharmalyte and 20 mg/ml DTT) and preheated at 37°C for 30 minutes.

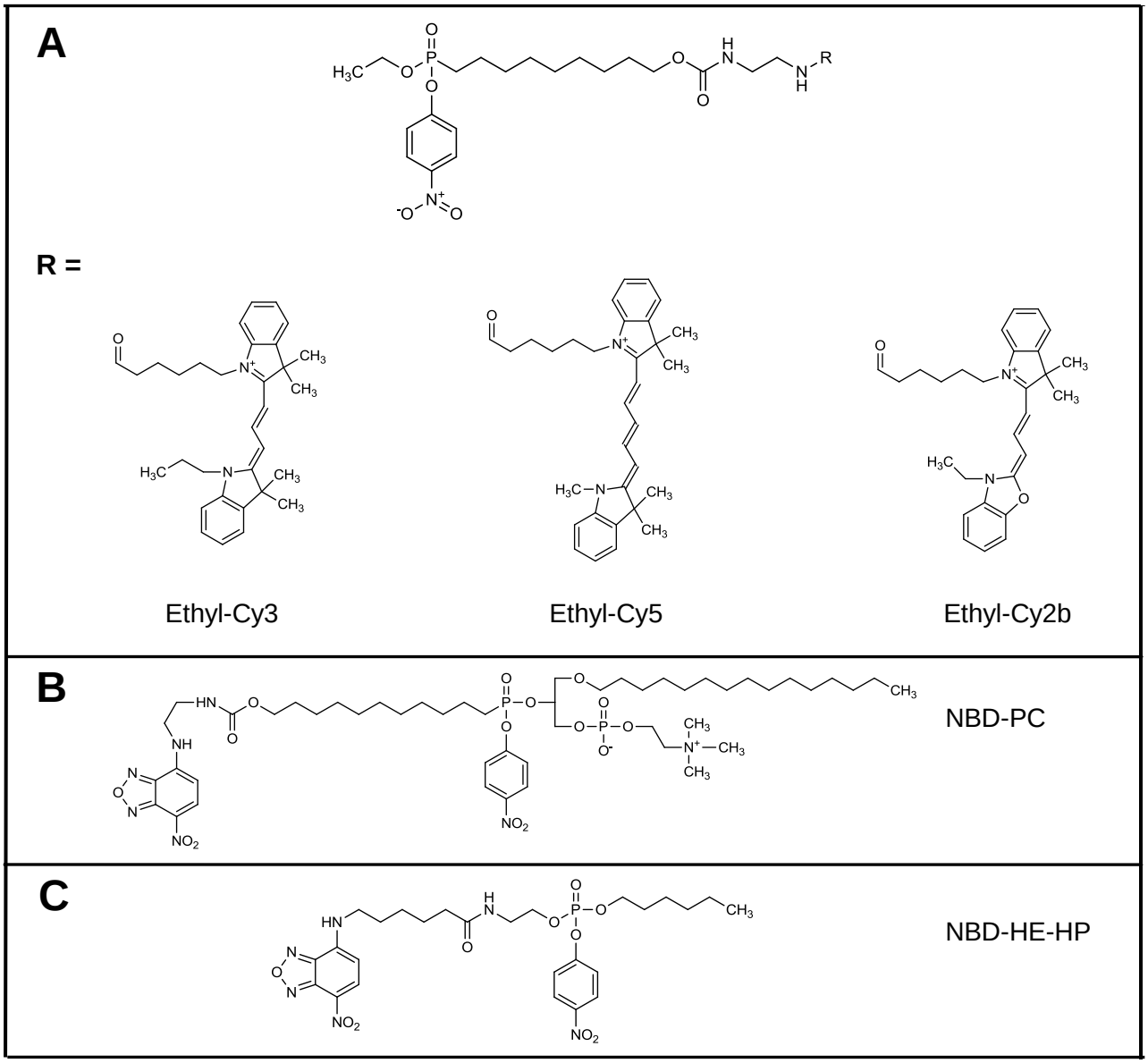

Figure 2. 1 Chemical structures of fluorescent p-nitrophenyl phosphonate probes: A: Ethyl-Cy- tagged phosphonic acid ester (Ethyl-Cy3, -Cy5 and -Cy2b); **B:** 1-O-Hexadecyl-2-NBD-undecylphosphonyl-sn-glycero-3-phosphocholine (NBD-PC) and **C:** NBD-HE-HP.

2.4.4 Transient expression of phospholipase A_2 group IVB and platelet-activating factor acetylhydrolase in COS 7 cells

Cells were seeded into 60 cm^2 Petri plates one day prior to use. The mouse constructs of phospholipases A_2: group IVB (gi|167900426) and platelet-activating factor acetylhydrolase (gi|225579136) were cloned in pcDNA3.1 and pcDNA3.1-CT-GFP. The

primers were Not I forward and Nhe I reverse. TurboFect^{TM} reagent (Fermentas , R0531) was used for the transfection of COS 7 cells. Briefly, 6 µg of DNA construct and 12 µl of TurboFect^{TM} reagent (ratio µg DNA / µl TurboFect = 1 / 2) was added in 1 ml of Optimem medium (supplemented with 1% Pen/Strep) and incubated at room temperature for 20 minutes followed by addition to the cells. Prior to vector addition, the cells were aspirated and 5 ml fresh culture medium was added. For transient enzyme expression, cells were incubated with the vectors at 37°C for 48 h. The enzyme-GFP fusion proteins were directly observed with a fluorescence microscope. The enzymes expressed without GFP tag were labeled with Ethyl-Cy-tagged and NBD-tagged inhibitors for isolation and MS identification.

2.4.5 Microscopy of PLA_2 - GFP fusion proteins

Prior to the transfection with pcDNA3.1-CT-GFP constructs, COS 7 cells were seeded into chamber slides (1 ml volume). 100 µl of PLA_2 constructs (prepared as described above) was added to 400 µl culture medium per chamber slide. Transfected cells were observed with an inverted fluorescence microscope Zeiss Axiovert 35 (excitation filter BP 450-490 nm, emission filter LP 520 nm, Xenon XBO lamp as the light source). The excitation and emission wavelengths of green fluorescence protein (GFP) are 395 nm / 480 nm and 509 nm, respectively.

2.4.6 One dimensional gel electrophoresis

Proteins were separated using one dimensional gel electrophoresis according to the method of Fling and Gregerson (21). We used 1x running buffer which contained: 3 g/L Tris, 0.334 g/L EDTA, 5 g/L SDS and 14,2 g/L glycine) in ddH_2O. Proteins were separated at constant current (10 mA per gel) for the first 15 minutes followed by 20 mA per gel for an hour using a Bio-Rad Mini PROTEAN 3 apparatus at 4°C.

2.4.7 Two dimension gel electrophoresis

2-D gel electrophoresis was preformed as described in (4). Briefly, for the first dimension 500 µg protein diluted in 2-D buffer was separated by isoelectric focusing in 18 cm immobilized nonlinear pH 3-10 strips (Immobiline^{TM} Dry Strip Gel strips; GE Healthcare, Germany) using Multiphor II (GE Healthcare, Germany). A discontinuous voltage gradient was used starting at 0 V. It increased to 3500 V during the following 1.5 h and was held at this level for another 9 h.

In the second dimension, proteins were separated by SDS-PAGE on 18 cm gels (10% SDS) at 100 V for 30 minutes and 200 V for 7 h.

2.4.8 Fluorescence detection of labeled proteins in electrophoresis gels

Gels were fixed in fixing solution (7% acetic acid and 10% ethanol) for at least 30 minutes and scanned at a resolution of 100 µm using a Bio-Rad Molecular Imager^{TM} FX Pro Plus. Fluorescence detection was carried out at different excitation wavelengths (488 nm, 488 nm, 532 nm and 635 nm) and emission wavelengths (530 nm, 530 nm, 555 nm and 695 nm) for NBD, Cy2b, Cy3 and Cy5, respectively.

Proteins were visualized after staining with Sypro ruby^{TM} solution. The staining solution was obtained after dilution of 100 µl of aqueous RuBPS stock solution (20 mM) in one liter of 20% Ethanol in ddH_2O. Gels were stained with Sypro ruby^{TM} solution for at least 2 h and incubated in fixing solution for at least 2 h. Sypro ruby^{TM} fluorescence was scanned at emission and excitation wavelengths of 605 nm and 488 nm, respectively.

2.4.9 LC-MS/MS analysis of target proteins

For the identification, protein bands or spots were excised from gels and tryptically digested according to the Method by Shevchenko et al. (22).

Peptide extracts were dissolved in 0.1% formic acid and separated by nano-HPLC (FAMOS^{TM} autosampler, SWITHOS^{TM} loading system, and ULTIMATE^{TM} dual gradientsystem system; LC-Packings, Amsterdam, The Netherlands) as described in (1), but using the following solvent gradient: solvent A: water, 0.3% formic acid; solvent B: acetonitrile/water 80/20 (v/v), 0.3% formic acid; 0 to 5 min: 4% B, after 40 min 55% B, then for 5 min 90% B, and 47 min reequilibration at 4% B. The samples were ionized in a Finnigan nano-ESI source equipped with NanoSpray tips (PicTip^{TM} Emitter; New Objective, Woburn, MA) and analyzed in a Thermo-Finnigan LTQ linear ion trap mass spectrometer (Thermo, San Jose, CA).

The MS/MS data were analyzed by searching the NCBI non redundant public database using SpectrumMill Rev A.03.03.084 SR4 software.

2.5 Results

In this study we report on the development and application of fluorescently tagged inhibitors (Figure 2.1) as activity-based probes (ABPs) for lipolytic enzymes. These compounds selectively detect active enzyme components containing nucleophilic serine or cysteine residues in an active site of e.g. (phospho)lipases and (thio)esterases.

Figure 2.2 illustrates the structure of ABPs and the mechanism of their activities. ABPs essentially contain three groups: p-nitrophenyl phosphonate ester residue as a reactive group; recognition element as a binding group and a fluorophore as a reporter group.

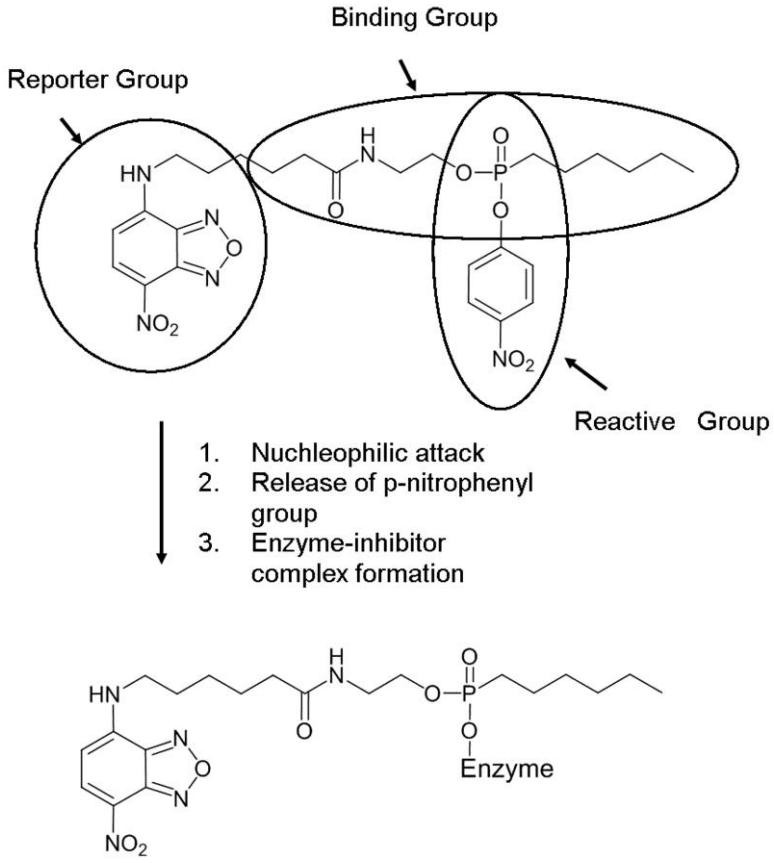

Figure 2. 2 The mechanism of enzyme labeling by activity-based probes. Serine/cysteine hydrolases irreversibly and stoichiometrically bind to an activity-based probes and form stable enzyme-inhibitor complex.

Firstly, the reactive group is responsible for formation of an irreversible enzyme-inhibitor complex due to covalent binding with nucleophilic serine and/or cysteine. As a consequence, a stable lipid-protein complex is formed which remains stable during SDS-gel electrophoresis. Secondly, the fluorescent group allows for the detection of lipid-protein complex in a gel. It can be visualized using fluorescence imager after separation and isolated for identification (5). Notably, structure and polarity of the fluorophores residues could slightly modify the binding to an enzyme. Lastly, the recognition group renders the inhibitor selectivity/specificity for the target enzymes. An important step of an enzyme-inhibitor complex formation is the solubilization of the inhibitors, which is accomplished by addition of the detergent Triton X 100 (1 mM) (4).

In order to screen all five ABPs listed in Figure 2.1 for phospholipases A_2 selectivity we used recombinant phospholipases GIVB and PAFAH. For this purpose, the PLA_2 were transiently expressed in COS 7 cells. Cell lysates were collected after 48 h and incubated with a fluorescent inhibitor. The protein was precipitated, separated by one dimensional gel electrophoresis and imaged with laser scanner (Figures 2.3 and 2.4).

Figure 2.3 shows the fluorescence patterns of both PLA_2 constructs which were labeled with Ethyl-Cy3, -Cy5 and -Cy2b inhibitors. Both, PLA_2GIVB (panel A) and PAFAH (panel C) could be detected in-gel at the expected molecular weights. Several other proteins of the cell lysate were also stained but were not identified. For comparison, panels B and D show the corresponding total protein stains with Sypro ruby^{TM}.

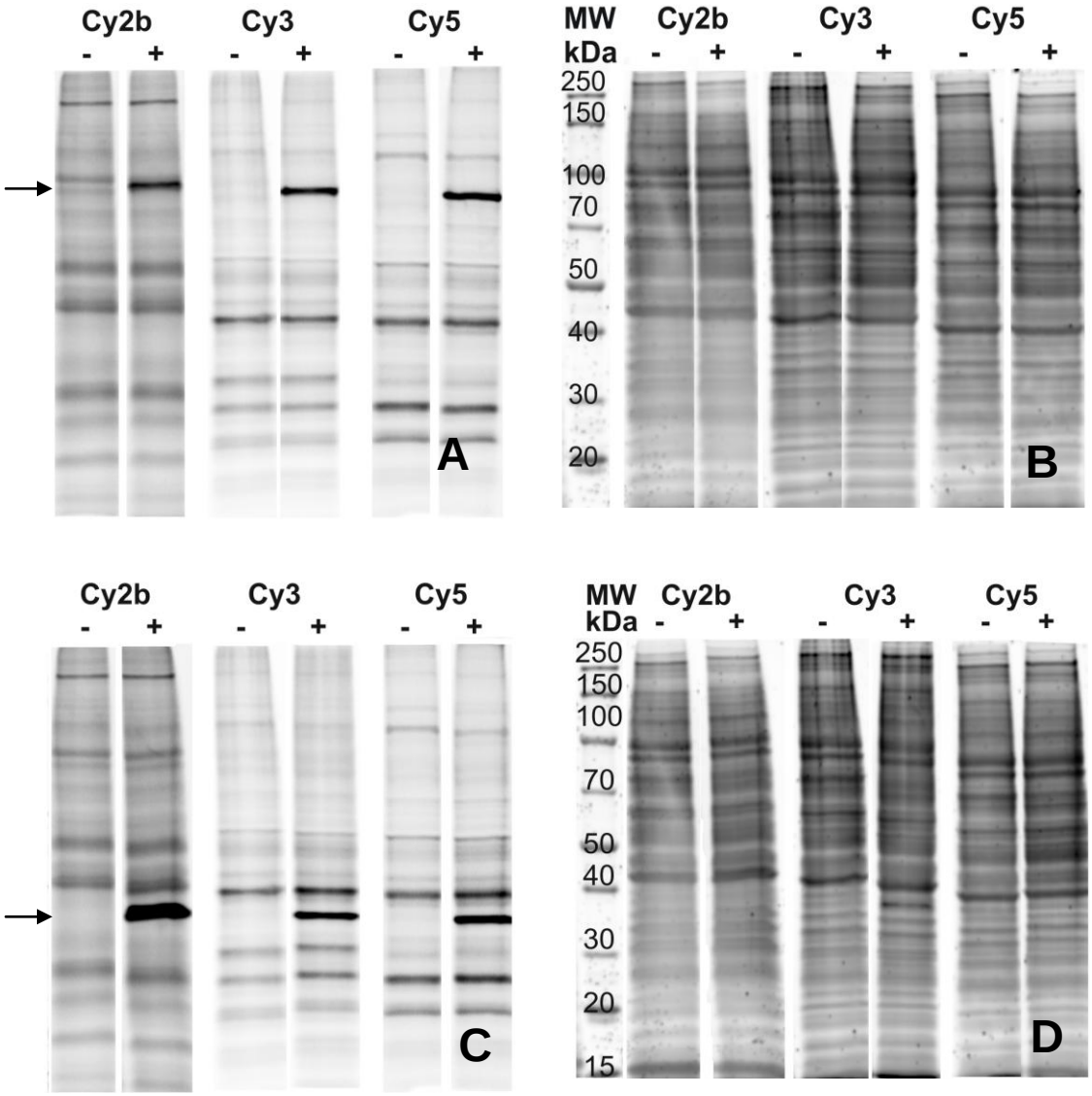

Figure 2. 3 Detection of recombinant phospholipases A_2 (PLA_2) with Ethyl-Cy-tagged inhibitors: group IVB (GIVB) and platelet-activating factor acetylhydrolase (PAFAH). COS 7 cell lysates containing transiently expressed PLA_2- constructs (GIVB and PAF-AH) (+) and the void vector (control (-)) were labeled with 10 µM Ethyl-Cy3, -Cy5- and -Cy2b -tagged inhibitors. After labeling, proteins were precipitated and separated by one-dimensional gel electrophoresis. Gels were scanned at a resolution of 100 µm using Bio-Rad Molecular Imager™ FX Pro Plus. Fluorescence detection was preformed at different excitation wavelengths (488 nm, 488 nm, 532 nm and 635 nm) and emission wavelengths (530 nm, 530 nm, 555 nm and 695 nm) for NBD, Cy2b, Cy3 and Cy5, respectively. Inhibitor fluorescence: PLA_2-GIVB (A) and PAFAH (C). Total protein stain with Sypro ruby™: PLA_2-GIVB (B) and PAFAH (D). The overexpressed enzymes were found at molecular weight ~89 kDa for PLA_2GIVB (A) and ~43 kDa for PAFAH (C).

Figure 2.4 shows the fluorescent complexes of PLA_2GIVB with NBD-PC (panel A) and NBD-HE-HP (panel B). Again, fluorescent band corresponding to the expected molecular weights of PLA_2GIVB (~89 kDa) was seen. In addition several other targets were detected in agreement with previous statement. However, NBD-PC reacted with less enzymes in the cell lysate compared to NBD-HE-HP pointing to higher selectivity of NBD-PC towards PLA_2.

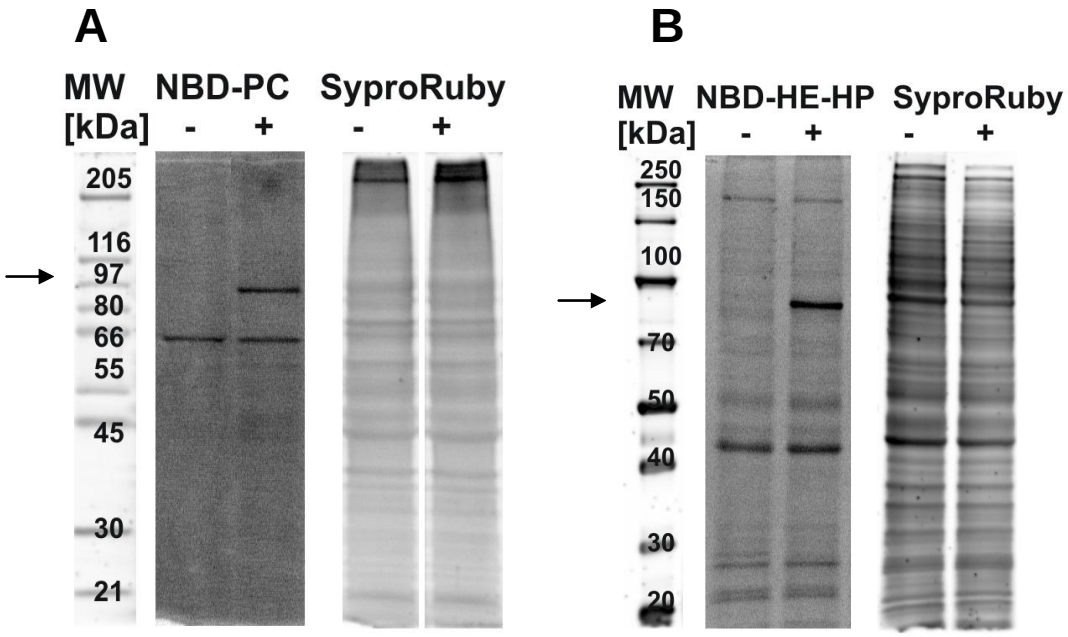

Figure 2. 4 Fluorescence detection of transiently expressed PLA_2 - GIVB in COS 7 cells after tagging with NBD-labeled inhibitors (NBD-PC and NBD-HE-HP). PLA_2GIV4 was expressed in COS 7 cells, followed by labeling with 50 µM NBD-PC or 50 µM NBD-HE-HP. Both inhibitors were solubilized with 1 mM Triton X-100 prior to incubation with cell lysates. Cell lysates from transfected (+) and non transfected (-) COS 7 cells were incubated with NBD-PC (A) or NBD-HE-HP (B) for 2h30. The fluorescence images of both inhibitors show an overexpressed protein at the expected molecular weight ~89 kDa. Total proteins were stained with Sypro ruby™.

The putative PLA_2GIVB (see arrow) shown in Figure 2.4 was cut out, tryptically digested and analyzed by mass spectrometry. The identified enzyme was phospholipase A_2, group

IVB (cytosolic). NCBI accession number: 220941523; molecular weight: 114,55 kDa; identified peptides: 10; amino acid coverage (%): 10.

To visualize and detect PLA_2GIVB and PAFAH in live cells, we expressed a fusion protein of the enzymes with green fluorescent protein. Figure 2.5 shows fluorescence micrographs of COS 7 cells transfection. The fluorescently tagged enzymes localize intracellularly and are bound at least in part in membrane structures.

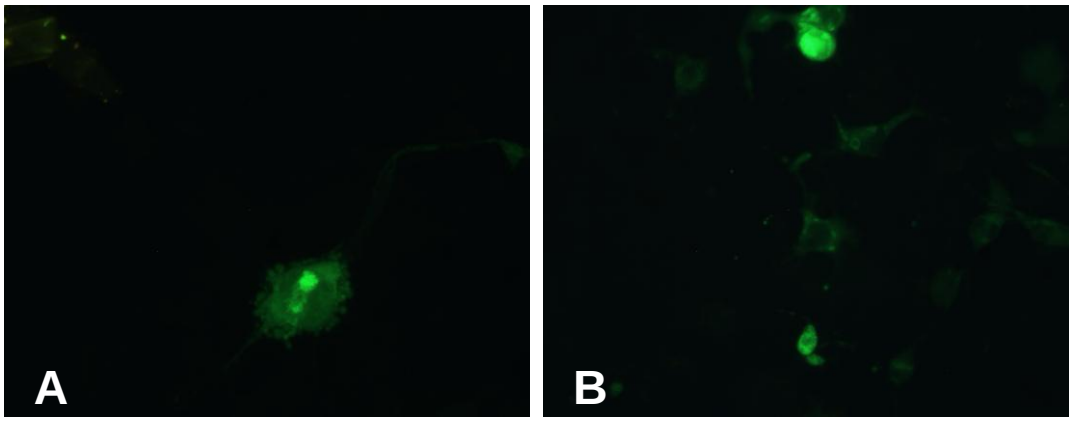

Figure 2. 5 Fluorescence microscopic images of GFP- tagged phospholipases (PLA_2GIVB and -PAFAH) in COS 7 cells. The emission of green fluorescence protein (GFP) (excitation at 395 nm / 480 nm and emission at 509 nm) was detected with excitation filter BP 450-490 nm, emission filter LP 520 nm and Xenon XBO lamp as the light source. **A:** Fluorescence image of GFP- PLA_2 GIVB, **B:** Fluorescence image of GFP- PAFAH.

Finally, the ABPs Ethyl-Cy5 and NBD-PC were used for detection of (phospho)lipases and esterases in lysates of mouse RAW 264.7 cells. Ethyl-Cy5 was chosen, because of its good sensitivity and the low fluorescence background in electrophoresis gel. Panels A and B of Figure 2.6 shows the Ethyl-Cy5-tagged proteins after separation by one and two dimensional gel electrophoresis, respectively. Panel C shows the fluorescent pattern of proteins labeled with the novel inhibitor NBD-PC. As a consequence of their largely different chemical structures (see Figure 2.1) Ethyl-Cy5 and NBD-PC still stained mostly

the same protein bands in the same cell lysates. However staining with the Cy dyes was more sensitive.

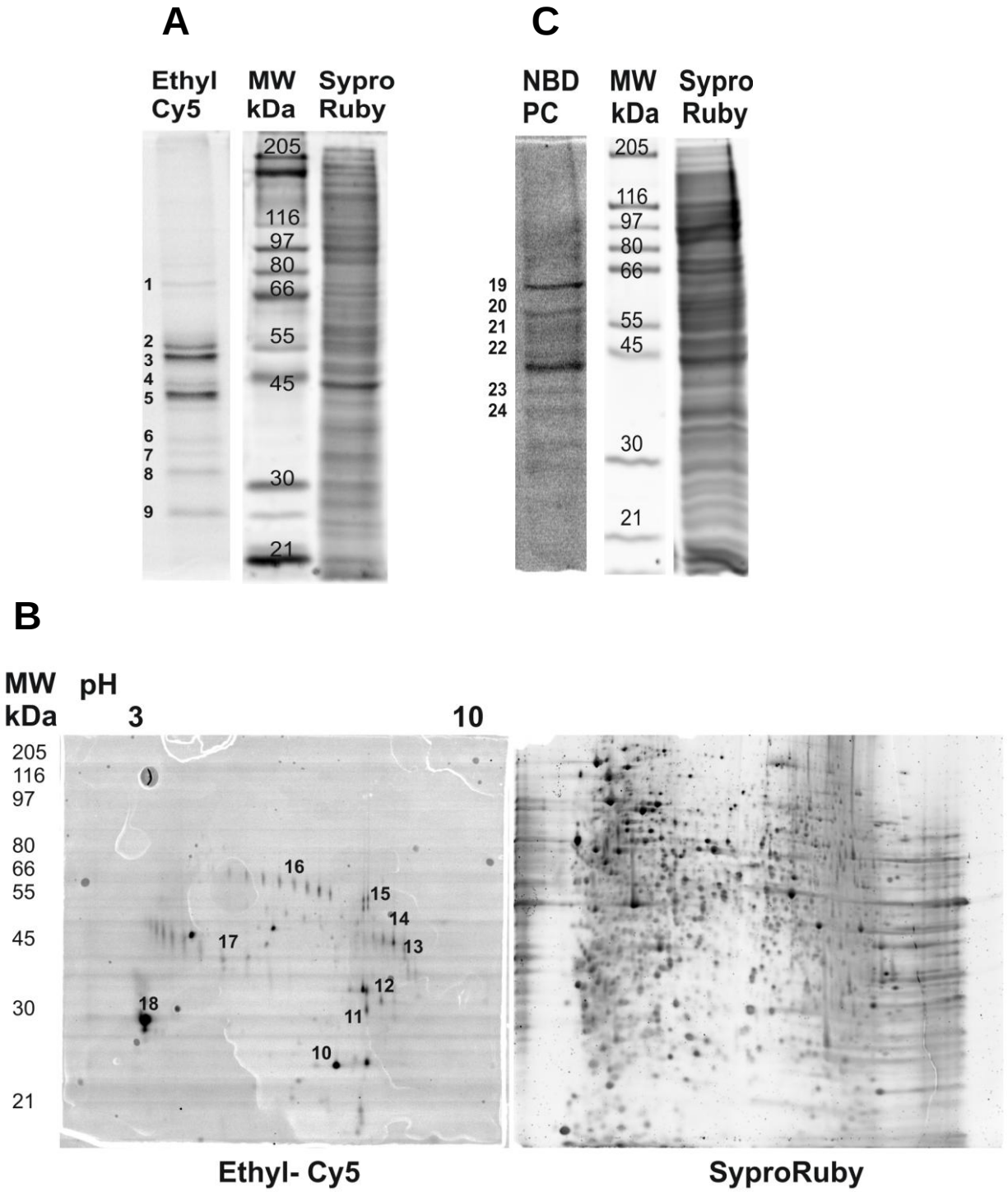

Figure 2. 6 Lipolytic proteomes of murine RAW 264.7 cells. Cell lysates were labeled with Ethyl-Cy5 or NBD-PC inhibitor. Protein was precipitated and separated by one and two dimensional gel electrophoresis. Gels were scanned at a resolution of 100 µm by Bio-Rad Molecular Imager^{TM} FX Pro Plus. Excitation: 488

nm, 488 nm and 635 nm; and the emission: 530 nm, 605 nm and 695 nm for NBD, Sypro ruby™ and Cy5 respectively. Detected spots were cut out, tryptically digested and analyzed with LC- MS/MS. Protein targets were identified using public databases. Ethyl-Cy5 labeled proteins after one-dimensional (A) and two-dimensional (B) gel electrophoresis. C) NBD-PC-labeled proteins after one-dimensional gel electrophoresis. Sypro ruby™ was used for total protein staining. Bands and spots marked from 1 through 24 correspond to target proteins listed in Table 2.1.

This observation was confirmed by MS analysis (Table 2.1). For this purpose, detected bands and spots shown in Figure 2.6 were excised, tryptically digested and analyzed by LC-MS/MS. The following group of proteins were found; Lipid hydrolases: phospholipases A-2-activating protein, neutral cholesterol ester hydrolase 1, alpha-enolase, cytosolic acyl coenzyme A thioester hydrolase, 3-ketoacyl-CoA thiolase (mitochondrial), 3-ketoacyl-CoA thiolase B (peroxisomal), serum paraoxonase (PON3), acyl-CoA thioesterase 2 (mitochondrial), esterase D, lysophospholipase 1 and 2, peroxiredoxin 6 (acidic calcium-independent phospholipases A2), acetyl-CoA acyltransferase 1 precursor, platelet-activating factor acetyl hydrolase (isoform 1b subunit 1); Proteases: adenosylhomocysteinase, cathepsin D, cathepsin D precursor, cathepsin B preprotein, cathepsin S; Proteins unrelated to both: fatty-acyl-CoA reductase 1, tubulin beta-5 chain, glyceraldehydes-3-phosphate dehydrogenase, peroxiredoxin-1, glutathione S-transferase Mu 1, protein DJ-1, protein disulfide-isomerase A3, disulfide-isomerase A4, disulfide-isomerase A6, prolyl 4 hydroxylase (beta polypeptide precursor), succinate dehydrogenase, tyrosine-protein phosphatase non-receptor type 1.

No	Name	NCBI No	MW [kDa]	pI	Id. Pep.	% AA Coverage
			Ethyl-Cy5 1-D PAGE			
1	Phospholipase A-2-activating protein	108935869	87,23	5,82	9	13
2	Neutral cholesterol ester hydrolase 1 (Kiaa1363)	50510901	47,08	6,90	4	13
3	Alpha-enolase	70794816	47,14	6,37	3	9
	Fatty acyl-CoA reductase 1	68448551	59,43	9,26	4	8
	Tubulin beta-5 chain	74141821	49,69	4,82	24	70
4	Adenosylhomocysteinase	74142455	47,78	6,03	10	28
	Cathepsin D	74220304	44,96	6,71	11	36
5	Cytosolic acyl coenzyme A thioester hydrolase	28376965	42,53	8,90	3	9
	3-ketoacyl-CoA thiolase, mitochondrial	73919875	41,85	8,33	10	34
	Serum paraoxonase (PON 3)	27370510	39,35	5,44	5	18
	Acyl-coenzyme A thioesterase 2, mitochondrial	12229867	49,65	6,91	4	10
	Cathepsin D precursor	74151850	45,02	6,51	4	11
6	Cathepsin B preprotein	74213457	37,32	5,65	5	15
7	Esterase D	12846304	34,9	8,51	8	40
	Cathepsin B preprotein	74213457	37,32	5,65	8	32
8	Cathepsin S	74214026	38,86	6,75	4	15
	Glyceraldehyde-3-phosphate dehydrogenase	74194852	35,84	8,43	2	8
9	Lysophospholipase1	71059731	24,68	5,76	4	20
	Lysophospholipase2	7242156	24,79	6,75	3	10
	Peroxiredoxin-6	6671549	24,82	5,98	8	44
	Glutathione S-transferase Mu 1	6754084	25,97	7,72	2	9
	Protein DJ-1	74212240	20,02	6,32	10	68
	Peroxiredoxin-1	12846314	22,23	8,26	8	37
			Ethyl-Cy5 2-D PAGE			
10	Lysophospholipase1 protein	71059731	24,68	5,76	1	5
11	Esterase D	12846304	34,9	8,51	2	7
12	Glyceraldehyde-3-phosphate dehydrogenase	74194852	35,84	8,43	3	12
13	3-ketoacyl-CoA thiolase B, peroxisomal	22122797	43,99	8,82	4	13
	Acetyl- CoA acyltransferase 1 precursor	74226209	43,99	8,58	2	8
14	3-ketoacyl-CoA thiolase, mitochondrial	73919875	41,85	8,33	9	30
15	Platelet-activating factor acetylhydrolase, isoform 1b, subunit 1	74204167	46,80	6,97	1	3
16	Protein disulfide-isomerase A3	112293264	56,67	5,88	2	4
17	Alpha-enolase	70794816	47,14	6,37	8	22
18	Prolyl 4 hydroxylase, beta polypeptide precursor	74220649	57,10	4,77	9	20
			NBD-PC 1-D PAGE			
19	Protein disulfide-isomerase A4	119531	71,97	5,13	19	30
	Succinate dehydrogenase	74219241	72,61	7,06	6	11
20	Protein disulfide-isomerase A3	112293264	56,67	5,88	16	39
21	Neutral cholesterol ester hydrolase 1	50510901	47,09	6,90	5	14
	Protein disulfide-isomerase A6	60502437	48,65	5,05	6	19
22	Alpha-enolase	70794816	47,14	6,37	20	66
	Tyrosine-protein phosphatase non-receptor type 1	133505845	49,59	5,78	3	8
	Adenosylhomocysteinase	74142455	47,78	6,03	10	33
23	Cytosolic acyl coenzyme A thioester hydrolase	28376965	42,53	8,9	2	5
	Acetyl- CoA acyltransferase 1 precursor	74226209	43,99	8,58	4	16
24	Esterase D	12846304	34,90	8,51	7	37

Table 2. 1 (Phospho)lipolytic and esterolytic proteomes of murine RAW 264.7 cells. Active serine hydrolases and other nucleophilic proteins were labeled with fluorescent phosphonate probes (Ethyl-Cy5 and NBD-PC) and separated by 1-D and 2-D PAGE (see Figure 2.6). The proteins were tryptically digested, analyzed by nano-HPLC-MS/MS and identified using public databases.

2.6 Discussion

We report on the detection of active enzymes containing nucleophilic serine or cysteine residue in an active site of complex biological samples using different fluorescent phosphonic acid esters as ABPs, Figure 2.1. These fluorescent lipids contain p-nitrophenyl phosphonate ester residue as reactive group, a recognition element as binding group and a fluorescent tag as a reporter group, Figure 2.2.

The ABPs listed in Figure 2.1 contain the same reactive groups, but differ with respect to binding and fluorescent groups. The fluorophores were nitrobenzo-2-oxa-1,3-diazole (NBD) and cyanine dyes (Cy2b, Cy3 and Cy5). NBD is widely used and is a cheap fluorophore. It can easily be attached to the acyl group of a lipid (23). The Cy-inhibitors are chosen because of their high sensitivity and good spectral separation of their signals and storage in a multichannel read out. These fluorophores as reporter tags were carefully selected in order to minimize interferences with target proteins (4).

Recombinant PLA_2-GIVB and PAFAH for transiently expression in COS 7 cells were used as reference enzymes for detection with ABPs. These two phospholipases A_2 preferably remove short *sn2* chains from glycerophospholipids. The overexpressed enzymes reacted with all the above mentioned inhibitors.

Figure 2.3 illustrates the detection of the overexpressed phospholipases PLA_2-GIVB and PAFAH in COS 7 cell lysates, with Ethyl-Cy-tagged inhibitors. These ABPs only differ in the fluorescent tag but exhibit similar reactivity. The structures and polarities of Cy3 and Cy5 slightly differ compared to Cy2b (4) (Figure 2.3 panels A and C) leading to slightly different protein mobility in electrophoresis. Nevertheless, all three ABPs carrying different fluorescent tags are similar enough to warrant comparison of two proteins in one

electrophoresis gel by differential activity-based gel electrophoresis (see chapters 3 and 4 of this thesis).

Overexpressed phospholipase PLA_2-GIVB was also labeled with NBD-PC (Figure 2.4, A) and NBD-HE-PE (Figure 2.4, B) in COS 7 cell lysates. These fluorescent analogues largely differed in their binding group but contained the same fluorophores.

NBD- and Ethyl-Cy-tagged inhibitors labeled a large number of proteins. The lack of selectivity could be due to short alkylphosphonyl chains (binding groups), their small size and low hydrophobicity (Figure 2.3, A and C; Figure 2.4, B) (3). Many more enzymes are labeled by these probes compared to the fluorescent NBD-PC. The latter compound contains a glycerol(phospho)lipid backbone (binding group). In *sn2*- position it is linked to an NBD- alkylphosphonyl chain. Due to its phospholipid analogous structure, this probe is more selective that the other inhibitors (Figure 2.4, panel A).

In summary, all five fluorescent analogues are useful baits for different serine hydrolases. A combination of these probes rather than single inhibitor is straight forward for detection of as many enzymes as possible. In mouse RAW 264.7 macrophage-like cells, protein patterns detected with Ethyl-Cy5 and NBD-PC inhibitors are different. Most of the indentified proteins are lipid-associated and proteases that contained nucleophilic serine or cysteines in an active site. These proteins were: phospholipase A_2-activating protein, neutral cholesterol ester hydrolase 1 (Kiaa1363), alpha-enolase, adenosylhomocysteinase, cytosolic acyl coenzyme A thioester hydrolase, 3-ketoacyl-CoA thiolase mitochondrial, 3-ketoacyl-CoA thiolase B, peroxisomal, serum paraoxonase (PON 3), acyl-Co A thioesterase 2 mitochondrial, cathepsin D precursor, cathepsin D, cathepsin B preprotein, cathepsin S, esterase D, glyceraldehyde-3-phosphate dehydrogenase, lysophospholipase 1, lysophospholipase 2, peroxiredoxin-6, peroxiredoxin-1, protein DJ-1,

acetyl- CoA acyltransferase 1 precursor, platelet-activating factor acetylhydrolase, isoform 1b, subunit 1, prolyl 4 hydroxylase beta polypeptide precursor, succinate dehydrogenase, protein disulfide-isomerase A3, A4 and A6. Other proteins unrelated to lipids were also found. These were: fatty acyl-CoA reductase 1, tubulin beta-5 chain and glutathione S-transferase Mu 1. Some of the protein targets shown in Figure 2.6 panels A, B (Ethyl-Cy5 inhibitor) and panel C (NBD-PC) were the same. Those are: protein disulfide-isomerase A3, neutral cholesterol ester hydrolase 1, alpha-enolase, adenosylhomocysteinase, cytosolic acyl-CoA thioester hydrolase, esterase D and acetyl-CoA acyltransferase 1 precursor.

In summary, we compared the capacity of five different activity-based probes, namely NBD- HE-HP, NBD-PC and Ethyl-Cy-inhibitors (Figure 2.1) to label active (phospho)lipases. The more polar and smaller NBD-HE-HP and Ethyl-Cy-inhibitors showed more complex protein profiles. In contrast, NBD-PC seemed to be more selective toward PLA_2 (Figure 2.4, A). It is still unclear why some of the known (phospho)lipolytic macrophage enzymes are not found with these activity-based probes. This could be due to the conditions used for inhibitor solubilization and presentation to the enzyme. In addition, enzyme stability may be affected directly by the detergent. Therefore, future studies will be required to screen for the effects of the detergent and the full potential of the ABPs to detect (phospho)lipases. Unexpectedly, we found proteins that seem to be entirely unrelated to lipid metabolism. Since the phosphonate used in this work react with nucleophilic serines or cysteines, these proteins might contain such a yet unidentified functional group. Unspecific binding of the hydrolytic fluorescent probes to the respective polypeptides might also be possible. The clarification of these open questions must be subject to an independent study.

2.7 Acknowledgment

This work was supported by grants from the Austrian Federal Ministry of Science and Research/FFG in the framework of the GEN-AU program (GOLD project).

2.8 References

1. Birner-Gruenberger, R., A. Hermetter. 2007. Activity-based proteomics of lipolytic enzymes. *Current Drug Discovery Technologies* **4:** 1-11.
2. Kopelman, P. G., N. Finer. 2001. Reply: Is obesity a disease? *Int. J. Obes.* **25:** 1405-1406.
3. Schmidinger, H., R. Birner-Gruenberger, G. Riesenhuber, R. Saf, H. Susani-Etzerodt, and A. Hermetter. 2005. Novel fluorescent phosphonic acid esters for discrimination of lipases and esterases. *ChemBioChem* **6:** 1776-1781.
4. Morak, M., H. Schmidinger, P. Krempl, G. Rechberger, M. Kollroser, R. Birner-Gruenberger, and A. Hermetter. 2009. Differential activity-based gel electrophoresis for comparative analysis of lipolytic and esterolytic activities. *J. Lipid Res.* **50:** 1281-1292.
5. Scholze, H., H. Stütz, F. Paltauf, and A. Hermetter. 1999. Fluorescent inhibitors for the qualitative and quantitative analysis of lipolytic enzymes. *Anal. Biochem.* **276:** 72-80.
6. Olga V. Oskolova, Robert Saf, Elfriede Zenzmaier and Albin Hermetter. 2003. Fluorescent organophosphonates as inhibitors of microbial lipases. Chemistry and Physics of Lipids **125:** 103-114.
7. Egloff, M. -., F. Marguet, G. Buono, R. Verger, C. Cambillau, and H. Van Tilbeurgh. 1995. The 2.46 Å resolution structure of the pancreatic lipase-colipase complex inhibited by a C11 alkyl phosphonate. *Biochemistry (N. Y.)* **34:** 2751-2762.
8. Gargouri, Y., S. Ransac, and R. Verger. 1997. Covalent inhibition of digestive lipases: An in vitro study. *Biochimica et Biophysica Acta - Lipids and Lipid Metabolism* **1344:** 6-37.
9. Mannesse, M. L. M., J. -. P. Boots, R. Dijkman, A. J. Slotboom, H. T. W. M. Van der Hijden, M. R. Egmond, H. M. Verheij, and G. H. De Haas. 1995. Phosphonate analogues of triacylglycerols are potent inhibitors of lipase. *Biochimica et Biophysica Acta - Lipids and Lipid Metabolism* **1259:** 56-64.
10. Marguet, F., C. Cudrey, R. Verger, and G. Buono. 1994. Digestive lipases: Inactivation by phosphonates. *Biochimica et Biophysica Acta - Lipids and Lipid Metabolism* **1210:** 157-166.

11. Moreau, H., A. Moulin, Y. Gargouri, J. -. Noël, and R. Verger. 1991. Inactivation of Gastric and Pancreatic Lipases by Diethyl p-Nitrophenyl Phosphate. *Biochemistry (N. Y.)* **30:** 1037-1041.
12. Patkar, S., F. Björkling. 1994. Their Structure, Biochemistry and Application. *In Lipases* 207-224.
13. Stadler, P., G. Zandonella, L. Haalck, F. Spener, A. Hermetter, and F. Paltauf. 1996. Inhibition of microbial lipases with stereoisomeric triradylglycerol analog phosphonates. *Biochimica et Biophysica Acta - Lipids and Lipid Metabolism* **1304:** 229-244.
14. Arpigny, J. L., K. -. Jaeger. 1999. Bacterial lipolytic enzymes: Classification and properties. Biochem. J. 343: 177-183.
15. Pleiss, J., M. Fischer, and R. D. Schmid. 1998. Anatomy of lipase binding sites: The scissile fatty acid binding site. Chem. Phys. Lipids 93: 67-80.
16. Kazlauskas, R. J. 1994. Elucidating structure-mechanism relationships in lipases: Prospects for predicting and engineering catalytic properties. Trends Biotechnol. 12: 464-472.
17. Brzozowski, A. M., U. Derewenda, Z. S. Derewenda, G. G. Dodson, D. M. Lawson, J. P. Turkenburg, F. Bjorkling, B. Huge-Jensen, S. A. Patkar, and L. Thim. 1991. A model for interfacial activation in lipases from the structure of a fungal lipase-inhibitor complex. Nature 351: 491-494.
18. Martinelle, M., M. Holmquist, and K. Hult. 1995. On the interfacial activation of Candida antarctica lipase A and B as compared with Humicola lanuginosa lipase. Biochimica et Biophysica Acta - Lipids and Lipid Metabolism 1258: 272-276.
19. Dijkstra, H. P., H. Sprong, B. N. H. Aerts, C. A. Kruithof, M. R. Egmond, and R. J. M. Klein Gebbink. 2008. Selective and diagnostic labelling of serine hydrolases with reactive phosphonate inhibitors. *Organic and Biomolecular Chemistry* **6:** 523-531.
20. Bradford, M. M. 1976. A rapid and sensitive method for the quantitation of microgram quantities of protein utilizing the principle of protein-dye binding. *Anal. Biochem.* **72:** 248-254.
21. Fling, S. P., D. S. Gregerson. 1986. Peptide and protein molecular weight determination by electrophoresis using a high-molarity tris buffer system without urea. *Anal. Biochem.* **155:** 83-88.

22. Shevchenko, A., M. Wilm, O. Vorm, and M. Mann. 1996. Mass spectrometric sequencing of proteins from silver-stained polyacrylamide gels. *Anal. Chem.* **68:** 850-858.

23. Rasmussen, J. -. M., A. Hermetter. 2008. Chemical synthesis of fluorescent glycero- and sphingolipids. *Prog. Lipid Res.* **47:** 436-460.

Chapter 3

Functional proteome analysis of (phospho)lipases as targets of Orlistat in HepG2 and 3T3-L1 cells

Bojana Stojčić[1], Gerald Rechberger[2], Manfred Kollroser[3]and Albin Hermetter[1]

[1] Institute of Biochemistry, Graz University of Technology, Austria

[2] Institute of Molecular Bioscience, University of Graz, Austria

[3] Institute of Forensic Medicine, University of Graz, Austria

3.1 Abbreviations

3T3-L1	Mouse embryonic fibroblast - adipose like cell line
ABHD5	Abhydrolase (alpha-beta hydrolase) domain
DABGE	Differential activity-based gel electrophoresis
DAG	Diacylglycerol
DI	Drugable inhibitor
DMEM	Dulbecco's Modified Eagle Medium
DMSO	Dimethyl Sulfoxide
FAS	Fatty acid synthase
FCS	Fetal Calf Serum
FDA	Federal and drug administrative
GAPDH	Glyceraldehyde 3-phosphate dehydrogenase
HepG2	Human liver hepatocellular carcinoma cell line
HLA	Histocompatibility antigen
HPLC	High pressure liquid chromatography
IBMX	3-Isobutyl-1-methylxanthine
LPA	Lysophosphatidic acid
MAG	Monoacylglycerol
PAF	Platelet activating factor
PAFAH	Platelet activating factor acetylhydrolase
PBS	Phosphate buffered saline
PC	Phosphatidylcholine

PE	Phosphatidylethanolamine
Pen/Strep	Penicillin/ Streptomycin
PNPLA2	Patatin-like phospholipase domain-containing protein
QTOF	Coupled to quadrupole time-of-flight
SDS-PAGE	Sodium dodecyl sulfate - polyacrylamide gel electrophoresis
TAG	Triacylglycerol
UPLC	Ultra-performance liquid chromatography
VLDL	Very low density lipoprotein

3.2 Abstract

We developed a novel functional proteomic approach that is generally applicable to the screening for protein targets of any drugable (phospho)lipase inhibitor. This is based on the differential activity-based gel electrophoresis (DABGE) method that allows for comparison of two functional proteomes in one electrophoresis gel. This technique is based on two types of fluorescent probes that are suicide inhibitors of lipases. The respective compounds are hydrophobic phosphonic esters that contain the same reactive group but differ by the fluorophores. In a typical experiment, a control sample A and a sample B preincubated with the drug are separately labeled with a green (dye swap: red) and a red (dye swap: green) fluorophore, respectively. After mixing the protein samples A and B, labeled proteins are separated by gel electrophoresis. Emission of fluorophore A shows all protein targets, whereas fluorophore B emission only shows proteins that do not bind the drug. Thus, the difference in the fluorescence patterns is representative for the drug targets in a given sample. This method was applied to identify protein targets of two commercial serine hydrolase inhibitors, namely Orlistat and CAY10499 in lysates of HepG2 cells and mouse adipocytes. The identified targets were lipases, fatty acid synthase, phospholipases and proteins unrelated to lipids.

3.3 Introduction

The regulation of energy homeostasis largely depends on the balance of lipid storage and mobilization. Mammals tend to store excess lipids as intracellular triacylglycerols (TAGs) or sterol esters preferably in adipose tissues. Upon energy demand free fatty acid mobilized by hydrolytic cleavage of this compounds are catalyzed by lipases or phospholipases (1). In many cases lipid degradation is also associated with the formation of lipid messengers that regulate cell physiology. This function of lipolytic enzymes gives rise to lipid-associated disorders (e.g. obesity, atherosclerosis, type 2 diabetes), which are among the most frequent diseases in the western civilized world (2, 3).

A current strategy towards the management of obesity is based on drugs that inhibit the enzymes of the digestive tract. Such compounds prevent TAGs from being degraded by lipolytic enzymes and therefore the fatty acids from dietary TAGs cannot be utilized by the organism. A typical anti-obesity drug which is approved by the FDA for administration to humans is Orlistat (4, 5). Orlistat is Tetrahydrolipstatin (THL), a lipase inhibitor of bacterial origin. It represents an amphiphatic compound containing a hydrophobic chain and a polar moiety with a lactone ring. The cyclic ester group covalently reacts with nucleophilic serine of lipases, esterases and phospholipases forming a stable ester bond with the target proteins (6, 7). Orlistat inhibits in digestive tract both pancreatic and gastric lipase. In vitro it inhibits lot more lipases including cholesterol esterase and bile-salt-stimulated lipase of human milk (7).

In pancreatic lipase Orlistat binds to the serine residue 152 (6). Regular doses of 120 mg three times daily results in reduced fatty acid uptake (5, 8). Taking into account the inhibitory effects of Orlistat it can be expected that other enzymes (inside cells or in the

vasculature) are also affected. According to several reports from the literature this probability should be low because of the low bioavailability of the drug (9). However, this assumption is at variance with other findings that oral administration of Orlistat may be associated with severe side effects (e.g. liver failure, fatty/oily stool etc.) (4, 5). For all these reasons considerable interest evolved to identify potential Orlistat targets. Peng Yu-Yang and colleagues developed functional proteomic approach for the identification of multiple Orlistat targets in a given sample using a fluorescent THL analog (10). These authors interestingly found not the classical targets of serine hydrolase inhibitors but also proteins that are virtually unrelated to lipolytic enzymes. One of the most prominent hits of the proteome analysis was fatty acid synthase (FAS) (10, 11). This enzyme is currently gaining much attention because its function is not only important for lipid-associated disorders but also for the growth of cancer cells. Therefore Orlistat has already been proposed in several reports as a potential anti-cancer drug (12-14).

Though technique by Yu-Yang et al., turned out to be very useful its application is restricted to Orlistat research. For that reason we developed a novel functional proteomic approach which is generally applicable to the screening for protein targets of any drugable (phospho)lipase inhibitor. This is based on the DABGE method (15) which allows for comparison of two functional proteomes in one electrophoresis gel. This technique is based on two types of fluorescent probes that are suicide inhibitors of lipases. The respective compounds are hydrophobic phosphonic esters that contain the same reactive group but differ by the fluorophores. In a typical experiment, a control sample A and a sample B preincubated with the drug are separately labeled with a green (dye swap: red) and a red (dye swap: green) fluorophore, respectively. After mixing the protein samples A and B, labeled proteins are separated by gel electrophoresis. Emission of fluorophore A shows all protein targets, whereas fluorophore B emission only shows proteins that do not bind the

drug. Thus, the difference in the fluorescence patterns is representative for the drug targets in a given sample. This method was applied to identify protein targets of two commercial serine hydrolase inhibitors, namely Orlistat and CAY10499 in lysates of HepG2 cells and mouse adipocytes. The identified targets were lipases, fatty acid synthase, phospholipases and proteins unrelated to lipids.

3.4 Experimental procedures

3.4.1 Cell culture

Cell lines: human liver hepatocellular carcinoma cells (HepG2 cells) and mouse embryonic fibroblast - adipose like cells (3T3-L1 cells) were provided by Juliane Gertrude Bogner-Strauß, Institute of Genomics and Bioinformatics, Technical University of Graz, Austria.

HepG2 cells were grown in DMEM low glucose (1 g/L), 25 mM HEPES and L-Glutamine from PAA (Pasching, Austria) supplemented with 10% FCS and 1% Pen/Strep (100 U). 3T3-L1 cells were grown in DMEM, high glucose (4,5 g/L), 25 mM HEPES from Invitrogen (Lofer, Austria) supplemented with 10% FCS, 1% Pen/Strep (100 U) and 2 mM L-Glutamine. Both cell lines were grown under an atmosphere containing 5% CO_2 at 37°C. Initially, 3T3-L1 cells were grown in standard medium (DMEM with 10 % FCS, 2 mM L-Glutamine and 1% Pen/Strep) until 100% confluency under an atmosphere containing 5% CO_2 at 37°C. Two days after (day 0) original medium was replaced by differentiation medium (standard medium supplemented with 0.05 mM IBMX, 1 µM Dexamethasone and 2 µg/ml Insulin) and the cells were cultured until day 3. The medium was changed stepwise:

Day 3 – medium was replaced by standard medium supplemented with 2 µg/ml insulin

Day 5 – medium was replaced by standard medium

Day 7 – cells were collected for experiments

To monitor cell differentiation, cellular lipid droplets and membranes were stained with Nile Red according to Greenspan et al. (16). The Lab-Tek™Chamber Slide System from Nunc (Nalgene, Rochester, USA) was used for microscopic inspection of stained cells. Briefly,

cells were seeded into chamber slides one day prior to use and fixed with 3.7% formaldehyde for 10 minutes. A stock solution of Nile Red (1 mg/ml) in acetone was prepared and diluted 100-fold with PBS. The resulting solution was used for staining. The cells were incubated with this solution (500 µl per slide / per 1 cm well) at room temperature under protection from light for 10 minutes. Thereafter, cells were washed three times with cold PBS and viewed under a fluorescence microscope (emission 637 nm).

3.4.2 Preparation of cell lysates

Cells were scraped and sonicated at 40 W for 20 seconds in 50 mM Tris/HCl buffer containing protease inhibitors (20 µg/ml leupeptin, 2 µg/ml antipain and 1 µg/ml pepstatin). To obtain the cytoplasmic fraction, cell debris was removed by centrifugation at 1.000 x g at 4°C for 15 minutes. Protein concentration was determined by the Bio-Rad protein assay based on the Bradford method (17). Supernatant was collected and used for further experiments.

3.4.3 Drug targeting and activity tagging of (phospho)lipolytic enzymes in cell lysates (DABGE)

Cell lysates were preincubated with drugable inhibitors (Orlistat or CAY10499) as follows: for 300 µl of cell lysate the following sample was prepared: 3 µl 100 mM Triton X-100 in $CHCl_3$ (final sample concentration: 1 mM) and 1,5 µl 20 mM inhibitor drugs (Orlistat or CAY10499) in DMSO (final concentration: 100 µM, if not stated otherwise) were mixed. The organic solvent was removed under the stream of argon. The cell lysate was added and samples were incubated at 37°C and 550 rpm for an hour.

Preincubated and untreated cell lysates were used for DABGE experiments. Typically, samples of 150 µl cell lysate containing 150 µg protein were labeled with fluorescence

inhibitors as follows: 1,5 µl of 100 mM Triton X-100 in $CHCl_3$ (final sample concentration: 1 mM) and a solution of 1,5 nmol of Ethyl-Cy-tagged inhibitors in $CHCl_3$ (final concentration: 10 µM) were mixed and the organic solvent was removed under a stream of argon. Cell lysates (1 µg/µl), preincubated with Orlistat and CAY10499, were incubated with 10 µM of Ethyl-Cy3 at 37°C and 550 rpm for 2 h. The same volume of untreated cell lysate was incubated with Ethyl-Cy5 under the same conditions. In a Dye-Swap experiment lysates pretreated with the drug were labeled with Ethyl-Cy5 and untreated lysates were labeled with Ethyl-Cy3. Identical volumes of both samples were mixed and protein was precipitated by addition of 500 µl acetone and the samples were stored overnight at -20°C. Precipitated protein was collected by centrifugation at 14.000 x g at 4°C for 20 minutes and resuspended in 1-D SDS-PAGE sample buffer (20 mM KH_2PO_4, 6 mM EDTA, 6 % SDS, 10 % glycine and 0,05 % bromophenol blue, pH 6,8 and 20 µl/ml mercaptoethanol). Samples were preheated for 5 minutes at 95°C prior to loading onto the gel.

3.4.4 One dimensional gel electrophoresis

For protein separation, we used one dimensional gel electrophoresis according to the method of Fling and Gregerson (18). We used 1x running buffer which contained: 3 g/L Tris, 0.334 g/L EDTA, 5 g/L SDS and 14,2 g/L glycine) in ddH_2O. Proteins were separated at constant current (10 mA per gel) for the first 15 minutes followed by 20 mA per gel for an hour using a Bio-Rad Mini PROTEAN 3 apparatus at 4°C.

3.4.5 Fluorescence detection of proteins in electrophoresis gels

Gels were fixed in fixing solution (7% acetic acid and 10% ethanol) for at least 30 minutes and scanned at a resolution of 100 µm using a Bio-Rad Molecular Imager^{TM} FX Pro Plus.

Fluorescence detection was carried out at different excitation wavelengths (532 nm and 635 nm) and emission wavelengths (555 nm and 695 nm) for Cy3 and Cy5, respectively.

Proteins were visualized after staining with Sypro ruby™ solution. The staining solution was obtained after dilution of 100 µl of aqueous RuBPS stock solution (20 mM) in one liter of 20% Ethanol in ddH_2O. Gels were stained with Sypro ruby™ solution for at least 2 h and incubated in fixing solution for at least 2 h. Sypro ruby™ fluorescence was scanned at emission and excitation wavelengths of 605 nm and 488 nm, respectively. Fluorescence signals were quantified by a Bio-Rad Image Lab™ Software Version 2.0.1.

3.4.6 LC-MS/MS analysis of target proteins

For the identification of drug – affected proteins, protein bands were excised from gels and tryptically digested according to the Method by Shevchenko et al. (19).

Peptide extracts were dissolved in 0.1% formic acid and separated by nano-HPLC (FAMOS™ autosampler, SWITHOS™ loading system, and ULTIMATE™ dual gradientsystem system; LC-Packings, Amsterdam, The Netherlands) as described in (1), but using the following solvent gradient: solvent A: water, 0.3% formic acid; solvent B: acetonitrile/water 80/20 (v/v), 0.3% formic acid; 0 to 5 min: 4% B, after 40 min 55% B, then for 5 min 90 % B, and 47 min reequilibration at 4% B. The samples were ionized in a Finning nano-ESI source equipped with NanoSpray tips (PicTip™ Emitter; New Objective, Woburn, MA) and analyzed in a Thermo-Finnigan LTQ linear ion trap mass spectrometer (Thermo, San Jose, CA).

The MS/MS data were analyzed by searching the NCBI non redundant public database with SpectrumMill Rev A.03.03.084 SR4.

3.4.7 Lipid extraction and analysis

HepG2 cells were seeded out a day prior to use onto 10 cm diameter cultured dishes. The cells were incubated with different concentrations of Orlistat in 3 ml standard medium. Cells were incubated with media obtained by stock solutions of Orlistat in DMSO to standard medium for 3 h. The final concentrations of Orlistat in the incubation media were 0 µM (control), 2 µM, 10 µM, 50 µM and 100 µM. After incubation, the medium was removed and cells were washed twice with cold PBS and followed by scraping into pyrex tubes on ice. The cell pellet was isolated by centrifugation at 1.000 rpm (Eppendorf Centrifuge 5810R) at 4°C for 5 minutes. 50 µl of a solution of 0.05 mg/ml of internal standard in chloroform (containing 45:0, 51:0, 57:0 glycerolipids, respectively) was added to the cell pellet. 3 ml of $CHCl_3$/MeOH (2:1, v/v) were added and the suspension was vortexed at 4°C for 1 h. 700 µl of (0,036%) $MgCl_2$- Solution was added and the sample was again shaken at 4°C for 15 minutes. Phase separation was completed after centrifugation at 2.400 rpm (Eppendorf Centrifuge 5810R) at room temperature for 2 minutes. The lower chloroform phase was isolated and the organic solvent was removed under a stream of nitrogen. The lipid extracts were further analyzed with UPLC-QTOF-MS. Briefly, samples were dissolved in chloroform/MeOH (2:1, v: v), diluted with 2-propanol (1:20, v: v) and lipids were separated with an AQUITY-UPLC system (Waters, Manchester, UK) using a BEH-C18-column, 2.1x150 mm, 1.7 µm column (Waters). Lipids were separated using a gradient solvent from 55% solvent A (water: MeOH 1:1, v:v) and 45% solvent B (2-propanol), both containing 1% ammonium-acetate, 0.1% formic acid and 8 µM H_3PO_4) to 100% solvent B. Separation time was 35 minutes and column temperature was 50°C.

Triacylglycerols (TAG), diacylglycerols (DAG), phosphatidylcholine (PC) and phosphatidylethanolamine (PE) were analyzed using the SYNAPT™G1 qTOF HDMS

(Waters), equipped with an ESI ion source (positive mode) using LeucinEnkephalin as lock mass. Capillary voltage was set 2.6 kV and capillary temperature to 100°C. The MS was operated in V-mode.

Data analysis was performed using the “Lipid Data Analyzer” software (20). The relative values of lipid content are normalized over the amount of internal lipid standard lipid and over the total protein concentration according to : $A_{Sample}/(A_{intern\ standard}$*mg Protein).

3.5 Results

Here we report on a new method for the identification of active lipolytic enzymes that are targeted by drugable inhibitors (e.g. Orlistat, CAY10499). For this purpose we used differential activity-based gel electrophoresis (DABGE) which allows the comparison of two different proteomes in one electrophoresis gel. This method is based on fluorescent suicide inhibitors (phosphonic acid esters) possessing the same functional structures but different fluorescent dyes (Figure 3.1). The reactive group is a phosphonic acid p-nitrophenyl ester. It reacts with nucleophilic serine of lipase by forming a covalent lipid-protein complex, which can be detected on polyacrylamide gels by fluorescence imaging (15).

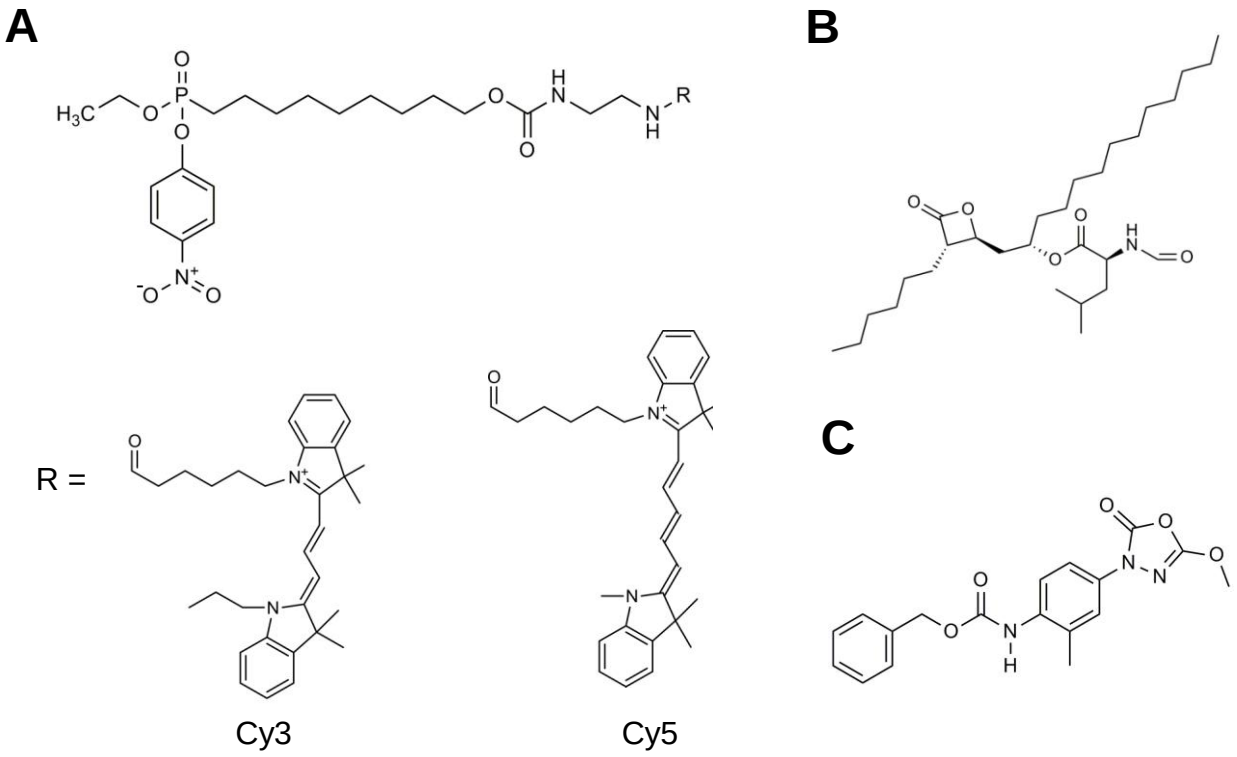

Figure 3. 1 Chemical structures of (fluorescent) lipase inhibitors. The compounds shown are **A:** cyanine tagged phosphonic acid esters containing Ethyl-Cy3 and –Cy5; **B:** Orlistat (THL) and **C:** A lipase inhibitor CAY10499.

Figure 3.2 illustrates how the technique works. A typical lipase sample (e.g. cell lysate) is divided in two aliquots. Sample A is preincubated with a drugable inhibitor (DI) for load by labeling with Cy3 phosphonate (Ethyl-Cy3). In sample A, only the proteins are stained by Cy3 (green fluorescence) that are not tagged by DI. The control sample B was labeled with Cy5 phosphonate (Ethyl-Cy5), red fluorescence, without pretreatment with the DI. In this sample all active lipases are fluorescently stained including those being DI targets. Labeled samples A and B are mixed (ratio 1/1), proteins are separated by 1-D PAGE and the labeled proteins were detected by fluorescence imaging. Proteins that are not tagged by the DI are labeled green and red and appear as yellow bands on the gel. Proteins that are targeted by the DI are exclusively labeled by Cy5 and appear as red bands on the gel. In order to avoid artifacts, due to fluorescent labeling, a Dye-Swap experiment was preformed. In this case, samples A and B were labeled red and green, respectively. Under these conditions the DI targets appear as green bands on the gel.

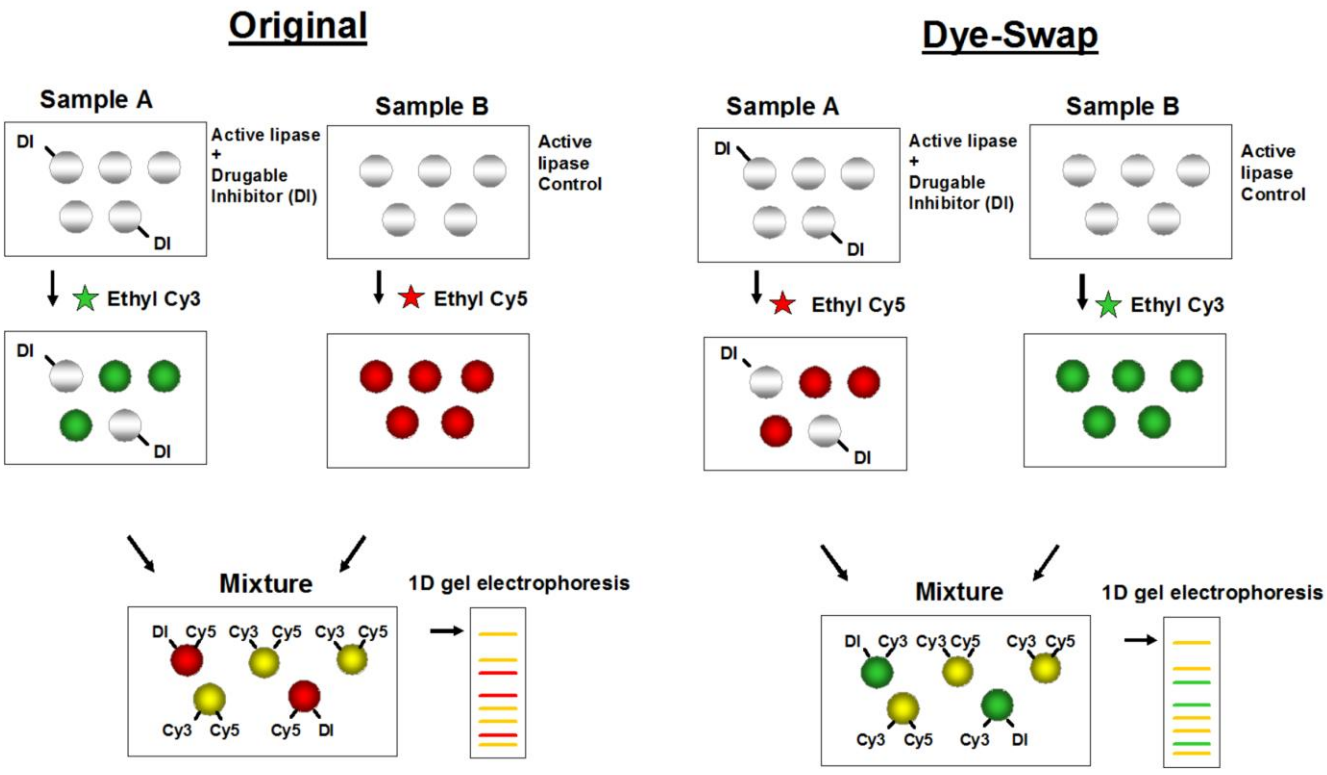

Figure 3. 2 DABGE imaging of drug/inhibitor-targeted (phospho)lipases. Cell lysates were incubated with the drug followed by fluorescence labeling with Cy3 phosphonate. An untreated cell lysate was labeled with

Cy5 phosphonate. Both lysates are mixed and proteins are separated by SDS-PAGE. Only the Orlistat binding proteins show red Cy5 emission (green Cy3 emission in a dye swap experiment). The yellow bands (Cy5 equal to Cy3 emission) show unaffected proteins. Sypro ruby™ stains all the proteins.

Table 3.1 shows the lipid-associated proteins that are tagged by Orlistat. In general proteins were found that either contain nucleophilic –OH or –SH groups. These functional groups covalently react with Orlistat and therefore are prevented from labeling by Cy-phosphonates (see above). The respective proteins are: 1-acylglycerol-3-phosphate O-acyltransferase ABHD5, 3-ketoacyl-CoA thiolase, acetyl-CoA acetyltransferase, acyl-CoA thioesterase 2, adenosylhomocysteinase, dipeptidyl peptidase 2, fatty acid synthase, glutathione S-transferase omega-1, glyceraldehydes-3-phosphate dehydrogenase, group XV phospholipase A_2, lipoprotein lipase, liver carboxylesterase 1, lysophospholipase 1 and 2, peroxiredoxin-1 and -6, platelet-activating factor acetylhydrolase IB subunit gamma, prolyl 4-hydroxylase subunit alpha-1/beta polypeptide isoform CRA_b, protein disulfide-isomerase A3, protein DJ-1, serine/threonine-protein phosphatase 2A catalytic subunit alpha, specific acyl-CoA dehydrogenase, trifunctional enzyme beta, ubiquitin carboxyl-terminal hydrolase. The additional proteins were found that do not contain such functional residue and to date it is unclear why they interact with the drug and the fluorescent label. Some of these proteins have been independently found by another group (10, 11). In their study they used functionalized Orlistat analogues for the identification of drug targets. However it has to be emphasized that they also found other proteins that could not be identified by our method. The method by Peng-Yu-Yang (10, 11) has the advantage that it makes use of probes closely related to the original drugs. However, it is only applicable to that specific drug. Our method is based on phosphonic acid esters displaying somewhat different structures but it can be used for the screening of any lipase targeted drug.

Figure 3.3 and 3.4 show the most pronounced relative activities of lipid-associated proteins. These proteins are listed in Table 3.1. It is interesting to note that patterns of protein inhibition of Orlistat (Figure 3.3) and CAY10499 (Figure 3.4) are similar. Various proteins in band number 1 (see Figure 3.3) are preferentially tagged by Orlistat. Proteins in bands 5 and 6 are almost equally tagged by CAY10499 (see Figures 3.3 and 3.4). Obviously lipase targeting depends on the chemical structure of the drug. In addition lipase targeting is specific for a cell(lysate).

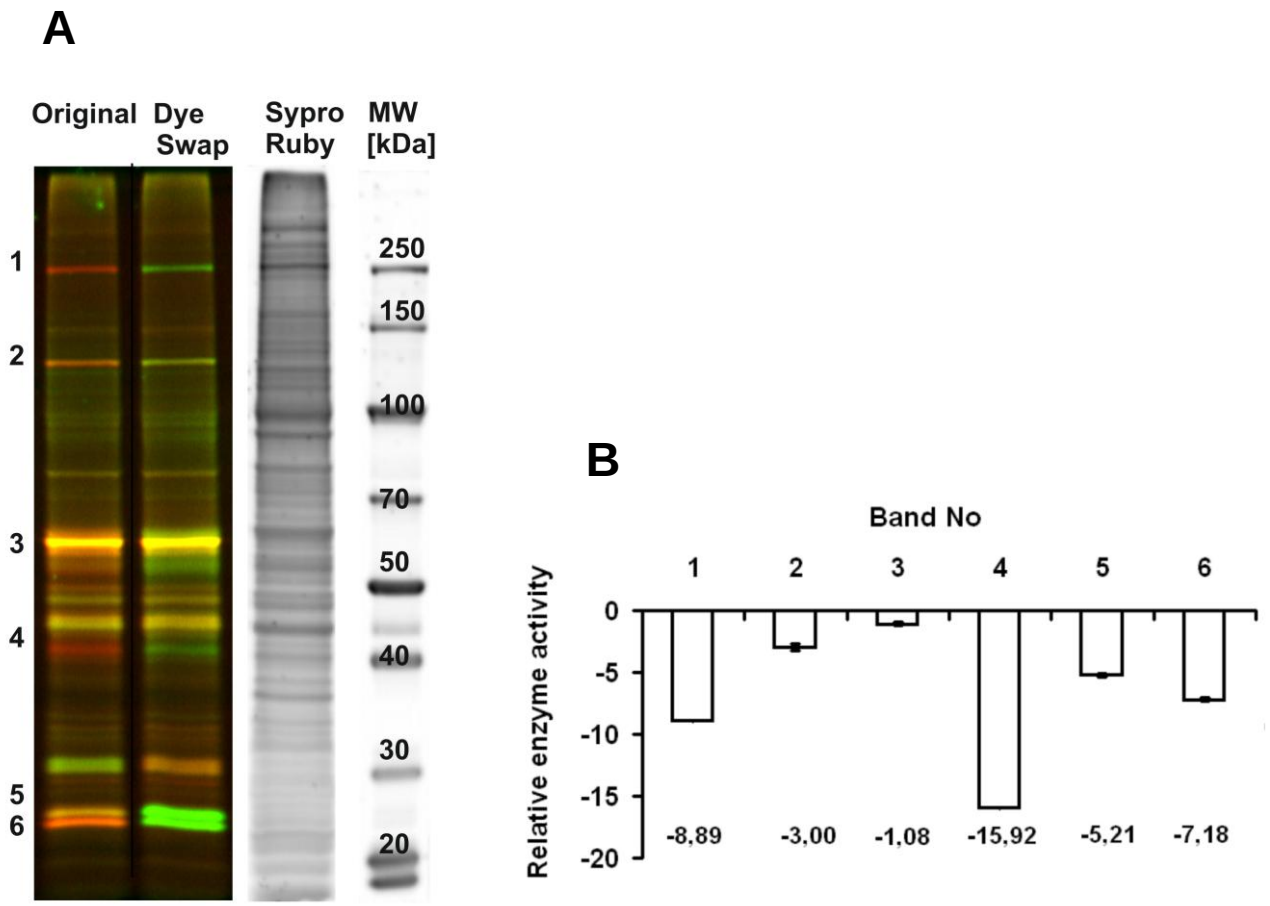

Figure 3. 3 DABGE analysis of Orlistat – tagged (phospho)lipolytic enzymes in HepG2 cell lysates. Cells were sonicated in 50 mM Tris/HCl buffer pH 7,4 containing protease inhibitors (20 µg/µl leupeptin, 2 µg/µl antipain and 1µg/µl pepstatin) at 40 W for 15 seconds. After centrifugation, the supernatant was incubated with 100 µM Orlistat at 37°C at 550 rpm for 1 h. The Orlistat treated samples and control cell lysates were incubated with Ethyl -Cy3 and -Cy5 phosphonates as described in legend to Figure 3.2. **A:** Fluorescence image of original (left lane) and dye swap sample (right lane). After imaging Cy3 and Cy5

fluorescence, total proteins were stained with Sypro ruby^{TM} stain. Molecular weights of proteins were compared with molecular weight standard (first lane from right); **B:** Relative enzyme activities in Orlistat treated cells determined from Cy3 and Cy5 fluorescence in the individual electrophoretic bands according to the formula: ratio = $\sqrt{\frac{Cy3(treated)*Cy5(treated)}{Cy3(untreated)*Cy5(untreated)}}$. Proteins found in bands **1:** fatty acid synthase; **2**: pyruvate carboxylase, ubiquitin carboxyl-terminal hydrolase; **3:** alpha enolase, dihydrolipoyl dehydrogenase, liver carboxylesterase 1, prolyl 4-hydroxylase subunit alpha-1 and beta, protein disulfide-isomerase A3, serum albumin, trifunctional enzyme subunit beta, tubulin beta chain and beta 2C; **4:** acetyl-CoA acetyltransferase, adenosylhomocysteinase, aminoacylase-1, Dnaj (Hsp40) homolog, fumarylacetoacetase, HLA class I histocompatibility antigen A-2 alpha chain, putative uncharacterized protein DKFZp686M24262, pyruvate dehydrogenase, short/branched chain specific acyl-CoA dehydrogenase; **5**: 60S ribosomal protein L14, enoyl-CoA hydratase, glutathione S- transferase; fumarylacetoacetase hydrolase domain containing 1platelet-activating factor acetylhydrolase IB subunit gamma, , lysophospholipase II, peroxiredoxin-6 and **6:** lysophospholipases 1, peroxoredoxin-1, protein DJ-1, ribosomal protein L14.

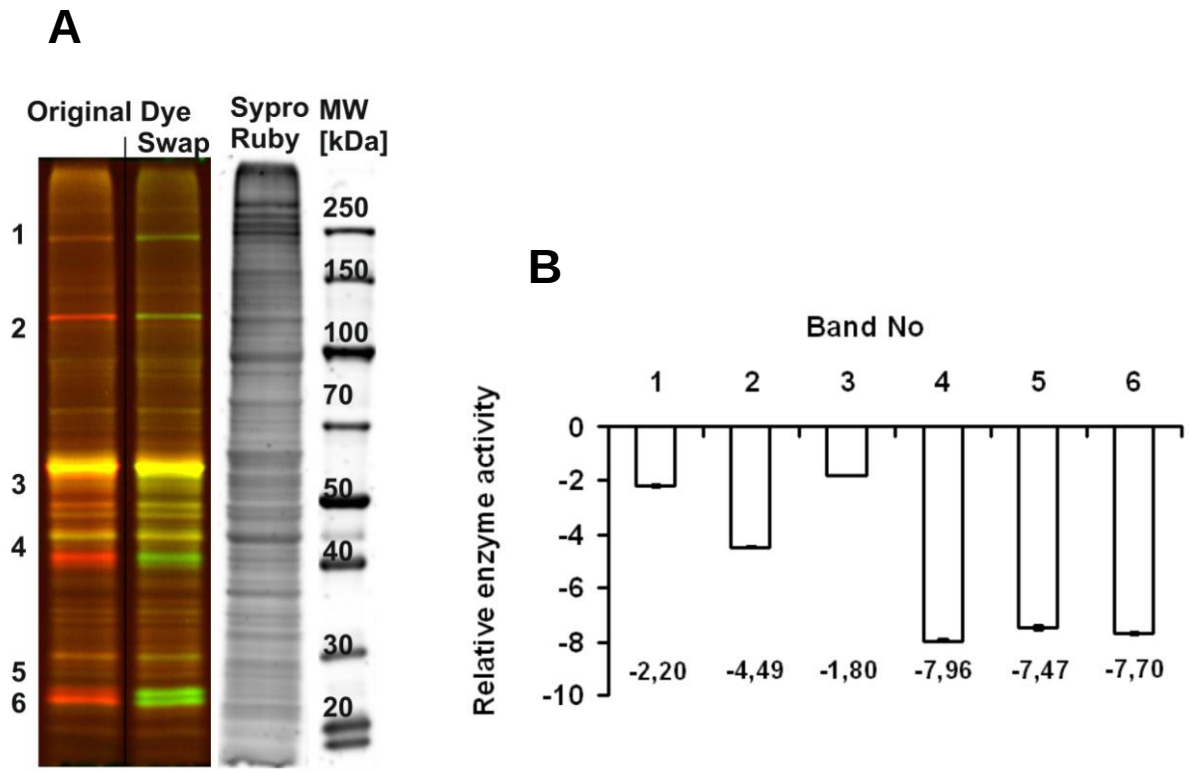

Figure 3. 4 DABGE analysis of CAY10499 – tagged (phospho)lipolytic enzymes in HepG2 cell lysates. Inhibitor-tagged enzymes and their relative enzyme activities were determined as described in legend to Figure 3.3. CAY10499 concentration was 100 µM.

We also determined Orlistat targets in differentiated mouse 3T3-L1 cells (Figure 3.5). Figure 3.5 shows that a set of different proteins is targeted in these cells as compared to HepG2 cells. Though certain proteins are identical (60S ribosomal protein L14 and L7; acetyl-CoA acetyltransferase; alpha enolase; glutathione S-transferase; lysophospholipase 1; peroxiredoxin-1; prolyl 4-hydroxylase; pyruvate dehydrogenase and tubulin beta). The proteins that are preferentially targeted by Orlistat in 3T3-L1 are: 1-acylglycerol-3-phosphate O-acyltransferase ABHD5; 3-ketoacyl-CoA thiolase, mitochondrial; 60S ribosomal protein L14; 60S ribosomal protein L7; acetyl-CoA acetyltransferase, mitochondrial; acyl-CoA thioesterase 2; aldehyde dehydrogenase family 6, subfamily A1, isoform CRA_a; alpha-enolase; annexin A2; cathepsin B preprotein; cathepsin D; dipeptidyl

peptidase 2; glutathione S-transferase omega-1; glyceraldehyde-3-phosphate dehydrogenase; group XV phospholipase A2; HLA-B-associated transcript 1 protein; lipoprotein lipase; lysophospholipase 1; peroxiredoxin-1; prolyl 4-hydroxylase, beta polypeptide, isoform CRA_b; pyruvate dehydrogenase E1 component subunit beta; serine/threonine-protein phosphatase 2A catalytic subunit alpha; sphingosine phosphate lyase 1; tubulin alpha-1B chain; tubulin, beta 5; tubulin beta-4A chain.

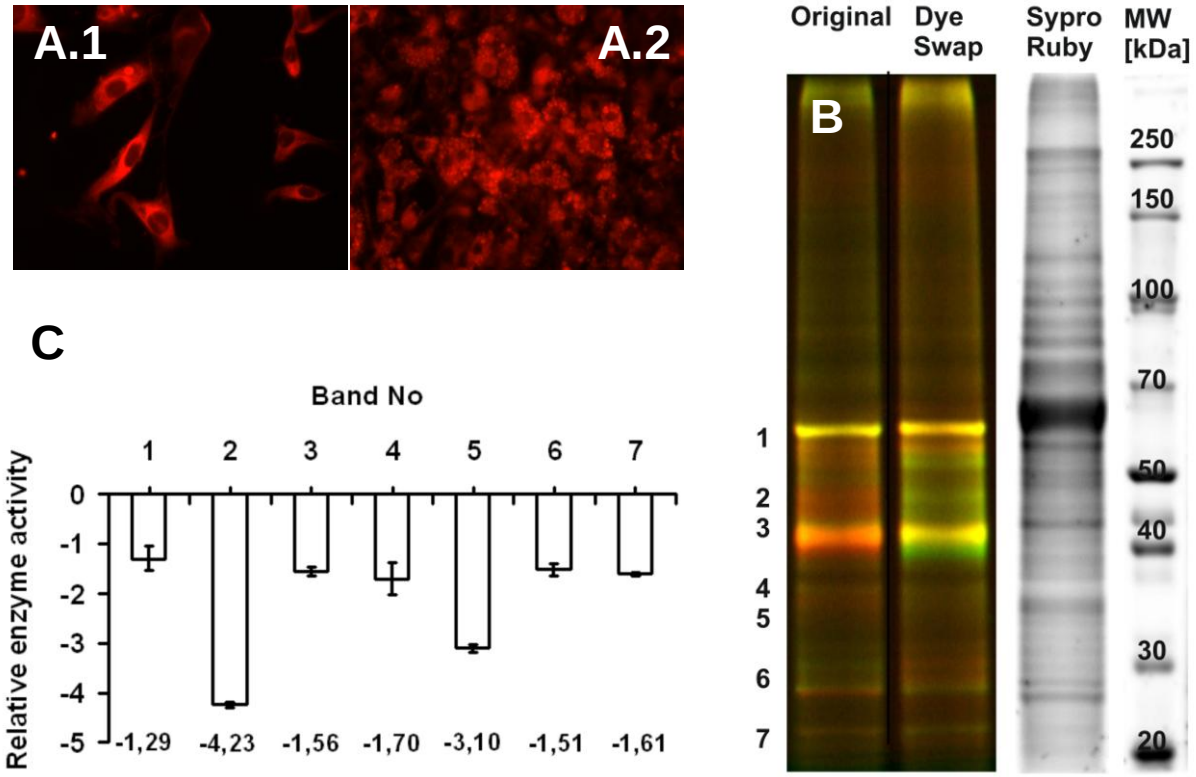

Figure 3. 5 Microscopic images of undifferentiated (A.1) and differentiated (A.2) 3T3-L1 mouse fibroblast and DABGE analysis of Orlistat – tagged (phospho)lipolytic enzymes in differentiated 3T3-L1 cell lysates (adiposities). Magnification was 320x. Cell culturing and differentiations was preformed as described in experimental procedures. Inhibitor-tagged enzymes and their relative enzyme activities were determined as described in legend to Figure 3.3 (panels B and C). Orlistat concentration was 100 µM. Proteins found in bands **1:** aldehyde dehydrogenase family 6 subfamily A1, dipeptidyl peptidase 2, lipoprotein lipase, prolyl 4-hydroxylase, sphingosine phosphate lyase 1, tubulin alpha-1B chain and beta 5; **2:** alpha-enolase, group XV phospholipase A2, HLA-B-associated transcript 1 protein, tubulin beta-4A chain; **3:** 1-acylglycerol-3-

phosphate O-acyltransferase ABHD5, 3-ketoacyl-CoA thiolase, acetyl-CoA acetyltransferase, acyl-coenzyme A thioesterase 2, annexin A2, cathepsin D; **4:** 60S ribosomal protein L7, glyceraldehyde-3-phosphate dehydrogenase, serine/threonine-protein phosphatase 2A catalytic subunit alpha; **5:** pyruvate dehydrogenase E1 component subunit beta; **6:** cathepsin B preprotein and **7:** glutathione S-transferaseomega-1, 60S ribosomal protein L14, lysophospholipase 1, peroxiredoxin-1.

In order to determine the effects of enzyme inhibition of Orlistat in HepG2 cells we analyzed lipid profiles of cellular lipid extracts after incubation with this inhibitor (Figure 3.6). TAG levels are hardly affected except for 2 µM concentration of Orlistat. In contrast, total DAG concentrations significantly change under the influence of the Orlistat. Again the lower concentrations (2 µM) show the most significant effects. The amounts of total PE and PC are not very much affected by different Orlistat concentrations either. It looks as impairment of lipolysis by Orlistat is compensated at least in part by other liposynthetic pathway.

Although total lipid concentrations of DAG, PC and PE stay almost the same, some preferences can be seen on the level of the individual lipid species (supplemented Figures S1 through S3). Figure S1, panel A shows that 54:3 TAG degradation is significantly inhibited by Orlistat. Among the DAG species (36:1 and 36:2) the effects are more significant at low concentrations of Orlistat. Species preferences for phospholipid species are much less pronounced.

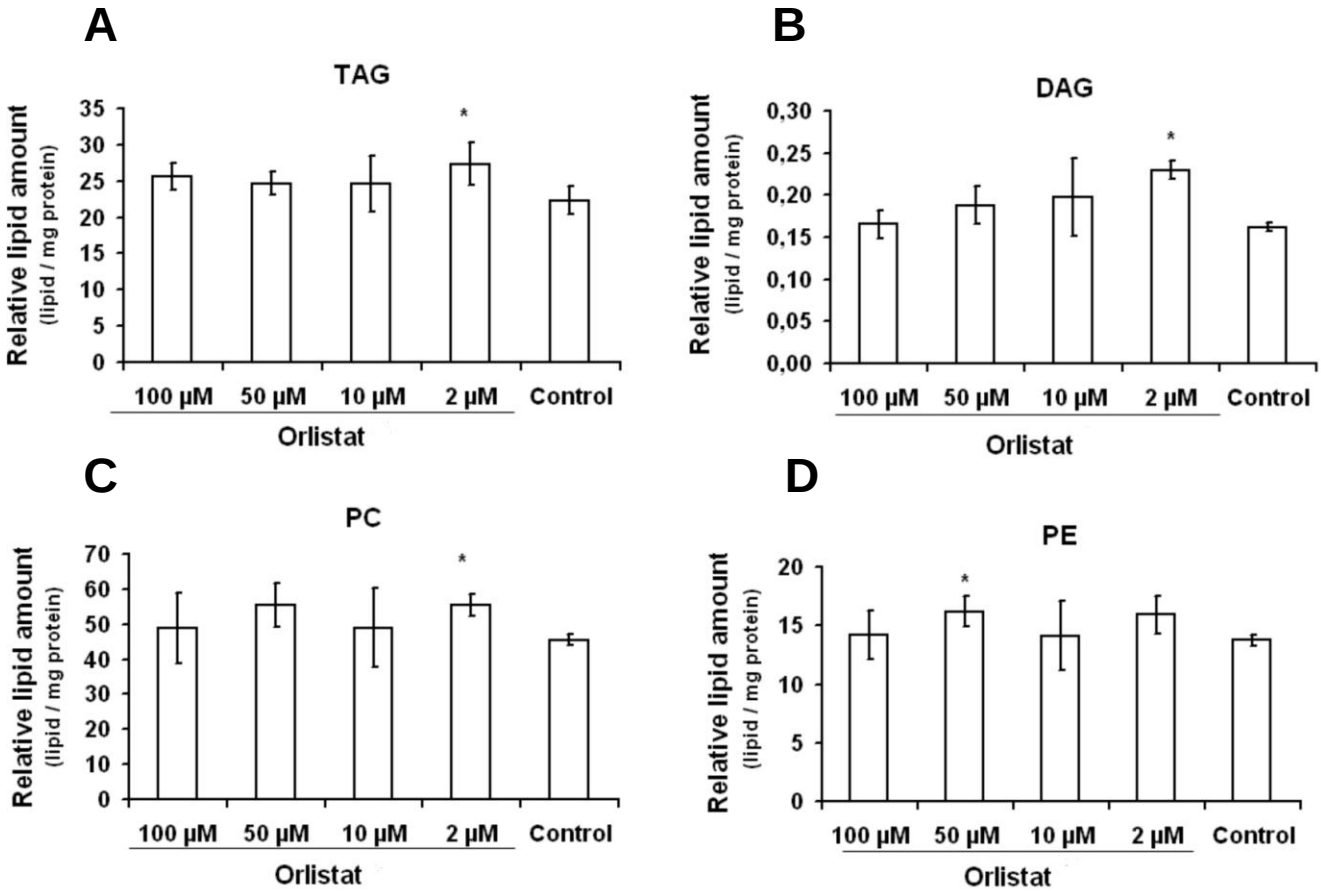

Figure 3. 6 Effects of Orlistat on glycerol(phospho)-lipid profiles in HepG2 cells. Cells were incubated for 3 h with different concentrations of Orlistat in serum rich medium. Lipids were extracted using $CHCl_3$/MeOH (2:1, v/v) as solvent as described in experimental procedures. Lipids were measured by UPLC-QTOF-MS and analyzed using SYNAPT™G1 qTOF HDMS. Data analysis was performed using the "Lipid Data Analyzer" software. The relative values of lipids are normalized over the amount of internal standard lipid and the total protein concentration according to: $A_{Sample}/(A_{intern\ standard}$*mg Protein). Data are expressed as means of 3 independent experiments ± SD (*, P ≤ 0, 05).

Name (Gene Name)	NCBI No	MW [kDa]	pI	Id.pep	Search Score	Seq cov %	Band No
1-acylglycerol-3-phosphate O-acyltransferase ABHD5 (protein CGI-58)	13385690	39,15	6,33	2	32,05	7	A_3
3-ketoacyl-CoA thiolase, mitochondrial	73919875	41,85	8,33	9	148,09	28	A_3
60S ribosomal protein L14	20810536	23,57	10,94	10	162,4	37	H_5
60S ribosomal protein L14	12846159	26,31	11,9	3	53,15	14	A_7
60S ribosomal protein L7	31981515	31,41	10,89	12	174,92	37	A_4
Acetyl-CoA acetyltransferase, cytosolic variant	62087566	42,13	7,2	4	63,62	9	H_4
Acetyl-CoA acetyltransferase, mitochondrial	21450129	44,81	8,71	10	158,65	32	A_3
Acyl-CoA thioesterase 2, mitochondrial	74196709	49,65	6,88	2	26,29	4	A_3
Adenosylhomocysteinase	9951915	47,7	5,92	12	207,43	27	H_4
Aldehyde dehydrogenase family 6, subfamily A1, isoform CRA_a	148670856	58,89	8,69	10	158,8	21	A_1
Alpha-enolase	70794816	47,14	6,37	17	294,23	42	A_2
Alpha-enolase	62897945	47,1	7,01	31	557,19	69	H_3
Aminoacylase-1	4501901	45,88	5,77	3	42,36	5	H_4
Annexin A2	6996913	38,67	7,55	29	362,45	49	A_3
Cathepsin B preprotein	74213457	37,32	5,65	3	44	10	A_6
Cathepsin D	26354406	48,37	6,86	7	113,52	20	A_3
Dipeptidyl peptidase 2	13626390	56,26	5,17	8	98,82	16	A_1
DnaJ (Hsp40) homolog, subfamily B, member 11	48146309	40,54	5,81	2	27,68	6	H_4
Dihydrolipoyl dehydrogenase	62088986	55,59	8,71	4	68,72	9	H_3
Enoyl-CoA hydratase, mitochondrial	14286220	31,39	8,34	6	86,06	19	H_5
Fatty acid synthase	68533031	273,4	6,2	23	924,98	56	H_1
Fumarylacetoacetase	4557587	46,37	6,46	3	48,12	6	H_4
Fumarylacetoacetase hydrolase domain containing 1	66348062	27,12	7,6	2	30,09	8	H_5
Glutathione S-transferase	825606	25,72	8,84	4	59,69	11	H_5
Glutathione S-transferase omega-1	6754090	27,49	6,91	2	38,4	10	A_7
Glyceraldehyde-3-phosphate dehydrogenase	62201487	35,83	8,43	13	230,57	47	A_4
Group XV phospholipase A2	19527008	47,3	6,02	2	35,04	5	A_2
HLA class I histocompatibility antigen, A-2 alpha chain	1644237	40,85	6,68	4	82,89	18	H_4
HLA-B-associated transcript 1 protein	9790069	49,03	5,44	4	67,43	10	A_2
Lipoprotein lipase	26347995	53,16	7,6	2	36,44	5	A_1
Liver carboxylesterase 1	68508967	62,59	6,15	5	82,04	12	H_3
Lypla1 protein	71059731	24,68	5,76	2	33,4	10	A_7
Lysophospholipase 1	5453722	24,66	6,29	3	38,3	13	H_6
Lysophospholipase II	119615487	30,76	9,62	5	75,04	12	H_5
Peroxiredoxin-1	12846314	22,23	8,26	9	151,74	45	A_7
Peroxiredoxin-1	4505591	22,11	8,27	15	265,28	66	H_6
Peroxiredoxin-6	4758638	25,03	6	6	102,76	30	H_5
Platelet-activating factor acetylhydrolase IB subunit gamma	4505587	25,73	6,33	2	27,02	7	H_5
Prolyl 4-hydroxylase subunit alpha-1	63252888	61,04	5,7	3	54,92	7	H_3
Prolyl 4-hydroxylase subunit beta	20070125	57,11	4,76	24	396,98	45	H_3
Prolyl 4-hydroxylase, beta polypeptide, isoform CRA_b	148702819	61,53	4,96	29	499,25	53	A_1
Protein disulfide-isomerase A3	1208427	56,79	5,99	33	401,92	44	H_3
Protein DJ-1	31543380	19,89	6,33	6	99,84	34	H_6
Putative uncharacterized protein DKFZp686M24262 (Acyl-CoA dehydrogenase)	57997529	50,3	7,94	7	112,78	17	H_4
Pyruvate carboxylase, mitochondrial	106049292	129,6	6,37	18	292,35	15	H_2
Pyruvate dehydrogenase E1 component subunit alpha, somatic form, mitochondrial	148357460	47,57	8,83	7	108,09	15	H_4
Pyruvate dehydrogenase E1 component subunit beta, mitochondrial	74177597	38,95	6,41	8	122,57	28	A_5
Ribosomal protein L14 - human	7513316	10,94	23,8	9	145,41	36	H_6
Serine/threonine-protein phosphatase 2A catalytic subunit alpha isoform	3342500	35,63	5,3	3	54,31	12	A_4
Serum Albumin	51476390	69,4	5,88	3	48,25	4	H_3
Short/branched chain specific acyl-CoA dehydrogenase, mitochondrial	4501859	47,48	6,53	5	90,39	14	H_4
Sphingosine phosphate lyase 1	50510859	65,44	9,27	3	43,05	5	A_1
Trifunctional enzyme subunit beta, mitochondrial	15778991	51,38	9,44	8	121,81	18	H_3
Tubulin alpha-1B chain	34740335	50,15	4,94	8	121,45	23	A_1
Tubulin beta chain	18088719	49,67	4,75	9	153,85	29	H_3
Tubulin beta-4A chain	12851187	49,52	4,81	5	76,34	12	A_2
Tubulin, beta 2C	23958133	49,84	4,83	7	118,43	23	H_3
Tubulin, beta 5	148691289	49,94	4,78	6	101,7	16	A_1
Ubiquitin carboxyl-terminal hydrolase	34851150	129	5,49	8	119,21	8	H_2

Table 3. 1 Orlistat targets in (phospho)lipolytic proteome of HepG2 (human) and differentiated 3T3-L1 (mouse) cell lysates in one dimensional gel electrophoresis. The proteins in this list were identified as described in experimental procedure. Protein band numbers are indicated as “Hx” and “Ax” for human HepG2 and mouse adiposities (3T3-L1), respectively. “X” corresponds to band numbers in Figures 3.3, 3.4 and 3.6.

3.6 Discussion

We established and applied DABGE method for the screening of proteins that are targeted by drugable inhibitors. This technique is based on fluorescence labeling of proteins by activity based probes that recognize nucleophilic serines and cysteines. Potential protein targets are therefore serine hydrolases, preferentially lipases and phospholipases, carboxyl esterases, thioesterases and amide hydrolases (15). In addition it cannot be ruled out that other unrelated proteins are tagged by probes. It has to be emphasized that the method presented in this work is generally applicable to the screening of potential inhibitor of lipolytic enzymes.

To demonstrate the feasibility of this technique for identifying drug targets in cells, we decided to analyze the targets of Orlistat as a drugable lipase inhibitor (e.g. pancreatic lipase) and CAY10499 as a commercially available as lipase inhibitor (e.g. hormone sensitive lipase) in lysates of HepG2 and 3T3-L1.

Table 3.1 summarizes the proteins that were identified as targets of these “drugs” using the novel technique. Basically, we found three main groups of proteins that is: 1. (phospho)lipases; 2. other lipid-associated proteins and 3. proteins virtually unrelated to lipids.

It is known that lipoprotein lipase (LPL) hydrolyzes triacylglycerols (TAG) and to lesser extent phospholipids (PLs) in chylomicrons and very low-density lipoproteins (VLDLs) (21). In addition LPL serves a role in binding of lipoproteins to cell surface receptor (22, 23, 24). LPL deficiency in the body is associated with severe disorders including hypertriglyceridemia (25). In studies by Lookene et al. (26) it is shown that LPL activity can

be inhibited by Orlistat *in vitro*. In agreement with this data LPL was identified in our study as a target of Orlistat in mouse adipocytes (3T3-L1 cells).

Another target protein found in mouse adipocytes is abhydrolase 5 (ABDH5), also known as CGI-58. This polypeptide is important for enzyme catalyzed lipid metabolism. First of all it is an activator of the main triacylglycerols hydrolase (phospholipase patatin-like phospholipase domain-containing protein 2, PNPLA2, ATGL). Secondly, it catalyzes the acylation of lysophosphatidic acid leading to the formation of phosphatidic acid. Therefore, CGI-58 plays at least indirectly an important role in lipid signaling since both compounds are second big messengers (27). It has already been found by previous studies in our group that CGI-58 is covalently tagged by Ethyl-Cy probe (15). Obviously, the sites of Ethyl-Cy binding and Orlistat binding in this proteins must be the same. Because in this study we found that fluorophore is no longer bound if the cell lysate is preincubated by Orlistat.

Among phospholipid hydrolyzing enzymes platelet activating factor acetylhydrolase (PAF AH) was identified as Orlistat target in HepG2 cells. Specifically we found platelet activating factor acetylhydrolase 1b subunit gamma (pafah 1b3). Alpha 1 subunit of this protein is a G-protein like (α1,α2)β trimer and can inactivate platelet activating factor (PAF). The same motif has already been found in p21 ras and other GTPases (28, 29). The effects of PAFAH 1b3 homozygosity is associated with mental retardation and ataxia (30) suggesting a functional importance of the catalytic subunits of Pafah1b in brain development. Interestingly we have not found PAFAH isoform in HepG2 cells that catalyze degradation of PAF and oxidized phospholipids. If these enzymes were affected by Orlistat this would have severe consequences for the detoxification of respective inflammatory and atherogenic lipids.

Notable lysophospholipase 1 and 2 have been found as targets of Orlistat. Providing additional evidence that Orlistat does not only interfere with neutral lipid but also with phospholipid catabolism.

Group XV phospholipase A_2 was targeted by Orlistat in mouse adipocytes. This protein represents an important enzyme at the cross road of sphingolipid and glycerophospholipid metabolism. *In vitro* it catalyzes transacylation and phospholipid degradation (31). In cells catalyzes the transfer of sn-2 acyl chains from PE and PC to the 1 hydroxy position of the ceramide. As the consequence this enzyme interferes with apoptotic signaling which may be mediated by distinct ceramide species (32-34).

An important target of Orlistat is fatty acid synthase (FAS). The drug covalently blocks the -SH group of the phosphopatatin domain of the enzyme which usually carries the growing fatty acyl chain in a thioester bound form (35). This enzyme has already been identified as Orlistat target by another group (10). Inhibition of FAS leads to severe consequences for cell physiology. It plays crucial role in energy homeostasis and proliferation of cells. FAS inhibition exhibits anti-proliferative effects in tumorigenic cells (36) and therefore makes this enzyme an interesting candidate for anti cancer therapies.

Yang and colleagues also identified targets of Orlistat in HepG2 cells. Some of the targets found by Yang et al. (10, 11) were also found in our studies. Those were lipid-associated enzymes: dihydrolipoyl dehydrogenase and acyl-CoA dehydrogenase. Other Orlistat – tagged proteins found by Yang et al. and also identified in our study are: annexin 2, β-tubulin, HLA class I histocompatibility antigen A-2 alpha chain (HLA-A), glyceraldehyde-3-phosphate dehydrogenase (GAPDH), 60S ribosomal protein L14 and L7, pyruvate carboxylase. Some studies indicate that GAPDH could be involved in cell proliferation of cancer cells (37). Tubulins are well studied targets of anticancer drugs (e.g. taxol (38)).

Ribosomal proteins are involved in protein synthesis, control of cellular transformation, tumor growth and aggressiveness and metastasis. Ribosomal proteins are overexpressed in some cancers (colon, brain, liver, breast and prostate (39-42) and their inhibition by Orlistat could be beneficial for anticancer therapy) (10). The functional consequences of protein binding to Orlistat must be subject to further clarification.

Another target identified in our study is pyruvate dehydrogenase. Interestingly, this enzyme contains the conserved lipase motif (GASAG). This unexpected structural motif in a dehydrogenase, could explain its tagging by a lipase inhibitor.

All proteins identified as Orlistat targets in our study also showed capacity of reacting with another commercial inhibitor, CAY10499. Therefore it looks as if Orlistat, which is pharmacological drug, does not display any specific targeting in cells compared to other serine hydrolase inhibitors. The situation could be different in live cells since drug efficiency also depends on cellular uptake. Such studies are currently under the way in our laboratory.

According to our data Orlistat inhibits FAS and glycerol lipid degradation. Thus, at the first glance steady state concentrations of acylglycero lipids can be expected not to change much. This assumption is in line with our observation that cellular levels of TAG, PE and PC are similar in control cells and Orlistat treated cells. Surprisingly, small changes are seen at 2 µM Orlistat concentration. So currently we do not have explanation for this effect. In contrast to TAG levels the amount of DAG in the cell significantly increased under the influence of 2 µM Orlistat. Since diacylglycerols represent biologically active second messengers (activation of protein kinase C) this effect would deserve further investigation. For instance, in some cancer cells fatty acid preferably incorporates in membrane instead of TAG reserves. The formation of DAG from phospholipids in plasma membrane leads to

activation of protein kinase C and therefore stimulates cell proliferation. DAG formation in lipid droplets would not induce such an effect (see Chapter 4).

In summary, we established DABGE as technique for drug screening using fluorescent activity-based probes. In this study we applied this method for the identification of Orlistat targets in HepG2 and 3T3-L1 adipocytes. We found that Orlistat inhibits a series of serine/cysteine-type lipid-hydrolases as well as lipid-associated proteins. The enzyme patterns affected by Orlistat are cell specific. The large number of lipid synthesizing and degrading enzymes affected by the drug helps understand the anti-obesity and possible anti-cancer activity of Orlistat. On the other hand, it also shows that this compound may be associated with number of unwanted side effects.

3.7 Acknowledgment

This work was supported by grants from the Austrian Federal Ministry of Science and Research/FFG in the framework of the GEN-AU program (GOLD project).

3.8 References

1. Birner-Gruenberger, R., H. Susani-Etzerodt, M. Waldhuber, G. Riesenhuber, H. Schmidinger, G. Rechberger, M. Kollroser, J. G. Strauss, A. Lass, R. Zimmermann, G. Haemmerle, R. Zechner, and A. Hermetter. 2005. The lipolytic proteome of mouse adipose tissue. *Mol. Cell. Proteomics* **4:** 1710-1717.
2. James, W. P. T. 2008. The epidemiology of obesity: The size of the problem. *J. Intern. Med.* **263:** 336-352.
3. Blaak, E. E. 2003. Fatty acid metabolism in obesity and type 2 diabetes mellitus. Proc. Nutr. Soc. **62:** 753-760.
4. Kang, J. G., C. Y. Park. 2012. Anti-Obesity Drugs: A Review about Their Effects and Safety. *Diabetes Metab. J.* **36:** 13-25.
5. Filippatos, T. D., C. S. Derdemezis, I. F. Gazi, E. S. Nakou, D. P. Mikhailidis, and M. S. Elisaf. 2008. Orlistat-associated adverse effects and drug interactions: A critical review. *Drug Safety* **31:** 53-65.
6. Luthi-Peng, Q., H. P. Marki, and P. Hadvary. 1992. Identification of the active-site serine in human pancreatic lipase by chemical modification with Orlistat. *FEBS Lett.* **299:** 111-115.
7. Borgstrom, B. 1988. Mode of action of Orlistat: A derivative of the naturally occurring lipase inhibitor lipstatin. *Biochimica et Biophysica Acta - Lipids and Lipid Metabolism* **962:** 308-316.
8. Dahlin, A., B. Beermann. 2007. Incorrect use of orlistat and sibutramine in clinical practice. *Eur. J. Clin. Pharmacol.* **63:** 205-209.
9. Zhi, J., A. T. Melia, H. Eggers, R. Joly, and I. H. Patel. 1995. Review of limited systemic absorption of orlistat, a lipase inhibitor, in healthy human volunteers. J. Clin. Pharmacol. **35:** 1103-1108.
10. Yang, P. -., K. Liu, M. H. Ngai, M. J. Lear, M. R. Wenk, and S. Q. Yao. 2010. Activity-based proteome profiling of potential cellular targets of orlistat - An FDA-approved drug with anti-tumor activities. *J. Am. Chem. Soc.* **132:** 656-666.

11. Yang, P. -., K. Liu, C. Zhang, G. Y. J. Chen, Y. Shen, M. H. Ngai, M. J. Lear, and S. Q. Yao. 2011. Chemical modification and organelle-specific localization of Orlistat-like natural-product-based probes. *Chemistry - An Asian Journal* **6:** 2762-2775.
12. Kuhajda, F. P. 2006. Fatty acid synthase and cancer: New application of an old pathway. *Cancer Res.* **66:** 5977-5980.
13. Kuhajda, F. P. 2000. Fatty-acid synthase and human cancer: New perspectives on its role in tumor biology. *Nutrition* **16:** 202-208.
14. Kuhajda, F. P., K. Jenner, F. D. Wood, R. A. Hennigar, L. B. Jacobs, J. D. Dick, and G. R. Pasternack. 1994. Fatty acid synthesis: A potential selective target for antineoplastic therapy. *Proc. Natl. Acad. Sci. U. S. A.* **91:** 6379-6383.
15. Morak, M., H. Schmidinger, P. Krempl, G. Rechberger, M. Kollroser, R. Birner-Gruenberger, and A. Hermetter. 2009. Differential activity-based gel electrophoresis for comparative analysis of lipolytic and esterolytic activities. *J. Lipid Res.* **50:** 1281-1292.
16. Greenspan, P., E. P. Mayer, and S. D. Fowler. 1985. Nile red: A selective fluorescent stain for intracellular lipid droplets. *J. Cell Biol.* **100:** 965-973.
17. Bradford, M. M. 1976. A rapid and sensitive method for the quantitation of microgram quantities of protein utilizing the principle of protein-dye binding. *Anal. Biochem.* **72:** 248-254.
18. Fling, S. P., D. S. Gregerson. 1986. Peptide and protein molecular weight determination by electrophoresis using a high-molarity tris buffer system without urea. *Anal. Biochem.* **155:** 83-88.
19. Shevchenko, A., M. Wilm, O. Vorm, and M. Mann. 1996. Mass spectrometric sequencing of proteins from silver-stained polyacrylamide gels. *Anal. Chem.* **68:** 850-858.
20. Hartler, J., M. Trotzmuller, C. Chitraju, F. Spener, H. C. Kofeler, and G. G. Thallinger. 2011. Lipid Data Analyzer: unattended identification and quantitation of lipids in LC-MS data. *Bioinformatics* **27:** 572-577.
21. Eckel RH. Lipoprotein lipase. A multifunctional enzyme relevant to common metabolic diseases. 1989. *N.Engl.J.Med.* **320:** 1060-1068.
22. Olivecrona, T., G. Bengtsson-Olivecrona. 1993. Lipoprotein lipase and hepatic lipase. *Curr. Opin. Lipidol.* **4:** 187-196.

23. Beisiegel U, Weber W, Bengtsson-Olivecrona G. 1991. Lipoprotein lipase enhances the binding of chylomicrons to low density lipoprotein receptor-related protein. *Proc. Natl Acad. Sci. USA* **88:** 8342-8346.
24. S Eisenberg, E Sehayek, T Olivecrona, and I Vlodavsky. 1992. Lipoprotein lipase enhances binding of lipoproteins to heparan sulfate on cell surfaces and extracellular matrix. *J. Clin. Invest.* **90:** 2013-2021.
25. Okubo M, Horinishi A, Saito M, et al. 2007. A novel complex deletion-insertion mutation mediated by Alu repetitive elements leads to lipoprotein lipase deficiency. Mol. *Genet. Metab.* **92 (3):** 229–33.
26. Lookene, A., N. Skottova, and G. Olivecrona. 1994. Interactions of lipoprotein lipase with the active-site inhibitor Orlistat (Orlistat)®. *European Journal of Biochemistry* **222:** 395-403.
27. Lord, C. C., J. L. Betters, P. T. Ivanova, S. B. Milne, D. S. Myers, J. Madenspacher, G. Thomas, S. Chung, M. Liu, M. A. Davis, R. G. Lee, R. M. Crooke, M. J. Graham, J. S. Parks, D. L. Brasaemle, M. B. Fessler, H. A. Brown, and J. M. Brown. 2012. CGI-58/ABHD5-derived signaling lipids regulate systemic inflammation and insulin action. *Diabetes* **61:** 355-363.
28. Hattori, M., H. Arai, and K. Inoue. 1993. Purification and characterization of bovine brain platelet-activating factor acetylhydrolase. *J. Biol. Chem.* **268:** 18748-18753.
29. Ho, Y. S., L. Swenson, U. Derewenda, L. Serre, Y. Wei, Z. Dauter, M. Hattori, T. Adachi, J. Aoki, H. Arai, K. Inoue, and Z. S. Derewenda. 1997. Brain acetylhydrolase that inactivates platelet-activating factor is a G-protein-like trimer. *Nature* **385:** 89-93.
30. Nothwang, H. G., H. G. Kim, J. Aoki, M. Geisterfer, S. Kübart, R. D. Wegner, A. Van Moers, L. K. Ashworth, T. Haaf, J. Bell, H. Arai, N. Tommerup, H. H. Ropers, and J. Wirth. 2001. Functional hemizygosity of PAFAH1B3 due to a PAFAH1B3-CLK2 fusion gene in a female with mental retardation, ataxia and atrophy of the brain. *Hum. Mol. Genet.* **10:** 797-806.
31. Abe, A., J. A. Shayman. 1998. Purification and characterization of 1-O-acylceramide synthase, a novel phospholipase A2 with transacylase activity. *J. Biol. Chem.* **273:** 8467-8474.
32. Abe, A., N. S. Radin, and J. A. Shayman. 1996. Induction of glucosylceramide synthase by synthase inhibitors and ceramide. *Biochimica et Biophysica Acta - Lipids and Lipid Metabolism* **1299:** 333-341.

33. Abe, A., J. A. Shayman, and N. S. Radin. 1996. A novel enzyme that catalyzes the esterification of n-acetylsphingosine: Metabolism of C2-ceramides. *J. Biol. Chem.* **271:** 14383-14389.
34. Rani, C. S. S., A. Abe, Y. Chang, N. Rosenzweig, A. R. Saltiel, N. S. Radin, and J. A. Shayman. 1995. Cell cycle arrest induced by an inhibitor of glucosylceramide synthase. Correlation with cyclin-dependent kinases. *J. Biol. Chem.* **270:** 2859-2867.
35. Pemble IV, C. W., L. C. Johnson, S. J. Kridel, and W. T. Lowther. 2007. Crystal structure of the thioesterase domain of human fatty acid synthase inhibited by Orlistat. *Nature Structural and Molecular Biology* **14**: 704-709.
36. Flavin, R., S. Peluso, P. L. Nguyen, and M. Loda. 2010. Fatty acid synthase as a potential therapeutic target in cancer. *Future Oncology* **6:** 551-562.
37. Phadke MS, Krynetskaia NF, Mishra AK, Krynetskiy E. GAPDH depletion induces cell cycle arrest and resistance to antimetabolites in human carcinoma cell lines. *J. Pharm. Exp. Therapy* (2009) **331:** 77-86
38. Kingston, D. G. I., D. J. Newman. 2007. Taxoids: Cancer-fighting compounds from nature. *Current Opinion in Drug Discovery and Development.* **10:** 130-144.
39. Zhu, Y., H. Lin, Z. Li, M. Wang, and J. Luo. 2001. Modulation of expression of ribosomal protein L7a (rpL7a) by ethanol in human breast cancer cells. *Breast Cancer Res. Treat.* **69:** 29-38.
40. Liu, Y., X. Zhu, J. Zhu, S. Liao, Q. Tang, K. Liu, X. Guan, J. Zhang, and Z. Feng. 2007. Identification of differential expression of genes in hepatocellular carcinoma by suppression subtractive hybridization combined cDNA microarray. *Oncol. Rep.* **18:** 943-951.
41. Wang, Y., D. Cheong, S. Chan, and S. C. Hooi. 2000. Ribosomal protein L7a gene is up-regulated but not fused to the tyrosine kinase receptor as chimeric trk oncogene in human colorectal carcinoma. *Int. J. Oncol.* **16:** 757-762.
42. Vaarala, M. H., K. S. Porvari, A. P. Kyllönen, M. V. J. Mustonen, O. Lukkarinen, and P. T. Vihko. 1998. Several genes encoding ribosomal proteins are over-expressed in prostate-cancer cell lines: Confirmation of L7a and L37 over-expression in prostate-cancer tissue samples. *International Journal of Cancer* **78:** 27-32.

3.9 Supplemental data

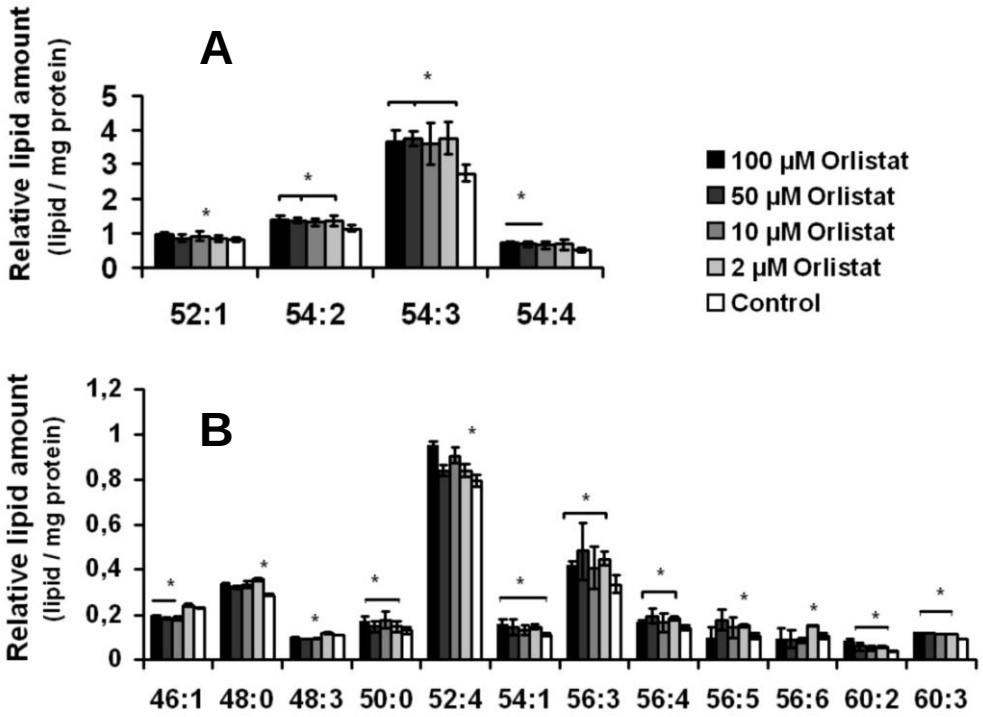

Figure S 1 Effects of Orlistat on triacylglycerol species. Cells were incubated for 3 h with different concentrations of Orlistat and lipids were analyzed as described in the legend to Figure 3.6.

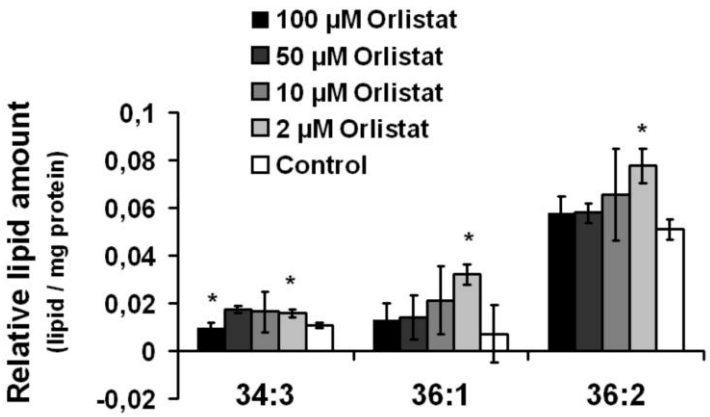

Figure S 2 Effects of Orlistat on diacylglycerol species. Cells were incubated for 3 h with different concentrations of Orlistat and lipids were analyzed as described in the legend to Figure 3.6.

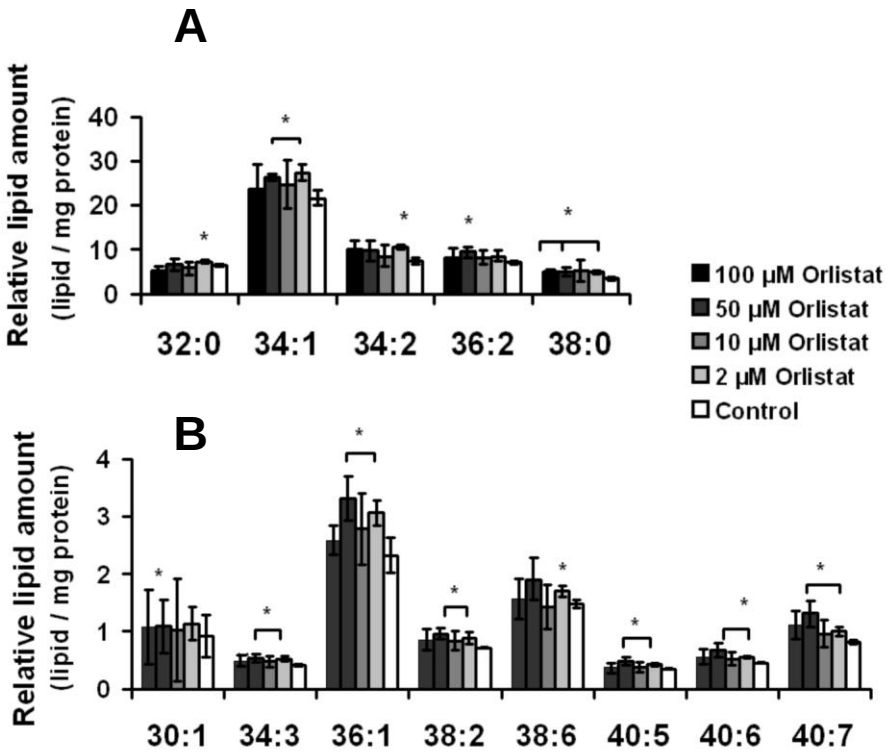

Figure S 3 Effects of Orlistat on glycerophospholipid – phosphatidylcholine species. Cells were incubated for 3 h with different concentrations of Orlistat and lipids were analyzed as described in the legend to Figure 3.6.

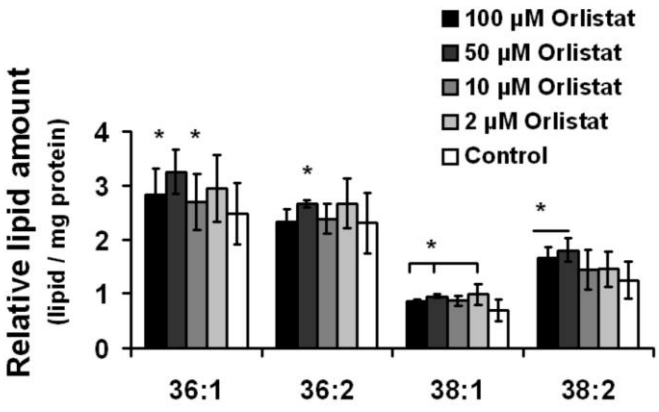

Figure S 4 Effects of Orlistat on glycerophospholipid – phosphatidylethanolamine species. Cells were incubated for 3 h with different concentrations of Orlistat and lipids were analyzed as described in the legend to Figure 3.6.

Chapter 4

Toxicity and protein targets of Orlistat in cultured human squamous carcinoma cells

Bojana Stojčić[1], Franziska Vogl[1], Gerald Rechberger[2], Manfred Kollroser[3], Helmut Schaider[4] and Albin Hermetter[1]

[1] Institute of Biochemistry, Graz University of Technology, Austria

[2] Institute of Molecular Bioscience, University of Graz, Austria

[3] Institute of Forensic Medicine, University of Graz, Austria

[4] Institute of Dermatology, Medical University of Graz, Austria

4.1 Abbreviations

AR	Androgen receptor
Co	Coenzyme
CPT-1	Carnitine palmitoyltranferase-1
DABGE	Differential activity-based gel electrophoresis
DMEM	Dulbecco's Modified Eagle Medium
Edelfosin	1-octadecyl-2-O-methyl-glycero-3-phosphocholin
EGFR	Epidermal growth factor receptor
ER	Estrogen receptor
FACS	Fluorescence activated cell sorter
FAS	Fatty acid synthase
HaCaT	Human Adult low Calcium high Temperature Keratinocytes
HaCaT-RT3	Ras transformed HaCaT cell line
HER2	Human epidermal growth factor receptor 2
MAPK	Mitogen activated pathway kinase
MET-4	Lymph node metastatic cell line
MH+	Positive ion mod
MS	Mass spectrometry
NADPH	Nicotinamide adenine dinucleotide phosphate
Pen/Strep	Penicillin/Streptomycin
PC	Phosphatidylcholine
PE	Phosphatidylethanolamine

PI3K	Phosphatidylinositol-3-kinase
PON2	Paraoxonase 2 (serum paraoxonase/arylesterase 2)
PR	Progesterone receptor
RPMI	Roswell Park Memorial Institute
SCC12	Squamous carcinoma cell line 12
SCC13	Squamous carcinoma cell line 13
SDS-PAGE	Sodium dodecyl sulfate – polyacrylamide gel electrophoresis
SREBP1c	Sterol regulating element binding protein 1-c
TAG	Triacylglycerol
UPLC	Ultra Performance Liquid Chromatography

4.2 Abstract

This study aimed at identifying protein targets of Orlistat in cultured human squamous carcinoma cells. For this purpose, we used differential activity-based gel electrophoresis (DABGE) for the detection of lipolytic enzymes and FAS in different skin cancer cell lines. This technique allows for comparative analysis of proteins from two different samples in one electrophoresis gel. Typically, proteins of control cells and cells pretreated with Orlistat were labeled with fluorescent p-nitrophenyl phosphonate esters as activity-based probes, which contained the same reactive group but only differed by their reporter fluorophore. After sample mixing, protein separation and fluorescence detection, Orlistat targets were identified as described in chapter 3. Various cancer cells were studied including the cell lines SCC12 and SCC13 as well as immortalized keratinocytes (HaCaT). The identified protein targets included fatty acid synthase, (phospho)lipases and lipid-unrelated proteins. Targeting of some of these polypeptides by Orlistat explains at least in part the profound apoptotic activity of this anti-obesity drug in cancer cells.

4.3 Introduction

Skin is the biggest organ in the body and has important protective and regulatory roles. It is composed of different layers (e.g. epidermis and dermis), which contain a number of different cell types. Depending on the cell type, different skin cancer can develop. Many different methods for treatment of skin cancers (surgery, chemotherapy etc.) are available (1) but improvement and development of new less invasive and harmful therapies are still needed.

Recently, it has been discovered that the anti-obesity drug Orlistat could be used as a potential anti-cancer drug. Orlistat is a pharmacological inhibitor of lipases and is administrated orally for anti-obesity treatment. As such it mainly inhibits the lipolytic enzymes of digestive tract and thus reduces the amount of absorbed lipid eventually leading to a reduction in depot fat weight (2). Apart from its anti-lipolytic activity, Orlistat targets the thiol domain of fatty acid synthase (FAS) and as a consequence inhibits the activity of this enzyme, too (3). It has been shown that the activity of FAS is upregulated in some cancerous cells such as prostate, breast and ovarian cancer as well as melanoma (4-13). Due to FAS inhibition, Orlistat reduces tumor proliferation and induces apoptosis (14). FAS is an important lipid synthesizing enzyme in mammalians as it catalyzes *de novo* production of long-chain fatty acids from acetyl-CoA and malonyl-CoA utilizing 14 ATP and 7 NADPH per fatty acid (15). Primarily, it generates palmitate in liver, adipose and cancer tissue. However, the fate of palmitic acid differs between cancer cells and lipogenic tissues. In lipogenic tissue, fatty acid synthase is highly active if energy is abundant to store excess in triacylglycerols. In cancer cells excess energy is not channeled in triacylglycerols, in this case synthesized fatty acids are predominantly esterified to phospholipids (16). FAS expression in normal cells is regulated through insulin, glucagon, glucocorticoids and

thyroid hormone (17). In contrary, FAS expression in cancer cells seems to be regulated at multiple levels (e.g. through kinase pathways including: mitogen-activated protein (MAP) kinase and phosphatidylinositol-3-kinase (PI3K), via the sterol regulating element binding protein 1-c (SREBP1c) (18, 19)), which contribute to the higher levels of FAS in cancer cells (14). There is evidence that FAS plays a role in tumor growth and survival (20). Inhibition of FAS induces cell death, though the molecular mechanisms of this (beneficial) effect which is still unknown (21). Both, fatty acid synthesis catalyzed by FAS and fatty acid liberation catalyzed by lipolytic enzymes contribute to the development of cancers (21). Therefore, the idea of using Orlistat (FAS and lipase inhibitor) for anti-cancer therapy has received much interest.

Knowing the protein targets of Orlistat could help better understand the mechanism of its anti-proliferative and apoptotic effects on cancer cells. Thus, we initiated a study to identify protein targets of Orlistat in cultured human squamous carcinoma cells. For this purpose, we used differential activity-based gel electrophoresis (DABGE) for the detection of lipolytic enzymes and FAS in different skin cancer cell lines. This technique allows for comparative analysis of proteins from two different samples in one electrophoresis gel. Typically, proteins of control cells and cells pretreated with Orlistat were labeled with fluorescent p-nitrophenyl phosphonate esters as activity-based probes, which contained the same reactive group but only differed by their reporter fluorophore. After sample mixing, protein separation and fluorescence detection, Orlistat targets were identified as described in chapter 3. Various cancer cells were studied including the cell lines SCC12 and SCC13 as well as immortalized keratinocytes (HaCaT). The identified protein targets included fatty acid synthase, (phospho)lipases and lipid-unrelated proteins. Targeting of some of these polypeptides by Orlistat explains at least in part the profound apoptotic activity of this anti-obesity drug in cancer cells.

4.4 Experimental procedures

4.4.1 Cell culture

HaCaT human keratinocytes were provided from Dr. Helmut Schaider (Cancer Biology Unit, Institute of Dermatology, Medical University of Graz, Austria). Squamous carcinoma cell lines SCC12 and SCC13 cells were provided by Dr. James G. Rheinwald (Department of Dermatology, Brigham and Women's Hospital, Harvard Medical School, Boston, Massachusetts). HaCaT-RT3 and MET-4 cells were kindly provided by Dr. Petra Boukamp (German Cancer Research Center, Heidelberg, Germany).

SCC13 and SCC12 cell lines were grown in RPMI-1640 medium from Invitrogen (Lofer, Austria) supplemented with 10% FCS, 1% Pen/Strep (100 U) and 2% L-Glutamine. HaCaT, HaCaT-RT3 and MET-4 were grown in DMEM, high glucose (4,5 g/L), 25 mM HEPES from Invitrogen (Lofer, Austria) supplemented with 10% FCS, 1% Pen/Strep (100 U). Cell lines were grown under an atmosphere containing 5% CO_2 at 37°C.

4.4.1.1 Origin of cell lines

Human Adult low Calcium high Temperature Keratinocytes or HaCaT are spontaneously immortalized human keratinocytes (22). Studies have shown that mutational inactivation of p53 as well as some other genetic aberrations are not enough to cause these cells as tumorigenic and therefore are similar to normal keratinocytes and used as healthy cells in experimental studies (22, 23).

The number of non-melanoma skin cancer malignancies is continuously increasing in our society (24). In order to study these cancers, models of cell lines derived from human skin carcinomas are needed. Squamous carcinoma cell lines are one the most important malignant variant of the keratinocytes (25). In this study we mainly focused on: SCC12, SCC13, MET-4 and HaCaT-RT3.

SCC12 and SCC13 were cultured from SCC's of the facial epidermis. SCC12 was isolated from a 60-year-old male kidney transplant recipient who had been treated with immunosuppressive drugs for the previous 7 years. SCC13 was isolated from a 56-yearold female who had received a series of radiation treatments for the tumor for several years before its surgical removal (25).

MET-4 is a metastatic cell line derived from metastatic lymph nodes isolated from a single renal transplant recipient who suffered from multiple SCC (26).

HaCaT-RT3 is a ras transformed HaCaT cells with a malignant phenotype (25).

4.4.2 Preparation of cell lysates

Cells were scraped and sonicated at 40 W for 20 seconds in 50 mM Tris/HCl buffer containing protease inhibitors (20 µg/ml leupeptin, 2 µg/ml antipain and 1 µg/ml pepstatin). To obtain the cytoplasmic fraction, cell debris was removed by centrifugation at 1.000 x g at 4°C for 15 minutes. Protein concentration was determined by the Bio-Rad protein assay based on the Bradford method (27). Supernatant was collected and used for further experiments.

4.4.3 Drug targeting and activity tagging of (phospho)lipolytic enzymes in cell lysates (DABGE)

Cell lysates were preincubated with Orlistat as follows: for 300 µl of cell lysate the following sample was prepared: 3 µl 100 mM Triton X-100 in $CHCl_3$ (final sample concentration: 1 mM) and 1,5 µl 20 mM Orlistat in DMSO (final concentration: 100 µM, if not stated otherwise) were mixed. The organic solvent was removed under the stream of argon. The cell lysate was added and samples were incubated at 37°C and 550 rpm for an hour.

Preincubated and untreated cell lysates were used for DABGE experiments (28). Typically, samples of 150 µl cell lysate containing 150 µg protein were labeled with fluorescence inhibitors as follows: 1,5 µl of 100 mM Triton X-100 in $CHCl_3$ (final sample concentration: 1 mM) and a solution of 1,5 nmol of Ethyl-Cy-tagged inhibitors in $CHCl_3$ (final concentration: 10 µM) were mixed and the organic solvent was removed under a stream of argon. Cell lysates (1 µg/µl), preincubated with Orlistat, were incubated with 10 µM of Ethyl-Cy3 at 37°C and 550 rpm for 2h. The same volume of untreated cell lysate was incubated with Ethyl-Cy5 under the same conditions. In a Dye-Swap experiment lysates pretreated with the drug were labeled with Ethyl-Cy5 and untreated lysates were labeled with Ethyl-Cy3. Identical volumes of both samples were mixed and protein was precipitated by addition of 500 µl acetone and the samples were stored overnight at -20°C. Precipitated protein was collected by centrifugation at 14.000 x g at 4°C for 20 min and resuspended in 1D SDS-PAGE sample buffer (20 mM KH_2PO_4, 6 mM EDTA, 6 % SDS, 10 % glycine and 0,05 % bromophenol blue, pH 6,8 and 20 µl/ml mercaptoethanol). Samples were preheated for 5 minutes at 95°C prior to loading onto the gel.

4.4.4 One dimensional gel electrophoresis

For protein separation, we used one dimensional gel electrophoresis according to the method of Fling and Gregerson (29). We used 1x running buffer which contained: 3 g/L Tris, 0.334 g/L EDTA, 5 g/L SDS and 14,2 g/L glycine) in ddH_2O. Proteins were separated at constant current (10 mA per gel) for the first 15 minutes followed by 20 mA per gel for an hour using a Bio-Rad Mini PROTEAN 3 apparatus at 4°C.

4.4.5 Fluorescence detection of proteins in electrophoresis gels

Gels were fixed in fixing solution (7% acetic acid and 10% ethanol) for at least 30 minutes and scanned at a resolution of 100 µm using a Bio-Rad Molecular Imager^{TM} FX Pro Plus. Fluorescence detection was carried out at different excitation wavelengths (532 nm and 635 nm) and emission wavelengths (555 nm and 695 nm) for Cy3 and Cy5, respectively.

Proteins were visualized after staining with Sypro^{TM} ruby solution. The staining solution was obtained after dilution of 100 µl of aqueous RuBPS stock solution (20 mM) in one liter of 20% Ethanol in ddH_2O. Gels were stained with Sypro ruby^{TM} solution for at least 2 h and incubated in fixing solution for at least 2 h. Sypro ruby^{TM} fluorescence was scanned at emission and excitation wavelengths of 605 nm and 488 nm, respectively. Fluorescence signals were quantified by a Bio-Rad Image Lab^{TM} Software Version 2.0.1.

4.4.6 LC-MS/MS analysis of target proteins

For the identification of drug – affected proteins, protein bands were excised from gels and tryptically digested according to the Method by Shevchenko et al. (30).

Peptide extracts were dissolved in 0.1% formic acid and separated by nano-HPLC (FAMOS^{TM} autosampler, SWITHOS^{TM} loading system, and ULTIMATE^{TM} dual gradientsystem system; LC-Packings, Amsterdam, The Netherlands) as described in (31), but using the following solvent gradient: solvent A: water, 0.3% formic acid; solvent B: acetonitrile/water 80/20 (v/v), 0.3% formic acid; 0 to 5 min: 4% B, after 40 min 55% B, then for 5 min 90 % B, and 47 min reequilibration at 4% B. The samples were ionized in a Finning nano-ESI source equipped with NanoSpray tips (PicTip^{TM} Emitter; New Objective, Woburn, MA) and analyzed in a Thermo-Finnigan LTQ linear ion trap mass spectrometer (Thermo, San Jose, CA).

The MS/MS data were analyzed by searching the NCBI non redundant public database with SpectrumMill Rev A.03.03.084 SR4.

4.4.7 Lipid extraction and analysis

SCC13 cells were seeded out a day prior to use onto 10 cm diameter cultured dishes. The cells were incubated with different concentrations of Orlistat in 3 ml standard medium. Cells were incubated with media obtained by stock solutions of Orlistat in DMSO to standard medium for 3 h. The final concentrations of Orlistat in the incubation media were 0 µM (control), 2 µM and 50 µM. Each sample contained 1 % DMSO in final incubation volume. After incubation, the medium was removed and cells were washed twice with cold PBS and followed by scraping into pyrex tubes on ice. The cell pellet was isolated by centrifugation at 1.000 rpm (Eppendorf Centrifuge 5810R) at 4°C for 5 minutes. 50 µl of a solution of 0.05 mg/ml of internal standard (containing 45:0, 51:0, 57:0 glycerolipids, respectively) in chloroform was added to the cell pellet. 3 ml of $CHCl_3$/MeOH (2:1, v/v) were added and the suspension was vortexed at 4°C for 1 h. 700 µl of (0,036%) $MgCl_2$- Solution was added and the sample was again shaken at 4°C for 15 minutes. Phase separation was completed after

centrifugation at 2.400 rpm (Eppendorf Centrifuge 5810R) at room temperature for 2 minutes. The lower chloroform phase was isolated and the organic solvent was removed under a stream of nitrogen. The lipid extracts were further analyzed with UPLC-QTOF-MS. Briefly, samples were dissolved in chloroform/MeOH (2:1, v: v), diluted with 2-propanol (1:20, v: v) and lipids were separated with an AQUITY-UPLC system (Waters, Manchester, UK) using a BEH-C18-column, 2.1x150 mm, 1.7 µm column (Waters). Lipids were separated using a gradient solvent from 55% solvent A (water: MeOH 1:1, v:v) and 45% solvent B (2-propanol), both containing 1% ammonium-acetate, 0.1% formic acid and 8 µM H_3PO_4) to 100% solvent B. Separation time was 35 minutes and column temperature was 50°C.

Triacylglycerols (TAG), diacylglycerols (DAG), phosphatidylcholine (PC) and phosphatidylethanolamine (PE) were analyzed using the SYNAPT™G1 qTOF HDMS (Waters), equipped with an ESI ion source (positive mode) using LeucinEnkephalin as lock mass. Capillary voltage was set 2.6 kV and capillary temperature to 100°C. The MS was operated in V-mode.

Data analysis was performed using the “Lipid Data Analyzer” software (32). The relative values of lipid content are normalized over the amount of internal lipid standard lipid and over the total protein concentration according to : $A_{Sample}/(A_{intern\ standard}$*mg Protein).

4.4.8 Microscopy

SCC12 and SCC13 cells were seeded out to 100% confluence into Lab-Tek™Chamber Slide System from Nunc (Nalgene, Rochester, USA) for microscopic inspection. Both cell lines were incubated with different samples in RPMI-1640 serum rich medium (no phenol red): 1 % DMSO, control; 10 mM H_2O_2, induces necrosis; 10 µM, 100 µM or 200 µM

Orlistat. Time dependent effects of Orlistat on morphology of human non-melanoma skin cancer cells were visualized with microscopic transmission light images (magnification 320x).

4.4.9 Caspase 3 activity Assay

Ten thousand SCC13 cells were seeded out in Corning/Costar 96 well microplates treated with flat clear bottom black TC from VWR (Vienna, Austria) 8 h prior to incubation. Cells were incubated with 100 µl of different samples in RPMI 164 serum rich medium (no phenol red): 0 µM Orlistat, control; 10 µM, 50 µM and 50 µM Orlistat for 20 h. Orlistat was diluted in DMSO. The end volume of DMSO in each sample was 0,5 %. In order to measure the caspase 3/7 activity we used Apo-ONE ® Homogeneous Caspase-3/7 Assay from Promega (Madison, USA). Briefly, the assay is based on cleavage of the non-fluorescent Substrate Z-DEVD-R110 by caspase 3/7. If active, caspase 3/7 cleaves the non-fluorescent substrate to rhodamine 110 leaving group, which becomes intensively fluorescent (excitation at 499 nm and emission at 521 nm).

To accomplish this reaction we added 100 µl of caspase 3/7 reagent to each sample (cells were incubated for 20 h with samples described above) following with shaking of 96 well microplates at 500 rpm at room temperature for 10 minutes. Caspase 3/7 activity was measured with POLARstar Galaxy plate reader (ServoLab Graz, Austria) repetitively every 15 minutes overnight. We took first 6 measuring points (15 minute intervals) and used it for determination of the linear slope for each sample. This linear slope corresponds to caspase 3/7 activity (ΔI / min).

4.5 Results

We used DABGE technique to identify Orlistat protein targets in cultured human skin cancer cells. This technique is described in detail in Chapter 3 in this thesis. Briefly, enzymes (proteins) containing nucleophilic –SH or –OH groups are selectively labeled with fluorescent phosphonic acid esters. If the protein sample is preincubated with Orlistat or any other enzyme inhibitor prior to incubation with the fluorescent reagent, the Orlistat targets are unaffected by the fluorophore. If proteins samples are compared in one gel, one being treated with Orlistat and one being untreated, the untreated samples show all enzymes, whereas the treated samples only show the proteins that are not targeted by the Orlistat. The difference represents Orlistat targets. A typical result is shown in Figure 4.1. Here we determined the Orlistat targets in lysates of SCC13 cells (squamous carcinoma cells).

Figure 4.1, A shows series of proteins targeted by the Orlistat (Original: red; Dye-Swap: green). Quantitative analysis of fluorescent intensities revealed that the individual targets are inhibited by Orlistat to a different extent (Figure 4.1, B). The most significant inhibitory effects are displayed by the protein in bands 4 and 6.

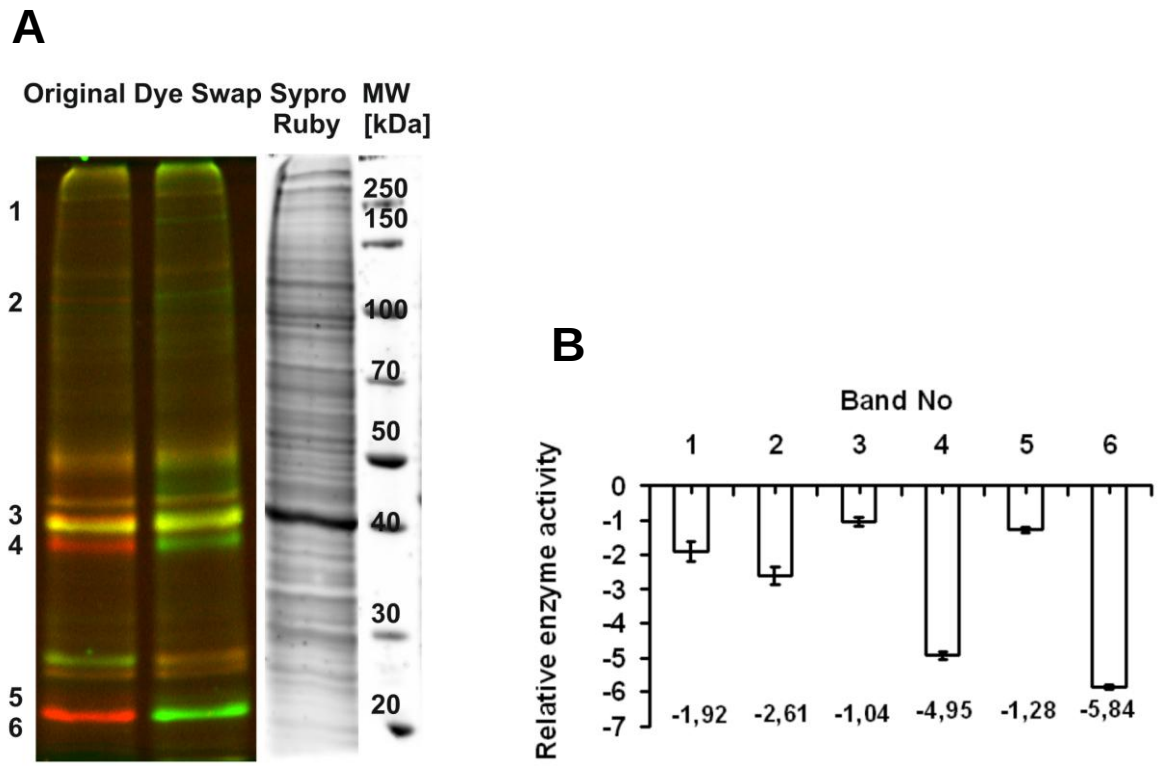

Figure 4. 1 DABGE analysis of Orlistat – tagged "(phospho)lipolytic" enzymes in SCC13 cell lysates. Cells were sonicated in 50 mM Tris/HCl buffer, pH 7,4, containing protease inhibitors (20 µg/µl leupeptin, 2 µg/µl antipain and 1µg/µl pepstatin) at 40 W for 15 seconds. After centrifugation, the supernatant was incubated with 100 µM Orlistat at 37°C and at 550 rpm for 1 h. The Orlistat treated samples and the control cell lysates were incubated with Ethyl -Cy3 and -Cy5 phosphonates as described in Chapter 3. **A:** Fluorescence image of original (left lane) and dye swap sample (right lane). After imaging of Cy3 and Cy5 – labeled proteins, total proteins were stained with Sypro ruby^{TM}. Molecular weights of proteins were compared with molecular weight standards (first lane from right); **B:** Relative enzyme activities in Orlistat treated cells determined from Cy3 and Cy5 fluorescence in the individual electrophoretic bands according to the formula: activity ratio = $\sqrt{\frac{Cy3(treated) * Cy5(treated)}{Cy3(untreated) * Cy5(untreated)}}$; (treated) refers to samples that were incubated with Orlistat prior to labeling with Cy dyes. Proteins found in bands of image A are listed in Table 4.1.

For identification of Orlistat protein targets by mass spectrometry, bands were cut out from electrophoresis gels, proteins were tryptically digested, peptides were analyzed by MS and

proteins were identified by database search. First of all we found series of lipid hydrolases as accepted (alpha enolase, neutral cholesterol hydrolase, platelet-activating factor acetylhydrolase 1b subunit gamma, serum paraoxonase, abhydrolase domain-containing protein 11 and acyl-protein thioesterase 1). In addition other (lipid unrelated) proteins have been identified including heat shock proteins. Targeting of these polypeptides is not currently understood. Table 4.1 shows the list of found proteins in SCC13 cells.

A particularly interesting hit is fatty acid synthase (FAS). This enzyme is key to endogenous fatty acid synthesis and in conjunction with enzymes utilizing exogenous lipid molecules (lipid hydrolases), which provide the cells with efficient energy supply.

Figure 4.2 shows a comparison of Orlistat targets in various cultured non-melanoma skin cancer cell lines and control keratinocytes. The cell lines SCC12 and SCC13 are derived from human squamous cell carcinoma, MET-4 is metastatic squamous carcinoma cell line, HaCaT are immortalized control keratinocytes and HaCaT-RT3 are cancer cells derived from metastatic HaCaT. Preliminary data shown in Figure 4.2 provide evidence that the cell lines under investigation show very similar patterns of Orlistat targets. It is remarkable that the HaCaT cells are missing the protein targets in band number 4. Among those proteins is serum paraoxonase, which is a hydrolase degrading short chain and oxidized phospholipids.

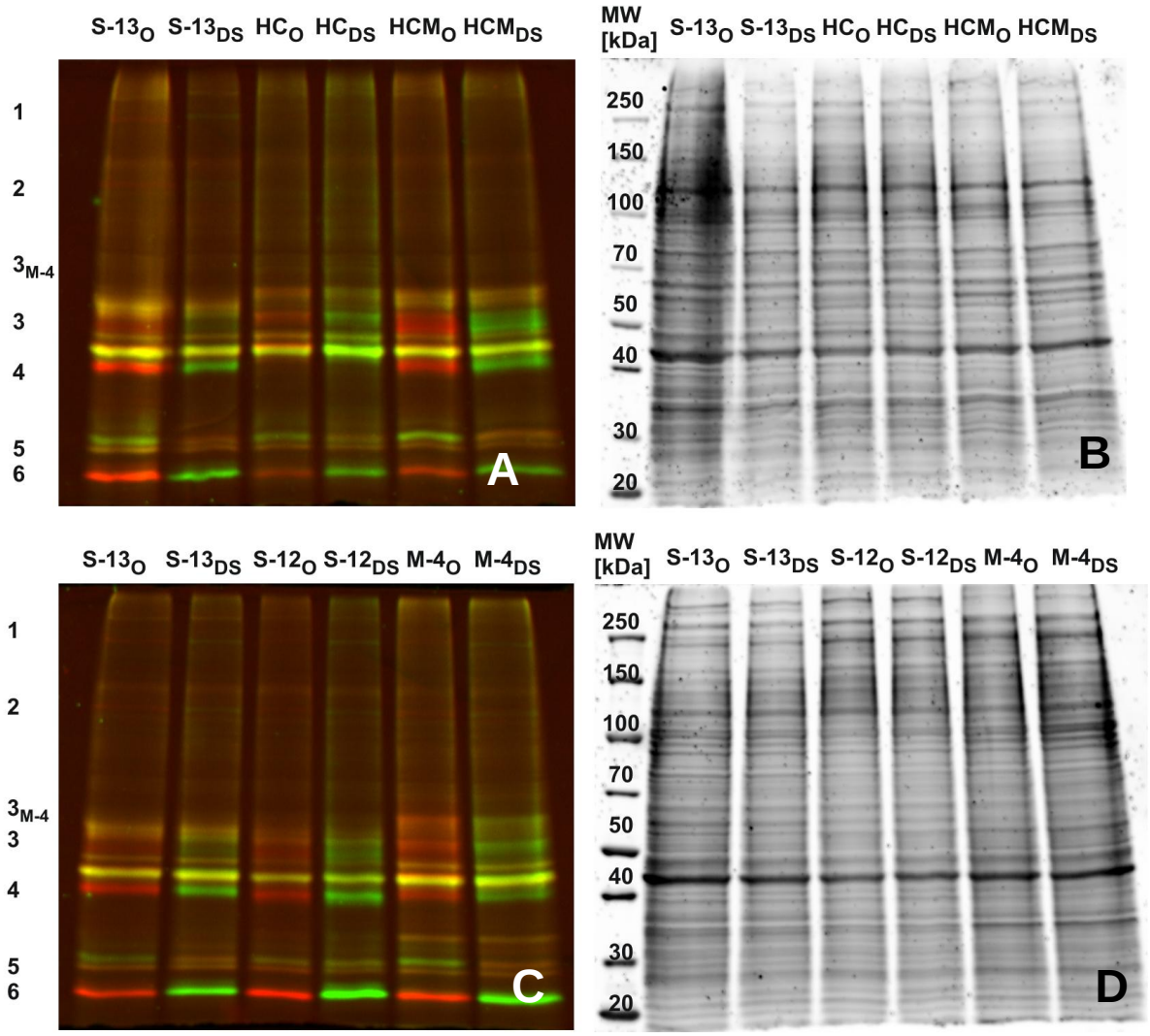

Figure 4. 2 DABGE analysis of Orlistat – tagged "(phospho)lipolytic" enzymes in lysates of different non-melanoma squamous cancer cells (SCC) and keratinocytes (HaCaT): SCC12 (S-12), SCC13 (S-13), HaCaT (HC), HaCaT-RT3 (HCM) and MET4 (M-4). Protein targets of Orlistat were fluorescently labeled, separated, detected and identified as described in the legend to Figure 4.1. Orlistat concentration was 100 µM. Panels A and C are fluorescence images (Cy3 and Cy5 excitation: 532 nm and 635 nm, respectively; Cy3 and Cy5 the emission: 555 nm and 695 nm, respectively). Panels B and D are the Sypro ruby^{TM} stains of total proteins (excitation 488 nm and emission 605 nm). O: Original , DS: Dye-Swap experiments. Proteins found in bands of images A and C are listed in Table 4.1.

In order to find out whether inhibition of lipid synthesizing and degrading enzymes is associated with lipid composition in the cancer cells, we analyzed the lipidome of SCC13

cells under the influence of Orlistat. Figure 4.3, A shows that cancer cells contain relative low amount of triacylglycerols (TAG). Orlistat treatment reduces the amount of this lipid to a small but significant extent. In addition phosphatidylcholine (PC) concentrations are also reduced due to Orlistat treatment. Figure 4.3, B to D show the effects of Orlistat on individual species. The most significant reduction is seen in the concentration of 50:1 TAG species. Orlistat does not show any preference for distinct PC species. Among phosphatidylethanolamines (PEs) the 36:0 species are most significantly reduced.

In summary, Orlistat affects neutral and phospholipid levels in SCC13 cells although to a rather small extent.

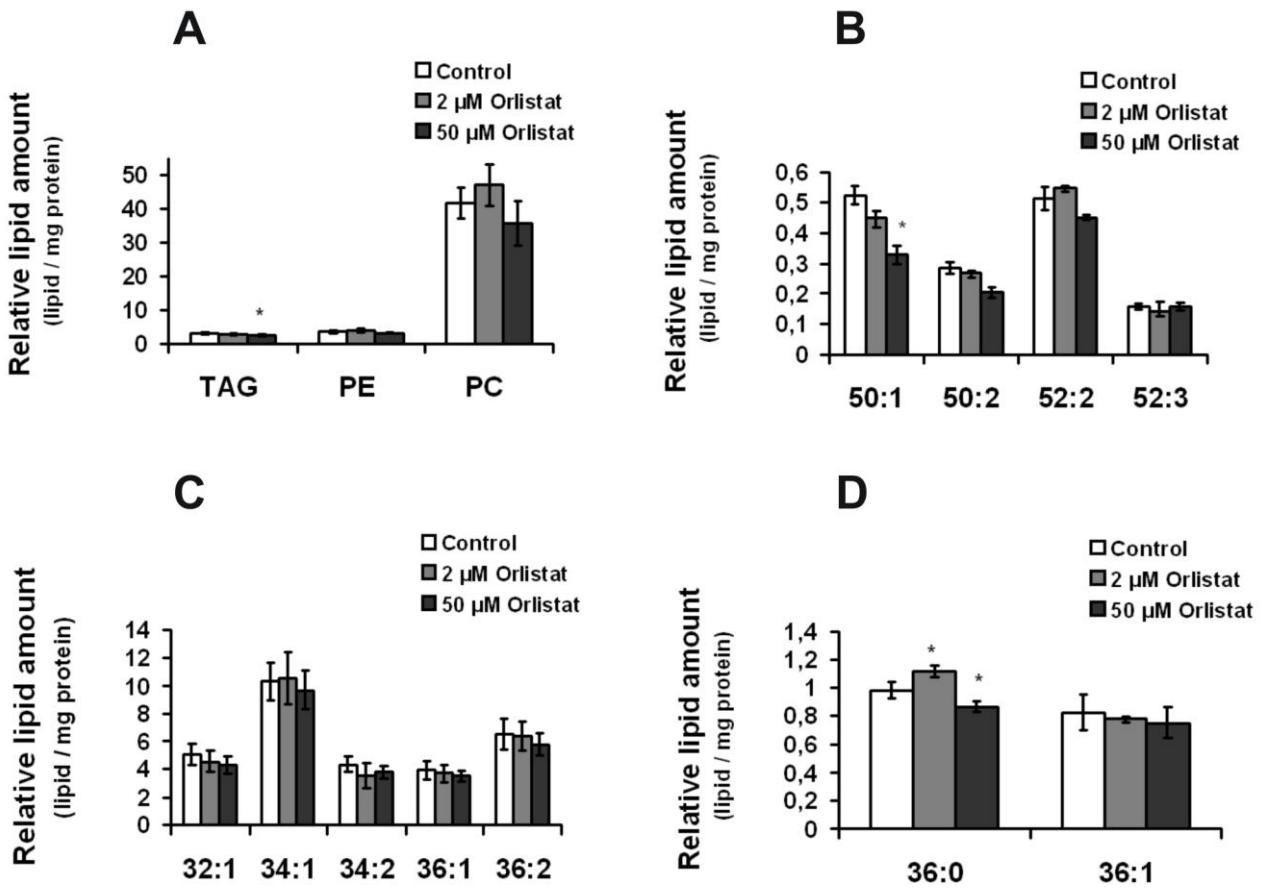

Figure 4. 3 Effects of Orlistat on glycero(phospho)-lipid profiles in SCC13 cells. Cells were incubated with different samples: 1 % DMSO or 0 µM, control; 2 µM and 50 µM Orlistat in serum rich medium for 3 h. Lipids were extracted using $CHCl_3$/MeOH (2:1, v/v) as solvent as described in experimental procedures. Lipids

were measured by UPLC-QTOF-MS and analyzed using SYNAPT™G1 qTOF HDMS. Data analysis was performed using the “Lipid Data Analyzer” software. The relative values of lipids are normalized over the amount of internal standard lipid and the total protein concentration according to: $A_{Sample}/(A_{intern\ standard}$*mg Protein). Data are expressed as means of 3 independent experiments ± SD (*, P ≤ 0, 05 relative to control). **A:** Effects of Orlistat on relative lipid amounts of TAG, PE and PC in SCC13 cells; Effects of Orlistat on relative amounts of TAG species **(B),** PC species **(C)** and PE species **(D)**. TAG: triacylglycerol, PC: phosphatidylcholine, PE: phosphatidylethanolamine.

Since Orlistat affects function of enzymes that are vital for lipid metabolism and energy supply we tested the potential of this drug of impairing cell viability or inducing cell death. Figure 4.4 shows the effect of Orlistat on cell morphology depending on Orlistat concentration and incubation time.

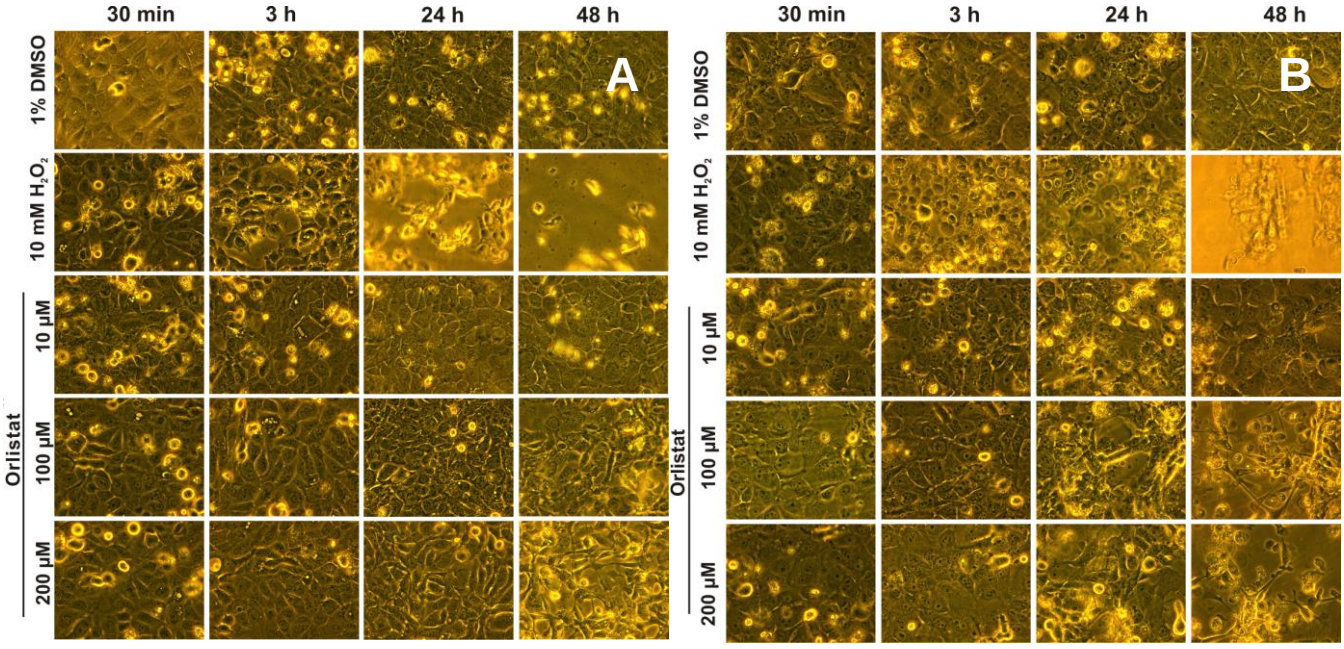

Figure 4. 4 Time dependent effects of Orlistat on morphology of human non-melanoma skin cancer cells. The cell lines, SCC12 (image A) and SCC13 (image B) were incubated with different samples in serum rich medium. 1 % DMSO, control; 10 mM H_2O_2, induces necrosis; 10 µM, 100 µM or 200 µM Orlistat. Shown are microscopic transmission light images (magnification 320x).

Data in panel A (SCC12) and panel B (SCC13) show that Orlistat is clearly cytotoxic on these cells. SCC13 cells seem to be even more susceptible to the drug as SCC12 cells. Low Orlistat concentration showed a small defect on SCC13 whereas higher concentrations led to total cell lysis in both cell lines.

Finally we analyzed the activity of caspase 3/7 which is an executer of apoptosis. Orlistat led to significant and concentration dependent activation of this enzyme after 20 h incubation (Figure 4.5).

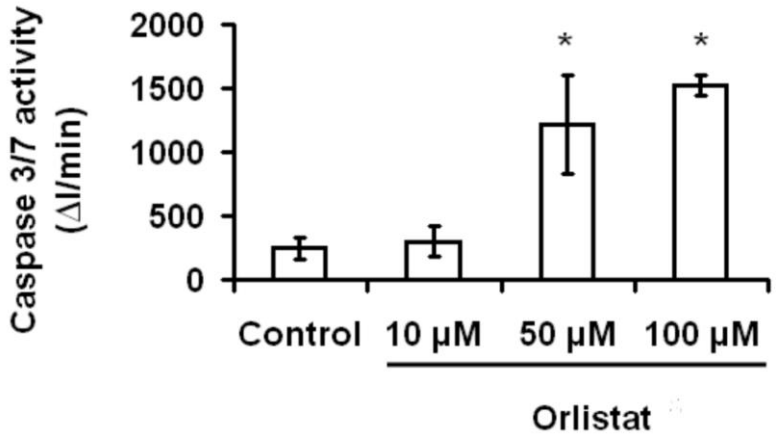

Figure 4. 5 Caspase 3/7 activity in skin cancer cells SCC13. Cells were incubated with different samples in serum rich medium (no phenol red): 0, 5 % DMSO or 0 µM Orlistat, control; 10 µM, 50 µM or 100 µM Orlistat for 20 h. Caspase 3/7 activity was detected by applying fluorescent Apo-ONE ® Homogeneous Caspase-3/7 Assay from Promega (Madison, USA) and was measured with POLARstar Galaxy plate reader (excitation: 499 nm and emission: 521 nm) overnight. The values were calculated as linear slope of measured fluorescent at different time points (ΔI/min).

It can be concluded that Orlistat induces programmed cell death in skin cancer cells (SCC13) which makes it useful candidate as therapeutic compound for treating malignant skin diseases.

No	Name	UniProt Accession No	Molecular Weight [kDa]	pI	Identified Peptide	Score	% AA Coverage
1	Fatty acid synthase	p49327	273,42	6,01	26	414,88	12
	Ubiquitin carboxyl-terminal hydrolase 7	q93009	128,3	5,33	4	53,96	3
2	Heat shock protein 105	q92598	96,86	5,28	8	126,26	12
	Heat shock protein 90	p07900	84,66	4,94	2	31,97	3
	60 kDa heat shock protein, mitochondrial	p10809	61,05	5,7	63	694.49	38
$^{*}3_{M-4}$	Pyruvate kinase isozymes M1/M2	p14618	57,93	7,95	57	480.74	27
	Alpha enolase	p06733	47,16	7,01	12	212,39	35
3	Neutral cholesterol ester hydrolase	q6piu2	45,8	6,75	2	37,62	6
	Protein disulfide-isomerase A6	q15084	48,12	4,95	2	25,66	6
	Serum paraoxonase (PON2)	q15165	39,39	5,33	1	19,2	4
4	Acetyl-CoA acetyltransferase, mitochondrial	p24752	45,19	8,98	6	100,92	19
	Adenosylhomocysteinase	p23526	47,71	5,92	3	44,5	9
	Heat shock protein beta-1	p04792	22,78	5,98	5	68,05	26
	Peroxiredoxin 4	q13162	30,54	5,86	3	56,62	15
5	Peroxiredoxin 6	p30041	25,03	6	2	24,33	10
	3-hydroxyacyl-CoA dehydrogenase type-2	q99714	26,92	7,65	5	85,59	26
	Platelet-activating factor acetylhydrolase 1b3	q15102	25,73	6,33	2	20,15	10
	Abhydrolase domain-containing protein 11	q8nfv4	34,69	9,5	2	23,63	6
	Peroxiredoxin 1	q06830	22,11	8,27	6	93,93	28
	Glutathione S-transferase kappa 1	q9y2q3	25,49	8,51	3	58,17	19
6	Acyl-protein thioesterase 1	o75608	24,66	6,29	3	43,18	13
	3-hydroxyacyl-CoA dehydrogenase type-2	q99714	26,92	7,65	4	69,69	21
	Glutathione S-transferase P	p09211	23,35	5,43	2	28,72	13

Table 4. 1 Orlistat targets in a "(phospho)lipolytic" proteome of human non-melanoma SCC13 cell lysates. Protein band numbers correspond to band numbers in Figures 4.1 and 4.2. ***** these enzymes have also been found as Orlistat targets in a proteome of the metastatic cell line MET-4. Protein targets of Orlistat were fluorescently labeled, separated, detected and identified as described in the legend to Figure 4.1.

4.6 Discussion

It was the aim of this study to identify the protein targets of Orlistat in carcinoma cells. We found different proteins as targets of Orlistat. Those were fatty acid synthase (FAS), lipid hydrolases and other proteins unrelated to lipids. Targeting of these enzymes is associated with cytotoxicity of Orlistat in cancer cells, specifically in our study to squamous carcinoma cells SCC13.

FAS contains a phosphopatatin group carrying a nucleophilic –SH function which usually binds the growing fatty acyl chain during lipid synthesis. This functional group is likely to be nucleophile, reacting with the electrophilic lactone ring of Orlistat forming a covalent drug-enzyme complex (3).

Experimental studies of Carvalho et al. have shown, that inhibition of FAS, due to higher Orlistat concentrations, in mouse melanoma B16-F10 induce apoptosis and reduce cell proliferation (33). In addition, Carvalho and colleagues tested the hypothesis that FAS has a role in spontaneous metastatic spread of B16-F10 cells from the peritoneal cavity of C57BL/6 mice through the lymphatic circulation. Thus, they ectopically injected metastatic B16-F10 melanoma cell in the peritoneal cavity of the C57BL/6 mice and observed that Orlistat - treated tumors were more dispersed among the abdominal organs. The inhibition of FAS by Orlistat apparently reduced metastasis to mediastinal lymph nodes (33). The exact role of FAS activity in this content is still unknown. One model suggest that Orlistat has antiangiogenic properties, which are due to preventing expression of vascular endothelial growth factor 2 at the endothelial cell surface, which could reduce cell viability in the lymphatic or blood circulation and interfere with their growth and colonization in the lymph nodes (34).

Zecchin et al. showed that inhibition of FAS by Orlistat in mouse melanoma B16-F10 reduces proliferation and triggers intrinsic apoptotic signaling. They found increased levels cytochrome c, caspase-9 and caspase-3 activity, which proceeded to increased levels of reactive oxygen species (ROS) and cytosolic calcium concentrations. On the other hand, cell death was independent of mitochondrial permeability transition and the activation of p53 (34). Since cytochrome c release was detected and in addition, increased levels of ROS and cytosolic calcium were involved in FAS associated cell death, it led to a conclusion that Orlistat activated the mitochondrial pathway (34). FAS inhibition by Orlistat leads to accumulation of malonyl-CoA. Specifically, it decreased carnitine palmitoyltransferase-1 (CPT-1) and fatty acid oxidation interaction with the anti-apoptotic protein Bcl-2 (20, 36-38). Palmitoyltransferase-1 is also inhibited leading to the accumulation of ceramide, which indicates apoptosis triggered by death receptors of an extrinsic pathway of apoptosis (39).

Recently, has been shown that the inhibition of FAS and FAS-induced apoptosis in the melanoma cell line B16-F10 involves mitochondria (34, 41, 43). Cellular effects due to the overexpression of FAS in neoplastic tissue, which catalyzes the formation of fatty acids for the phospholipid synthesis (40), suggest that this pathway is responsible for the activity of potential anti-cancer drug (41). After mouse melanoma B16-F10 cells were treated with Orlistat the free fatty acid (FFA) profile in mitochondria significantly changed. This effect probably influences cytosolic levels of FFA, which freely cross the outer mitochondrial membrane (42). Nevertheless, if FAS is inhibited it can consequently reduce elongation of palmitic acid, which can lead to reduction of unsaturated product such as arachidonic acid (41). Hence, the lower proliferation rates could also be due to the effect of FFA deficiency on the synthesis of membrane phospholipid (33, 43). In our studies with SCC13 cells, we also found that concentrations of TAG, PC and PE were decreased after exposure of cells

to 50 µM Orlistat for 3 h. This effect could be due to the some Orlistat activities as described above for melanoma cells. At lower Orlistat concentration such as 2 µM, the relative lipid amounts were higher, which could be due to the inhibition of (phospho)lipolytic enzymes.

In the human colorectal HT-29 cell line, inhibition of FAS by Orlistat correlated with G1 arrest leading to reduced cell growth. In addition, due to Orlistat, caspase 3/7 activity was elevated, which is a mass for apoptosis and the endogenous fatty acid synthesis was decreased prior to apoptosis (44). FAS inhibition can lead to alterations of membrane phospholipid synthesis as consequence to disruption of lipid rafts and thereby affect the function of epidermal growth factor receptor and tyrosine kinase on the surface of the tumor cells (45-47), so that the membrane disturbance induced by Orlistat could be relevant to the cell death in colorectal cancer. Hence, FAS inhibition in cancer cells is correlated to alterations of cell cycle progression, the inhibition of PI3-Akt pathway and the caspase-associated cell apoptosis (44).

In summary, it has been shown that in different cancer cell lines Orlistat has apoptotic or anti-proliferative effects. The mechanism of its action is not completely understood but most likely it involves inhibition of FAS which eventually leads to apoptosis and involves both intrinsic and extrinsic pathways. On the other hand, it seems that it can also influence cell growth by interfering with cell cycle progression during the S phase (34, 33, 39, 41).

Our studies showed that Orlistat also affects FAS in non-melanoma skin cancer cells, reduces levels of membrane phospholipids at least to a small extent and that it activates caspase 3/7. It will be the aim of more detailed investigations to find out whether the mechanism of Orlistat toxicity in cancer cells described above apply to non-melanoma skin cancers, too.

Lipid hydrolases degrading toxic oxidized phospholipids in oxLDL have also been identified as targets of Orlistat in SCC13 cells. The respective enzymes are platelet-activating factor acetylhydrolase IB subunit gamma and serum paraoxonase 2 (PON2). Both of them contain a nucleophilic serine in their active site and are therefore likely candidates for inhibition by Orlistat. PON2 is basically a lactonase and therefore Orlistat is an optimal “substrate” for this enzyme (48). Inhibition of both lipid hydrolases by the drug can also be expected to reduce cell proliferation and viability of (cancer) cells, because the function of the enzymatic defense against oxidative lipid stress is impaired.

In agreement with reports from Yu-Yang et al. we also detected the Orlistat target proteins that seem not to be related to lipids. Those are heat shock proteins (49), whose targeting still needs to be elucidated.

The mechanism of Orlistat effects on some of the targeted proteins are still unknown and additional studies will be needed to elucidate the molecular basis for effects.

4.7 Acknowledgment

This work was supported by grants from the Austrian Federal Ministry of Science and Research/FFG in the framework of the GEN-AU program (GOLD project).

4.8 References

1. US Department of Health and Human Services, editor. 2010. Melanoma and other skin cancers. National Institute of Health, 10-7625.
2. Kang, J. G., C. -. Park. 2012. Anti-obesity drugs: A review about their effects and safety. *Diabetes and Metabolism Journal* **36:** 13-25.
3. Pemble IV, C. W., L. C. Johnson, S. J. Kridel, and W. T. Lowther. 2007. Crystal structure of the thioesterase domain of human fatty acid synthase inhibited by Orlistat. *Nature Structural and Molecular Biology* **14:** 704-709.
4. Alò, P. L., P. Visca, M. L. Framarino, C. Botti, S. Monaco, V. Sebastiani, D. E. Serpieri, and U. Di Tondo. 2000. Immunohistochemical study of fatty acid synthase in ovarian neoplasms. *Oncol. Rep.* **7:** 1383-1388.
5. Dhanasekaran, S. M., T. R. Barrette, D. Ghosh, R. Shah, S. Varambally, K. Kurachi, K. J. Pienta, M. A. Rubin, and A. M. Chinnaiyan. 2001. Delineation of prognostic biomarkers in prostate cancer. *Nature* **412:** 822-826.
6. Kuhajda, F. P. 2000. Fatty-acid synthase and human cancer: New perspectives on its role in tumor biology. *Nutrition* **16:** 202-208.
7. Pizer, E. S., F. D. Wood, H. S. Heine, F. E. Romantsev, G. R. Pasternack, and F. P. Kuhajda. 1996. Inhibition of fatty acid synthesis delays disease progression in a xenograft model of ovarian cancer. *Cancer Res.* **56:** 1189-1193.
8. Pizer, E. S., C. Jackisch, F. D. Wood, G. R. Pasternack, N. E. Davidson, and F. P. Kuhajda. 1996. Inhibition of fatty acid synthesis induces programmed cell death in human breast cancer cells. *Cancer Res.* **56:** 2745-2747.
9. Gansler, T. S., W. Hardman III, D. A. Hunt, S. Schaffel, and R. A. Hennigar. 1997. Increased expression of fatty acid synthase (OA-519) in ovarian neoplasms predicts shorter survival. *Hum. Pathol.* **28:** 686-692.

10. Swinnen, J. V., T. Roskams, S. Joniau, H. Van Poppel, R. Oyen, L. Baert, W. Heyns, and G. Verhoeven. 2002. Overexpression of fatty acid synthase is an early and common event in the development of prostate cancer. *International Journal of Cancer* **98:** 19-22.
11. Rossi, S., E. Graner, P. Febbo, L. Weinstein, N. Bhattacharya, T. Onody, G. Bubley, S. Balk, and M. Loda. 2003. Fatty acid synthase expression defines distinct molecular signatures in prostate cancer. *Molecular Cancer Research* **1:** 707-715.
12. Van de Sande, T., T. Roskams, E. Lerut, S. Joniau, H. Van Poppel, G. Verhoeven, and J. V. Swinnen. 2005. High-level expression of fatty acid synthase in human prostate cancer tissues is linked to activation and nuclear localization of Akt/PKB. *J. Pathol.* **206:** 214-219.
13. Visca, P., V. Sebastiani, C. Botti, M. G. Diodoro, R. P. Lasagni, F. Romagnoli, A. Brenna, B. C. De Joannon, R. P. Donnorso, G. Lombardi, and P. L. Alo. 2004. Fatty Acid Synthase (FAS) is a marker of increased risk of recurrence in lung carcinoma. *Anticancer Res.* **24:** 4169-4173.
14. Kridel, S. J., F. Axelrod, N. Rozenkrantz, and J. W. Smith. 2004. Orlistat Is a Novel Inhibitor of Fatty Acid Synthase with Antitumor Activity. *Cancer Res.* **64:** 2070-2075.
15. Kuhajda, F. P. 2006. Fatty acid synthase and cancer: new application of an old pathway. *Cancer Res.* **66:** 5977-5980.
16. Kuhajda, F. P., K. Jenner, F. D. Wood, R. A. Hennigar, L. B. Jacobs, J. D. Dick, and G. R. Pasternack. 1994. Fatty acid synthesis: A potential selective target for antineoplastic therapy. *Proc. Natl. Acad. Sci. U. S. A.* **91:** 6379-6383.
17. Fukuda, H., N. Iritani, T. Sugimoto, and H. Ikeda. 1999. Transcriptional regulation of fatty acid synthase gene by insulin/glucose, polyunsaturated fatty acid and leptin in hepatocytes and adipocytes in normal and genetically obese rats. *European Journal of Biochemistry* **260:** 505-511.
18. Yang, Y., W. F. Han, P. J. Morin, F. J. Chrest, and E. S. Pizer. 2002. Activation of fatty acid synthesis during neoplastic transformation: Role of mitogen-activated protein kinase and phosphatidylinositol 3-kinase. *Exp. Cell Res.* **279:** 80-90.

19. Van de Sande, T., E. De Schrijver, W. Heyns, G. Verhoeven, and J. V. Swinnen. 2002. Role of the phosphatidylinositol 3′-kinase/PTEN/Akt kinase pathway in the overexpression of fatty acid synthase in LNCaP prostate cancer cells. *Cancer Res.* **62:** 642-646.
20. Pizer, E. S., J. Thupari, W. F. Han, M. L. Pinn, F. J. Chrest, G. L. Frehywot, C. A. Townsend, and F. P. Kuhajda. 2000. Malonyl-coenzyme-A is a potential mediator of cytotoxicity induced by fatty-acid synthase inhibition in human breast cancer cells and xenografts. *Cancer Res.* **60:** 213-218.
21. Mashima, T., H. Seimiya, and T. Tsuruo. 2009. De novo fatty-acid synthesis and related pathways as molecular targets for cancer therapy. *Br. J. Cancer* **100:** 1369-1372.
22. Boukamp, P., R. T. Petrussevska, D. Breitkreutz, J. Hornung, A. Markham, and N. E. Fusenig. 1988. Normal keratinization in a spontaneously immortalized aneuploid human keratinocyte cell line. *J. Cell Biol.* **106:** 761-771.
23. Boukamp, P. 2005. Non-melanoma skin cancer: What drives tumor development and progression? *Carcinogenesis* **26:** 1657-1667.
24. Corona, R. 1996. Epidemiology of nonmelanoma skin cancer: a review. Ann *1st Super Sanita.* **32:** 37–42,
25. Rheinwald, J. G., M. A. Beckett. 1981. Tumorigenic keratinocyte lines requiring anchorage and fibroblast support cultured from human squamous cell carcinomas. *Cancer Res.* **41:** 1657-1663.
26. Proby, C. M., K. J. Purdie, C. J. Sexton, P. Purkis, H. A. Navsaria, J. N. Stables, and I. M. Leigh. 2000. Spontaneous keratinocyte cell lines representing early and advanced stages of malignant transformation of the epidermis. *Exp. Dermatol.* **9:** 104-117.
27. Bradford, M. M. 1976. A rapid and sensitive method for the quantitation of microgram quantities of protein utilizing the principle of protein-dye binding. *Anal. Biochem.* **72:** 248-254.
28. Morak, M., H. Schmidinger, P. Krempl, G. Rechberger, M. Kollroser, R. Birner-Gruenberger, and A. Hermetter. 2009. Differential activity-based gel electrophoresis for comparative analysis of lipolytic and esterolytic activities. *J. Lipid Res.* **50:** 1281-1292.
29. Fling, S. P., D. S. Gregerson. 1986. Peptide and protein molecular weight determination by electrophoresis using a high-molarity tris buffer system without urea. *Anal. Biochem.* **155:** 83-88.

30. Shevchenko, A., M. Wilm, O. Vorm, and M. Mann. 1996. Mass spectrometric sequencing of proteins from silver-stained polyacrylamide gels. *Anal. Chem.* **68:** 850-858.

31. Birner-Gruenberger, R., H. Susani-Etzerodt, M. Waldhuber, G. Riesenhuber, H. Schmidinger, G. Rechberger, M. Kollroser, J. G. Strauss, A. Lass, R. Zimmermann, G. Haemmerle, R. Zechner, and A. Hermetter. 2005. The lipolytic proteome of mouse adipose tissue. *Mol. Cell. Proteomics* **4:** 1710-1717.

32. Hartler, J., M. Trotzmuller, C. Chitraju, F. Spener, H. C. Kofeler, and G. G. Thallinger. 2011. Lipid Data Analyzer: unattended identification and quantitation of lipids in LC-MS data. *Bioinformatics* **27:** 572-577.

33. Carvalho, M. A., K. G. Zecchin, F. Seguin, D. C. Bastos, M. Agostini, A. L. C. A. Rangel, S. S. Veiga, H. F. Raposo, H. C. F. Oliveira, M. Loda, R. D. Coletta, and E. Graner. 2008. Fatty acid synthase inhibition with Orlistat promotes apoptosis and reduces cell growth and lymph node metastasis in a mouse melanoma model. *International Journal of Cancer* **123:** 2557-2565.

34. Zecchin, K. G., F. A. Rossato, H. F. Raposo, D. R. Melo, L. C. Alberici, H. C. Oliveira, R. F. Castilho, R. D. Coletta, A. E. Vercesi, and E. Graner. 2011. Inhibition of fatty acid synthase in melanoma cells activates the intrinsic pathway of apoptosis. *Laboratory Investigation* **91:** 232-240.

35. Browne, C. D., E. J. Hindmarsh, and J. W. Smith. 2006. Inhibition of endothelial cell proliferation and angiogenesis by orlistat, a fatty acid synthase inhibitor. *FASEB Journal* **20:** 2027-2035.

36. Bandyopadhyay, S., R. Zhan, Y. Wang, S. K. Pai, S. Hirota, S. Hosobe, Y. Takano, K. Saito, E. Furuta, M. Iiizumi, S. Mohinta, M. Watabe, C. Chalfant, and K. Watabe. 2006. Mechanism of apoptosis induced by the inhibition of fatty acid synthase in breast cancer cells. *Cancer Res.* **66:** 5934-5940.

37. Thupari, J. N., M. L. Pinn, and F. P. Kuhajda. 2001. Fatty acid synthase inhibition in human breast cancer cells leads to malonyl-CoA-induced inhibition of fatty acid oxidation and cytotoxicity. *Biochem. Biophys. Res. Commun.* **285:** 217-223.

38. Zhang, Y., C. Guo, and G. Yu. 2005. A pilot study of fatty acid metabolism in oral squamous cell carcinoma. *Int. J. Oral Maxillofac. Surg.* **34:** 78-81.

39. Paumen, M. B., Y. Ishida, H. Han, M. Muramatsu, Y. Eguchi, Y. Tsujimoto, and T. Honjo. 1997. Direct interaction of the mitochondrial membrane protein carnitine palmitoyltransferase I with Bcl-2. *Biochem. Biophys. Res. Commun.* **231:** 523-525.
40. Swinnen, J. V., P. P. Van Veldhoven, L. Timmermans, E. De Schrijver, K. Brusselmans, F. Vanderhoydonc, T. Van De Sande, H. Heemers, W. Heyns, and G. Verhoeven. 2003. Fatty acid synthase drives the synthesis of phospholipids partitioning into detergent-resistant membrane microdomains. *Biochem. Biophys. Res. Commun.* **302:** 898-903.
41. Zecchin, K. G., L. C. Alberici, M. F. Riccio, M. N. Eberlin, A. E. Vercesi, E. Graner, and R. R. Catharino. 2011. Visualizing inhibition of fatty acid synthase through mass spectrometric analysis of mitochondria from melanoma cells. *Rapid Communications in Mass Spectrometry* **25:** 449-452.
42. Schrauwen, P., W. H. M. Saris, and M. K. C. Hesselink. 2001. An alternative function for human uncoupling protein 3: Protection of mitochondria against accumulation of nonesterified fatty acids inside the mitochondrial matrix. *FASEB Journal* **15:** 2497-2502.
43. Zecchin, K. G., F. A. Rossato, and H. F. Raposo. 2010. *Lab. Invest.*
44. Chuang, H. -., Y. -. Chang, and J. -. Hwang. 2011. Antitumor effect of orlistat, a fatty acid synthase inhibitor, is via activation of caspase-3 on human colorectal carcinoma-bearing animal. *Biomedicine and Pharmacotherapy* **65:** 286-292.
45. Simons, K., E. Ikonen. 1997. Functional rafts in cell membranes. *Nature* **387:** 569-572.
46. Helms, J. B., C. Zurzolo. 2004. Lipids as targeting signals: Lipid rafts and intracellular trafficking. *Traffic* **5:** 247-254.
47. Nagy, P., G. Vereb, Z. Sebestyén, G. Horváth, S. J. Lockett, S. Damjanovich, J. W. Park, T. M. Jovin, and J. Szöllosi. 2002. Lipid rafts and the local density of ErbB proteins influence the biological role of homo- and heteroassociations of ErbB2. *J. Cell. Sci.* **115:** 4251-4262.
48. Draganov, D. I., J. F. Teiber, A. Speelman, Y. Osawa, R. Sunahara, and B. N. La Du. 2005. Human paraoxonases (PON1, PON2, and PON3) are lactonases with overlapping and distinct substrate specificities. J. Lipid Res. 46: 1239-1247.

49. Yang, P. -., K. Liu, M. H. Ngai, M. J. Lear, M. R. Wenk, and S. Q. Yao. 2010. Activity-based proteome profiling of potential cellular targets of orlistat - An FDA-approved drug with anti-tumor activities. J. Am. Chem. Soc. 132: 656-666.